This is to certify that the
thesis entitled

OPTIMIZATION OF A MICROWAVE-ASSISTED EXTRACTION PROCEDURE FOR THE EXTRACTION OF ORGANIC IMPURITIES FROM SEIZED MDMA TABLETS

presented by

PATRICIA JEAN JOINER

has been accepted towards fulfillment
of the requirements for the

M.S. degree in Forensic Science

Major Professor's Signature

September 3, 2009

Date

OPTIMIZATION OF A MICROWAVE-ASSISTED EXTRACTION PROCEDURE FOR THE EXTRACTION OF ORGANIC IMPURITIES FROM SEIZED MDMA TABLETS

By

Patricia Jean Joiner

A THESIS

Submitted to
Michigan State University
in partial fulfillment of the requirements
for the degree of

MASTER OF SCIENCE

Forensic Science

2009

ABSTRACT

OPTIMIZATION OF A MICROWAVE-ASSISTED EXTRACTION PROCEDURE
FOR THE EXTRACTION OF ORGANIC IMPURITIES
FROM SEIZED MDMA TABLETS

By

Patricia Jean Joiner

The controlled substance 3,4-methylenedioxymethamphetamine (MDMA), also known as ecstasy, is often ingested in tablet form. Because of the lack of quality control in the synthesis of MDMA, impurities from the starting materials as well as intermediates and by-products of reactions during the synthesis are often present in the tablets. The organic impurities are extracted using a liquid-liquid extraction (LLE) procedure and are analyzed by gas-chromatography-mass spectrometry (GC-MS) to obtain the organic impurity profile. Due to the limitations using LLE, alternative extraction procedures are desired for the extraction of impurities.

In this work, a microwave-assisted extraction (MAE) procedure in conjunction with a headspace solid-phase microextraction (HS-SPME) procedure is optimized for the extraction of organic impurities from MDMA tablets. The extraction buffer, pH, and concentration were optimized for use in the MAE. Using a full factorial design, the MAE parameters of ramp time, extraction time, and extraction temperature were determined to be significant and were then optimized using a circumscribed central composite (CCC) design. The HS-SPME parameters of extraction time and extraction temperature were optimized empirically. The optimized MAE/HS-SPME procedure was compared to a HS-SPME procedure and a LLE procedure based on the literature [1] showing that MAE/HS-SPME and HS-SPME are possible alternatives to LLE.

[1] Van Deursen *et al.* Sci Justice 2006; 46: 135-152.

ACKNOWLEDGEMENTS

I would first like to thank my advisor Dr. Ruth Smith for all of her guidance and patience throughout the project start to finish. Without her help and support, this work would not have reached its potential.

I thank my committee members Mr. Frank Schehr and Dr. Christina DeJong for their input and help in preparing my thesis.

I would like to acknowledge the Michigan State Police for the supply of MDMA tablets. The tablets were essential in the practical application of this work which could not have been completed otherwise.

I would also like to thank the Forensic Sciences Foundation Lucas Grant and the Michigan State University Graduate School for partial funding of this project. The funds were essential in the completion of this work.

I thank my fellow forensic chemistry students who were always available for a second opinion and for support whenever I needed it. Their thoughts and ideas helped to remind me of the big picture and the overall goal of the work.

Finally, I would like to thank my family for their continued support. I especially want to thank Adam Giebink for his love and support even when things were tough.

TABLE OF CONTENTS

LIST OF TABLES

LIST OF FIGURES

KEY TO ABBREVIATIONS

amu	Atomic mass unit
ANOVA	Analysis of variance
BZP	N-benzylpiperazine
CAR	Carboxen™
CCC	Circumscribed central composite
CSA	Controlled Substances Act
DEA	Drug Enforcement Administration
DVB	Divinylbenzene
DVB/CAR/PDMS	Divinylbenzene/Carboxen™/polydimethylsiloxane
EM	Electron multiplier
FDA	Food and Drug Administration
FTIR	Fourier transform infrared spectroscopy
GC	Gas chromatography (gas chromatograph)
GC-MS	Gas chromatography-mass spectrometry
HPLC	High performance liquid chromatography
HS-SPME	Headspace solid-phase microextraction
ICP-MS	Inductively-coupled plasma mass spectrometry
LLE	Liquid-liquid extraction
MAE	Microwave-assisted extraction
MAE/HS-SPME	Microwave-assisted extraction/headspace solid-phase microextraction
MANOVA	Multivariate analysis of variance

MDA	3,4-Methylenedioxyamphetamine
MDEA	3,4-Methylenedioxyethylamphetamine
MDMA	3,4-Methylenedioxymethamphetamine
MDP2P	3,4-Methylenedioxyphenyl-2-propanone
MDP2P-oxime	3,4-Methylenedioxyphenyl-2-propanone oxime
MDP2-propanol	3,4-Methylenedioxyphenyl-2-propanol
MS	Mass spectrometry (mass spectrometer)
m/z	Mass to charge ratio
N-formyl-MDA	N-formyl-methylenedioxyamphetamine
N-formyl-MDMA	N-formyl-methylenedioxymethamphetamine
PDMS	Polydimethylsiloxane
PDMS/DVB	Polydimethylsiloxane/divinylbenzene
PPMC	Pearson product moment correlation
RSD	Relative standard deviation
SPME	Solid-phase microextraction
TFMPP	1-(3-Triflouromethyl)phenylpiperazine

Chapter 1 Introduction

1.1. MDMA Background

The controlled substance 3,4-methylenedioxymethamphetamine (MDMA), also known as the club drug "ecstasy," is a dangerous and illegal substance. MDMA is a synthetic amphetamine-type stimulant often ingested in tablet form. This psychedelic drug has many effects on the body including euphoria and distortions in perceptions [1].

1.1.1. MDMA History

MDMA was synthesized in the early 1900s by the German pharmaceutical company Merck as an intermediate product in an attempt by the company to synthesize a drug to stop bleeding [2]. The compound was patented in 1914 by Merck under German Patent number 274350 [3]. In the 1950s, the US Army was reported to have conducted studies with the drug, testing its toxicity in several animals including mice, and rats [4,5].

A major resurgence of the drug occurred in the mid-1970s. Dr. Alexander Shulgin synthesized MDMA for experimentation. He ingested the drug and took careful notes of its effects including euphoria [6]. Around the same time, psychiatrists were utilizing the compound with patients to enhance communication; however, MDMA had never been tested by the Food and Drug Administration (FDA) for this use [7]. In the 1980s the drug first became available on the streets. After being emergency scheduled in Schedule I of the Controlled Substances Act (CSA) in 1985, MDMA was permanently placed in Schedule I by the Drug Enforcement Administration (DEA) in 1988. As a Schedule I controlled substance, MDMA was thought to have a high potential for abuse and no proven medical uses [8,9].

1.1.2. MDMA Use

The term "ecstasy" encompasses a broad range of synthetic tablets that are ingested orally, often in a club or rave setting [10,11]. Other names for these tablets include Adam, XTC, Beans, E, X, Hug Drug, and Disco Biscuit [12]. Most ecstasy tablets contain MDMA, though not all do. Ecstasy mimic tablets often contain a mixture of N-benzylpiperazine (BZP), a Schedule I controlled substance under the CSA, and 1-(3-triflouromethyl)phenylpiperazine (TFMPP) which is not currently controlled [13]. Ecstasy tablets which include MDMA often also contain methamphetamine and 3,4-methylenedioxyamphetamine (MDA) in addition to other substances such as ketamine, caffeine, and diazepam [10]. The tablets can vary in size, shape, color, and markings with masses ranging from approximately 0.2 g to 0.3 g. The percentage of MDMA in tablets ranges from approximately 30-50% of the total mass [10].

According to an ongoing study by the University of Michigan, MDMA use has fluctuated over the last 13 years [14]. The study surveyed 8th grade, 10th grade, and 12th grade students concerning their use and attitudes towards illicit drugs. The number of students who reported having used MDMA at least once in their life peaked in 2001 with 12% of 12th grade students reporting MDMA use. Since 2001, the number of students reporting MDMA use has decreased to approximately 6% of 12th grade students. However, the study also reported the perceived risk associated with using MDMA once or twice. The percentage of students who associate a risk with using MDMA has slowly decreased since 2005 with less than half of the 8th grade and 10th grade students responding that risk is involved. Because of the trend of attitudes towards MDMA, there is a concern that a resurgence of the drug's popularity may occur.

1.1.3. MDMA Chemistry and Pharmacology

MDMA is a member of the phenethylamine class of compounds. It is structurally similar to amphetamine and methamphetamine with the addition of a methylenedioxy group on the aromatic ring (Figure 1.1). The methylenedioxy substitution on the aromatic ring gives MDMA its hallucinogenic properties while the methyl group on the α-carbon gives MDMA its stimulant properties [15].

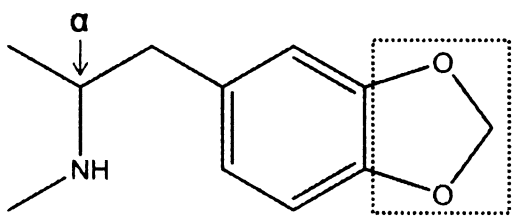

Figure 1.1: Chemical structure of MDMA with the methylenedioxy substitution on the aromatic ring outlined and the α-carbon labeled

When ingested orally, MDMA enters the blood stream and reaches peak levels about two hours later [11]. In the body, MDMA may remain unchanged or be metabolized to MDA as it is excreted. Because the half life of MDMA is eight hours, effects of the MDMA can last for several days after the drug has been ingested [11]. Effects of MDMA on the body can include euphoria, distortions in perception, increased energy, and a feeling of closeness with other people [1,11]. MDMA can also cause increased heart rate, nausea, blurred vision, faintness, and hyperthermia [1].

When MDMA reaches the brain, it has the most effect on serotonin neurons [16]. The MDMA acts as a substrate for the serotonin transporter on the pre-synaptic cell. Once in the nerve terminal, MDMA displaces serotonin from vesicles which increases the amount of serotonin released into the synapse between neurons. The areas of the brain most affected by the increase in serotonin levels include the prefrontal cortex, which is

involved in decision making; the thalamus, which is involved in sensory processing; and the amygdala, which is involved with fear and anxiety reactions [16].

1.2. MDMA Production

1.2.1. MDMA Synthetic Routes

Several routes are available for synthesizing MDMA with routes using 3,4-methylenedioxyphenyl-2-propanone (MDP2P) as the starting material being the most common [17]. Because MDP2P is now regulated by the DEA, it too must be synthesized in the clandestine laboratory. Two of the more common routes for MDP2P synthesis are shown in Appendix A [18]. In the first synthesis, safrole is extracted from sassafras oil, a naturally occurring substance in eastern North America and eastern Asia [19]. Safrole is then converted to isosafrole through isomerization using potassium hydroxide and ethanol. Isosafrole can also be obtained from industrial sources thus bypassing the safrole extraction and isomerization steps [18]. Isosafrole glycol is produced by the oxidation of isosafrole using formic acid and hydrogen peroxide. Finally MDP2P is generated by dehydration of isosafrole glycol using sulfuric acid [18].

The second synthesis of MDP2P begins in the same way with safrole being converted to isosafrole. However, using sulfuric acid and sulfanilic acid, isosafrole is oxidized to form piperonal. Piperonal is then converted to β-nitroisosafrole via the Knoevenagel-Walter condensation using nitroethane. After the formation of an intermediate oxime, 1-(3,4-methylenedioxyphenyl)-2-propanone oxime (MDP2P oxime), through oxide-reduction, MDP2P is formed by hydrolysis using acetic acid [18].

After MDP2P is synthesized, the MDMA synthesis begins. While there are other synthesis methods that can be used, the two most common are reductive amination and

the Leukart synthesis [17,18]. Appendix B shows a schematic of the synthesis of MDMA from MDP2P by both of these routes.

For the reductive amination route, the MDP2P is reacted with methylamine to form an imine intermediate: 1,2-(methylenedioxy)-4-(2-N-methyl-iminopropyl) benzene. This compound is then reduced to MDMA using one of several reducing agents such as sodium cyanoborodhydride or sodium borohydride [18,20]. During the reduction of the imine, 3,4-methylenedioxyphenyl-2-propanol (MDP2-pronanol) is formed from a side reaction which lowers the yield of MDMA. To limit the production of MDP2-propanol and increase the production of MDMA, a laboratory may use the "cold method." When the cold method is used, the temperature of the mixture during synthesis is cooled to -20 °C which increases the selectivity of the reducing agent to form MDMA [21].

Two variations of the Leukart synthesis are commonly used. The first involves the reductive amination of MDP2P to N-formyl-methylenedioxymethamphetamine (N-formyl-MDMA) using methylformamide [22]. Through hydrolysis, MDMA is then formed [20]. Alternatively, MDP2P can be converted to N-formyl-methylenedioxyamphetamine (N-formyl-MDA) using formamide through reductive amination [22]. Then, through reduction with lithium aluminum hydride, MDMA is formed [20].

1.2.2. Tablet Production

Using one of the aforementioned synthetic routes, MDMA is synthesized in clandestine laboratories [17,23]. The impurities from chemicals used as starting materials as well as by-products and intermediates of reactions during the synthesis are present in the MDMA powder, though often in low concentrations [17]. The synthesized

MDMA is then mixed with additives including adulterants and diluents. Adulterants, such as caffeine, are compounds that are added to the drug to enhance its effects. Other controlled substances such as methamphetamine and amphetamine may also be added to further enhance the effects of the MDMA. Diluents, such as lactose, are added to dilute the MDMA so that more tablets can be produced from a single batch of MDMA. Additionally, color dyes are also used to dilute the MDMA and to give the tablets their color.

The mixture of MDMA and additives is then pressed into tablets using various tablet presses that give the tablets different shapes and logos (or imprints). In a clandestine laboratory, a single batch of MDMA can be divided and pressed into tablets with different colors and logos. Therefore, exhibits that look physically different may in fact contain MDMA that was synthesized in the same batch and therefore have the same chemical properties [10,17]. The percentage of MDMA present in the final tablets varies by batch and manufacturer [10]. Tablets currently being seized by law enforcement contain about 30% MDMA (by mass) as well as methamphetamine and caffeine. Also, some tablets being seized contain a mixture of MDMA and BZP [24].

1.3. MDMA Profiling

The goal of profiling MDMA tablets is to link tablets from different exhibits to a common batch of MDMA or link tablets to a common production source in an effort to determine drug trafficking routes. Historically, physical characteristics of tablets have been used in MDMA tablet profiling [10]. However, the physical characteristics alone may not be sufficient to compare tablets from different exhibits because clandestine laboratories can manufacture tablets that appear physically different [10,23].

The limitations of profiling MDMA tablets based only on the physical appearance of the tablets were demonstrated by Cheng *et al.* [10]. Using over 123,000 MDMA tablets seized from 613 cases in Hong Kong, the group recorded physical characteristics and studied the chemical composition of tablets using Fourier transform infrared spectroscopy (FTIR), high performance liquid chromatography (HPLC), and gas chromatography-mass spectrometry (GC-MS). Many of the physically similar tablets were likely not from a common production source because different impurities and additives were present. On the other hand, some tablets that had different physical characteristics were found to possess similar impurity profiles (similar impurities present at similar concentrations), indicating that the tablets may have originated from the same production source. This study demonstrated the downfalls of tablet profiling based on physical characteristics alone and highlighted the need for profiling tablets based on the chemical composition.

The profiling of tablets based on chemical composition can be completed at different levels. The overall chemical components of the tablet can be used in compositional profiling or the organic impurities present in the tablet can be used in organic impurity profiling [25]. To study the organic impurities in MDMA tablets, the tablets are typically ground and dissolved in an aqueous solvent and then extracted into an organic medium. The extraction is referred to as liquid-liquid extraction (LLE). After LLE, the extract is analyzed, often by GC-MS, with the resulting chromatogram referred to as the organic impurity profile of the tablet. By studying and comparing the impurity profiles of the tablets, a more complete comparison of tablets from different exhibits can be obtained. The identity of impurities present can be used to determine the synthetic

route used to manufacture the MDMA. In addition, tablets from different exhibits can possibly be linked based on the impurities.

Van Deursen *et al.* developed a LLE method for the extraction of organic impurities from seized MDMA tablets [26]. In the developed procedure, whole MDMA tablets were ground and dissolved in 0.33 M phosphate buffer at pH 7. After several agitation steps, including vortexing, centrifugation, and sonication, 400 μL of toluene were added to the solution. After a few final agitation steps, such as rotative shaking and centrifugation, the toluene layer was extracted and analyzed by GC-MS. Good repeatability (average relative standard deviation, RSD, without outliers was 6%) over six extractions was achieved based on the peak areas of 22 selected impurities in the chromatograms (for example MDP2P, MDP2-propanol, and N-formyl-MDMA). Also, good reproducibility among days over a two week time span was reported with RSD values of 7% and 8% (without outliers) using two separate MDMA exhibits. Based on the impurities detected and identified in the MDMA exhibits, the group determined that the MDMA present in many tablets seized in the Netherlands was manufactured using the reductive amination route. The group also noted that differences between the tablets were likely due to different reducing reagents used in the manufacturing process.

In addition to between exhibit comparisons, the impurities present in MDMA tablets can be utilized to determine the method used to synthesize the MDMA. Palhol *et al.* identified 29 impurities in 52 MDMA samples seized in France using LLE followed by GC-MS [17]. Impurities from starting materials and side reactions were present in the final tablets with different synthetic routes yielding different impurities. For example, the Leukart reaction gave N-formyl-MDMA, an impurity not observed in other routes. Also,

the bromopropane route was the only route to show brominated impurities. The most common synthetic route in Europe was determined to be reductive amination from MDP2P based on the impurities in the analyzed tablets. The group also compared tablets from different exhibits based on the impurities present and determined that similar levels of the same impurities indicated that the MDMA was produced in a common batch. The same impurities present at different levels indicated that, while the same synthetic route was used, the MDMA originated from different batches from the same clandestine laboratory. Different impurities present indicated that the samples were unrelated. (However, a clandestine laboratory may produce batches of MDMA using different synthetic routes yielding different impurities.) Therefore, a more definitive comparison of tablets is possible when organic impurities contained in the tablets are considered, rather than only the physical characteristics.

Using organic impurity profiles obtained by the LLE procedure developed by van Deursen *et. al* [26], Weyermann *et al.* created a standardized procedure that could be used across many laboratories. With participating laboratories using the same procedure, the results can be pooled to create a database. Throughout the work, the differences in eight impurities among 26 MDMA exhibits were studied [23]. Some of these impurities included: MDP2P, MDP2-propanol, and N-formyl-MDMA. These eight organic impurities were selected to compare tablets based on good reproducibility between replicate analyses and large variability among samples from different exhibits. The correlation among the samples was assessed using Pearson product moment correlation (PPMC) coefficients based on the peak areas of the eight impurities. Using this method, successful discrimination of many of the exhibits was achieved (although it is not clear

how many exhibits were discriminated). However, because only eight impurities were considered in the comparison, potentially discriminatory information found elsewhere in the chromatogram was overlooked.

1.4. Alternative Extraction Procedures

Despite the successful use of LLE for organic impurity profiling there are many limitations of LLE. For example, LLE can efficiently extract components such as methamphetamine, MDMA, and caffeine. The efficient extraction of these components is not desirable because the compounds can result in large, broad peaks in the chromatogram that can potentially mask impurities present at lower concentrations. Also, a relatively large sample mass is required. For the van Deursen method, a full tablet is used for each extraction. Therefore, when exhibits contain a small number of tablets, possibly only one tablet, re-testing cannot be performed [26]. Because organic solvents are used for LLE, costs increase and organic waste is generated. Therefore, alternative extraction methods to LLE are desirable to overcome these limitations.

1.4.1. Headspace Solid-Phase Microextraction

Solid-phase microextraction (SPME) is an extraction procedure in which a polymer coated fiber is introduced to the sample either directly in contact with the sample (immersion SPME) or in the headspace of the sample (HS-SPME). Solid-phase microextraction allows for the pre-concentration of analytes onto the fiber thus allowing for the detection of components present at low concentrations. Headspace solid-phase microextraction has been used as an alternative method of extraction to LLE for profiling synthetic illicit drugs such as methamphetamine.

Kuwayama *et al.* optimized HS-SPME parameters such as sample mass, extraction time, extraction temperature, and fiber type for the extraction of organic impurities from methamphetamine [27]. In the developed procedure, t he opt imized extraction procedure included exposing a divinylbenzene/Carboxen^{TM}/ polydimethylsiloxane (DVB/CAR/PDMS) fiber to the headspace of 50 mg solid sample for 30 minutes at 85°C. Because the HS-SPME pre-concentrated the analytes on the fiber, less sample mass was required for this extraction compared to LLE. The group applied statistical procedures such as Euclidian distance, cosine distance, and correlation coefficients to compare the samples based on the abundance of eight impurities. It was determined that a logarithmic conversion followed by a cosine distance calculation was best for discriminating tablets from different batches and classifying tablets from the same batch. The group demonstrated that HS-SPME was a quick and simple extraction method for organic impurities while minimizing the extraction of methamphetamine.

Koester *et al.* also used HS-SPME to obtain impurity profiles of methamphetamine [28]. The HS-SPME profiles were compared to profiles obtained using other extraction procedures including LLE, acid dissolution, base dissolution, and solvent dissolution. The HS-SPME procedure, which involved sampling the headspace of the solid sample, extracted 30 impurities while the LLE procedure extracted only eight impurities. Methamphetamine was present in the HS-SPME profiles; however, it was present at lower concentrations and did not dominate the profile, as observed in the LLE profiles.

The application of SPME to MDMA was described by Kongshaug *et al.* [29]. The MDMA sample was dissolved in 0.1 M acetate buffer at pH 5 which was chosen to

avoid the over-extraction of MDMA. A polydimethylsiloxane/divinylbenzene (PDMS/DVB) fiber was exposed to the sample for 30 minutes at 90 °C. The two different SPME sampling modes (immersion and headspace) were investigated. The HS-SPME sampling mode was preferred due to the increased lifetime of the fiber. In immersion SPME, the fiber degraded more quickly because it was in direct contact with the liquid sample. The PDMS/DVB fiber extracted more impurities (though it is unclear how many more) than the PDMS fiber because the PDMS/DVB fiber extracted analytes with a wider range of polarities. To assess the precision of the extraction, the RSD values of peak areas was calculated to be 2-13%, showing that the HS-SPME procedure was precise. The HS-SPME procedure extracted a similar number of impurities to LLE with similar chromatography but without the need for organic solvents.

Bonadio *et al.* optimized a HS-SPME procedure for the extraction of impurities from a ground MDMA tablet [30]. The developed method involved pre-heating the vial with 40 mg of ground MDMA sample for 15 minutes at 80 °C and then exposing a PDMS/DVB fiber to the headspace for 15 minutes at 80 °C. The group chose the 10 impurities with the most repeatable peak areas and applied data pre-treatments such as a normalization using the 4^{th} square root and the logarithm. Principal components analysis was then used to identify clusters of similar MDMA samples. The group also compared their developed method to a LLE procedure [31]. The LLE procedure extracted 15 more impurities than the HS-SPME procedure, but the HS-SPME sample preparation was simpler because fewer steps were required.

1.4.2. Microwave-Assisted Extraction

Microwave-assisted extraction (MAE) uses microwave energy to heat a solution under pressure. The pressure allows the heating of the solvent to temperatures higher than its atmospheric boiling point. The higher MAE temperatures are achieved in a few minutes which is faster than heating a sample by conventional heating. Theoretically, MAE offers a highly efficient extraction in part because the sample is heated more evenly due to the heating mechanisms (discussed in chapter 2).

So far, MAE has had limited use in drug analysis applications. The procedure has been applied to the extraction of the active ingredients in pharmaceuticals by Hoang *et al.* [32]. Using MAE, the group achieved 97-102% extraction efficiency when the amount extracted was compared to the amount given on the label of the pharmaceutical. The extraction efficiency compares to conventional extraction procedures; however, the MAE took only seven minutes compared to the conventional 30 minutes. The RSD values between replicate extractions were 1.4% showing that the MAE procedure had good repeatability that compared well with the conventional extraction.

The use of MAE in combination with SPME has been reported in the literature as a method that offers a highly efficient extraction (MAE) while maintaining the desired selectivity (SPME). Bieri *et al.* used focused MAE (microwave-assisted extraction at atmospheric pressure) followed by immersion SPME to extract cocaine from coca leaves, and the fiber extract was analyzed by GC-MS [33]. The MAE involved placing 100 mg of coca leaves in 5 mL methanol and exposing it to microwave energy for 30 seconds. The effects of pH, extraction time, and extraction temperature on immersion SPME were also studied. The group determined that the optimum SPME procedure involved diluting

the microwave extract (50:1) in 50mM phosphate buffer at pH 8.1. The PDMS fiber was immersed in a sample for 15 minutes at 25 °C. By using MAE with HS-SPME, the total extraction time was reduced by 29 minutes. The MAE procedure allowed a quick and efficient extraction while the addition of the SPME step allowed for more selective extraction of the cocaine from coca leaves.

Carro *et al.* applied a combined MAE/HS-SPME procedure to the extraction of polybrominated compounds from aquaculture samples [34]. Using a central composite experimental design, MAE parameters, such as solvent type, solvent volume, extraction temperature, and extraction time were studied and optimized. Following MAE, a clean-up step and HS-SPME step were performed. Because of the pre-concentration ability of the fiber in HS-SPME, lower detection limits were achieved when the HS-SPME step was included compared to analyses where HS-SPME was not included. For example, for the compound heptachlor, the limit of detection for MAE/HS-SPME was 80 pg/g of sample whereas, with MAE alone, the limit of detection was 690 pg/g of sample. This study demonstrated the possibility of MAE used in conjunction with HS-SPME to achieve lower limits of detection.

1.5. Research Objectives

The objective of this research is to develop a MAE/HS-SPME procedure for the extraction of organic impurities from seized MDMA tablets. Microwave-assisted extraction allows for an efficient extraction; however, because of the high efficiency, a more selective extraction procedure is desired to follow the MAE. Headspace solid-phase microextraction was chosen because it allows for the selective extraction of the

organic impurities while minimizing the extraction of the more concentrated components such as methamphetamine, MDMA, and caffeine.

This work was completed in two parts. The MAE/HS-SPME procedure was optimized first. This involved determining an appropriate extraction buffer and HS-SPME parameters and then optimizing the MAE parameters. The pH, concentration, and type of the extraction buffer for MAE were optimized to achieve a precise extraction that limited sample carry-over between extractions. The HS-SPME extraction time and extraction temperature were optimized empirically to allow for the extraction of impurities without overloading the fiber. The MAE parameters ramp time, extraction time, and extraction temperature were optimized using experimental design procedures. A full factorial design was used to determine the significant parameters and a circumscribed central composite (CCC) design was used to optimize the significant parameters.

After the method was optimized, three MDMA exhibits were utilized to compare the optimized MAE/HS-SPME procedure to a HS-SPME procedure and a LLE procedure based on the literature [26]. The goal was to determine which extraction procedure extracted the most impurities and would be the most useful in crime laboratories.

1.6. References

[1] National Institute on Drug Abuse. NIDA InfoFacts: MDMA. 2008. Available at http://www.drugabuse.gov/infofacts/ecstasy.html. (Accessed 22 December 2008).

[2] Freudenmann R, Oxler F, Bernschneider-Reif S. The Origin of MDMA (Ecstasy) Revisited: The True Story Reconstructed from the Original Documents. Addiction 2006; 9: 1241-1245.

[3] E Merck, assignee. Verfahren zur Darstellung von Alkyloxyaryl-, Dialkyloxyaryl- und Alkylendioxyarylaminopropanen bzw. Deren am Stickstoff monoalkylierten Derivaten. German Patent 274350. 16 May 1914.

[4] Parrot AC. Human Psychopharmacology of Ecstasy (MDMA): A Review of 15 Years of Empirical Research. Hum Psychopharmacol Clin Exp 2001; 16: 557-577.

[5] Hardman HF, Haavik CO, Seevers MH. Relationship of the Structure of Mescaline and Seven Analogs to Toxicity and Behavior in Five Species of Laboratory Animals. Toxicol Appl Pharmacol 1973; 25: 299-309.

[6] Shulgin A, Shulgin A. PiHKAL: A Chemical Love Story. Transform Press, Berkeley, CA; 1991.

[7] National Institute on Drug Abuse. Research Report Series: MDMA (Ecstasy) Abuse. 2006. Available at http://www.drugabuse.gov/ResearchReports/MDMA/default.html. (Accessed 22 December 2008).

[8] Drug Enforcement Administration. Drug Scheduling. Available at http://www.usdoj.gov/dea/pubs/scheduling.html. (Accessed 5 January 2009).

[9] Drug Enforcement Administration. Irma Perez Story. Available at http://www.usdoj.gov/dea/pubs/states/newsrel/perez_story.html. (Accessed 05 January 2009).

[10] Cheng WC, Poon NL, Chan MF. Chemical Profiling of 3,4-Methylenedioxymethamphetamine (MDMA) Tablets Seized in Hong Kong. J Forensic Sci 2003; 48: 1249-1259.

[11] McKim WA. Drugs and Behavior: An Introduction to Behavioral Pharmacology. Prentice Hall, Upper Saddle River, NJ; 2003.

[12] Drug Enforcement Administration. MDMA (Ecstasy). 2006. Available at http://www.usdoj.gov/dea/concern/mdma.html. (Accessed 7 April 2008).

[13] Microgram Bulletin. Ecstasy Mimic Tablets (actually containing BZP, 1-(3-Trifluoromethyl)phenylpiperazine (TFMPP), Caffeine , and 1,4-Dibenzylpiperazine) in Olathe, Kansas. Vol 42, No 5, May 2009. Available at http://www.usdoj.gov/dea/programs/forensicsci/microgram/mg0509/mg0509.pdf (Accessed 2 Aug 2009).

[14] Johnston LD, O'Malley PM, Bachman JG, Schulenberg JE. "Various Stimulant Drugs Show Gradual Decline among Teens in 2008, Most Illicit Drugs Hold Steady." University of Michigan News Service: Ann Arbor, MI. Available at http://www.monitoringthefuture.org. (Accessed 5 January 2009).

[15] Smith FP ed., Siegel JA series ed. Handbook of Forensic Drug Analysis. Elsevier Academic Press, Burlington, MA; 2005.

[16] Parrott AC. Recreational Ecstasy/MDMA, the Serotonin Syndrome, and Sertonergic Neurotoxicity. Pharm Biochem Behav 2002; 71: 837-844.

[17] Palhol F, Boyer S, Naulet N, Chabrillat M. Impurity Profiling of Seized MDMA Tablets by Capillary Gas Chromatography. Anal Bioanal Chem 2002; 374: 274-281.

[18] Gimeno P, Besacier F, Bottex M, Dujourdy L, Chaudron-Thozet H. A Study of Impurities in Intermediates and 3,4-Methylenedioxymethamphetamine (MDMA) Samples Produced via Reductive Amination Routes. Forensic Sci Int 2005; 155: 141-157.

[19] Nie ZL, Wen J, Sun H. Phylogeny and Biogeography of Sassafras (Lauraceae) Disjunct Between Eastern Asia and Eastern North America. Plant Systematics and Evol 2007; 267: 191-203.

[20] Swist M, Wilamowski J, Parczewski A. Determination of Synthesis Method of Ecstasy based on the Basic Impurities. Forensic Sci Int 2005; 152: 175-184.

[21] Swist M, Wilamowski J, Zuba D, Kochana J, Parczewski. Determination of Synthesis Route of 1-(3,4-Methylenedioxyphenyl)-2-propanone (MDP2P) based on Impurity Profiles of MDMA. Forensic Sci Int 2005; 149: 181-192.

[22] Li JJ. Name Reactions: A Collection of Detailed Reaction Mechanisms. Springer Berlin Heielberg, New York; 2006.

[23] Weyermann C, Marquis R, Delaporte C, Esseiva P, Lock E, Aalberg L, Bozenko Jr. JS, Dieckmann S, Dujourdy L, Zrcek F. Drug Intelligence based on MDMA Tablets Data: I Organic Impurities Profiling. Forensic Sci Int 2007; 177: 11-16.

[24] Microgram Bulletin. Ecstasy Combination Tablets (containing MDMA and Methamphetamine) in Haltom City and Fort Worth Texas. Vol 42, No 4, April 2009. Available at http://www.usdoj.gov/dea/programs/forensicsci/microgram/mg0409/mg0409.pdf. (Accessed 2 Aug 2009).

[25] Teng SF, Wu SC, Tsay WI, Liu C. The Composition of MDMA Tablets Seized in Taiwan. Huaxue 2005; 63: 468-480.

[26] van Deursen MM, Lock ERA, Poortman-van der Meer AJ. Organic Impurity Profiling of 3,4-Methylenedioxymethamphetamine (MDMA) Tablets Seized in the Netherlands. Sci Justice 2006; 46: 135-152.

[27] Kuwayama K, Tsujikawa K, Miyaguchi H, Kanamori T, Iwata Y, Inoue H, Saitoh S, Kishi T. Identification of Impurities and the Statistical Classification of Methamphetamine using Headspace Solid Phase Microextraction and Gas Chromatography-Mass Spectrometry. Forensic Sci Int 2006; 160: 44-52.

[28] Koester CJ, Andresen BD, Grant PM. Optimum Methamphetamine Profiling with Sample Preparation by Solid-Phase Microextraction. J Forensic Sci 2002; 47: 1002-1007.

[29] Kongshaug KE, Pedersen-Bjergaard S, Rasmussen KE, Krogh M. Solid-Phase Microextraction/Capillary Gas Chromatography for the Profiling of Confiscated Ecstacy and Amphetamine. Chromatographia 1999; 50: 247-252.

[30] Bonadio F, Margot F, Delemont O, Esseiva P. Optimization of HS-SPME/GC-MS Analysis and Its Use in the Profiling of Illicit Ecstasy Tablets (Part 1). Forensic Sci Int 2009; 187: 73-80.

[31] Bonadio F, Margot P, Delemont O, Esseiva P. Headspace solid-phase Microextraction (HS-SPME) and liquid-liquid extraction (LLE): Comparison of the Performance in Classification of Ecstasy Tablets (Part 2). Forensic Sci Int 2008; 182: 52-56.

[32] Hoang TH, Sharma R, Susanto D, Di Maso M, Dwong E. Microwave-Assisted Extraction of Active Pharmaceutical Ingredient from Solid Dosage Forms. J Chromatogr 2007; 1156: 149-153.

[33] Bieri S, Ilias Y, Bicchi C, Veuthey J, Christen P. Focused Microwave-Assisted Extraction Combined with Solid-Phase Microextraction and Gas Chromatography-Mass Spectrometry for the Selective Analysis of Cocaine from Coca Leaves. J Chromatogr 2006; 1112: 129-132.

[34] Carro AM, Lorenzo RA, Fernandez F, Phan-Tan-Luu R, Cela R. Microwave-Assisted Extraction Followed by Headspace Solid-Phase Microextraction and Gas Chromatography with Mass Spectrometry Detection (MAE-HSSPME-GC-MS/MS) for Determination of Polybrominated Compounds in Aquaculture Samples. Anal Bioanal Chem 2007; 388: 1021-1029.

Chapter 2 Theory

2.1. Microwave-Assisted Extraction

Microwave-assisted extraction (MAE) utilizes microwave energy to extract a sample from a matrix into solution. The solution is heated under pressure which allows for the solvent to be heated above its atmospheric pressure boiling point resulting in efficient extractions [1].

The heating of the sample takes place through two mechanisms which occur at the same time: diopolar rotation and ionic conduction [2,3]. The dipolar rotation phenomenon is due to solvent's molecular dipoles aligning with the electrical field. As the electric field oscillates, the dipoles are forced into motion to stay in alignment, thus creating friction and heating the solvent. Ionic conduction is caused by the electrophoretic movement of the ions as a result of the applied electric field. Ions with a small charge will generally move more slowly than ions with a higher charge. Also, as the mass of the ion increases, the movement of the ion decreases. As the solvent resists this movement, the friction created heats the solvent [2,3]. Due to these heating mechanisms, the solvent is theoretically heated more uniformly than with conventional heating methods such as a hot plate.

Several considerations must be taken into account when choosing a solvent for MAE. The first is the polarity of the solvent. As mentioned earlier, the dipole of the solvent molecules aligns with the electric field. A more polar molecule with a larger dipole is more vigorously realigned with the electric field creating more heat than a non-polar molecule with a smaller dipole. Therefore, polar solvents such as alcohols and water will absorb more microwave energy than non-polar solvents such as hexane [1].

The dielectric loss coefficient (ε'') indicates the ability of a material to absorb microwave energy and convert it to heat. Molecules with a larger dielectric loss coefficient are able to absorb the microwave energy more effectively therefore achieving more optimal heating than molecules with a lower dielectric loss coefficient. The dielectric constant (ε') is the ability of the material to be polarized by the electric field [1]. The ratio of the dielectric loss coefficient and the dielectric constant, known as the loss tangent or tangent delta (tan δ), describes the material's ability to convert electromagnetic energy to heat [1]. With a dipole moment of 1.87, a dielectric constant of 78.3, and a tan δ of 1570×10^{-4}, water is a good solvent for microwave chemistry because it adequately absorbs the microwave energy and converts it to heat. In contrast, non-polar solvents which are not heated efficiently by microwave energy have lower dipole moments and dielectric constants. For example, hexane has a dipole moment of less than 0.1 and a dielectric constant of 1.88 [1].

Commercially available microwave lab stations are generally used to perform microwave chemistry due to the dangers involved with the higher pressures, sometimes as much as 65 bar, that can be achieved. After the sample and solvent have been placed in the microwave vessels, the vessel is assembled and placed on a rotor inside the unit to allow rotation of the vessels during the extraction. This overcomes the limitation of a non-uniform electrical field by altering the location of the microwave vessels throughout the extraction. The temperature is monitored during the extraction and microwave energy can be supplied at varying levels to ensure that the system remains at the desired temperature. After the extraction, the samples are cooled and then analyzed directly or subsequently extracted by additional procedures.

2.2. Headspace Solid-Phase Microextraction

Headspace solid-phase microextraction (HS-SPME) is an analytical extraction technique that utilizes a polymer coated fiber to extract analytes from the sample headspace. A solid sample or aqueous sample is placed in a vial with a septum cap. The fiber is placed in the headspace above the sample for a specified extraction time at a specified extraction temperature. When sampling above an aqueous solution, the analytes move from the solution into the headspace. Then, from the headspace, the analytes absorb onto the fiber. Figure 2.1 shows a schematic of HS-SPME.

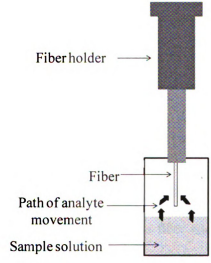

Figure 2.1: Schematic of HS-SPME with the arrows representing the movement of the analytes

At the end of the extraction, the fiber is retracted, removed from the sample, and typically placed in the heated inlet of a gas chromatograph for analysis. In the GC inlet, the analytes are thermally desorbed from the fiber and carried onto the column in the flow of the mobile phase for subsequent separation [4].

Headspace solid-phase microextraction is an equilibrium based technique. During the process, analytes form an equilibrium among three phases: the fiber coating and the

aqueous phase, the headspace and the aqueous phase, and the fiber coating and the headspace. The concentration of analytes in the different phases at equilibrium is given by Equation 2.1 [5]

$$C_o V_s = C_h V_h + C_s V_s + C_f V_f \tag{2.1}$$

where, C_o is the initial concentration of the analyte in the aqueous sample, variables C and V are the concentrations and volumes, respectively, of the analyte in the different phases that are represented by the following subscripts: h corresponds to the headspace, s corresponds to the sample matrix, and f corresponds to the fiber.

The equilibrium formed by the analyte is based on the partition coefficients of the analyte between the phases. The partition coefficient between the phases is the ratio of the concentration of the analyte in each of those phases. The partition coefficient K_{fh} for an analyte between the fiber and the headspace is given by Equation 2.2

$$K_{fh} = \frac{C_f}{C_h} \tag{2.2}$$

where, C_f is the concentration of the analyte on the fiber and C_h is the concentration of the analyte in the headspace. Similarly, the partition coefficient K_{hs} of the analyte between the headspace and the sample matrix is given by Equation 2.3

$$K_{hs} = \frac{C_h}{C_s} \tag{2.3}$$

and the partition coefficient K_{fs} of the analyte between the sample matrix and the fiber is given by Equation 2.4

$$K_{fs} = \frac{C_f}{C_s} \tag{2.4}$$

Based on the partition coefficients, the mass of analyte that is absorbed on the fiber (n_f) is summarized by Equation 2.5 [4].

$$n_f = \frac{K_{fs} V_f V_s C_o}{K_{fs} V_f + K_{hs} V_h + V_s} \tag{2.5}$$

In the denominator, the terms $K_{fs}V_f$ and $K_{hs}V_h$ describe the analyte on the fiber and in the headspace. Based on Equation 2.5, several alterations can be made to the system to increase the mass of the analyte that is absorbed by the fiber [4]. One way is to increase the concentration C_o of the analyte in the sample. If more of the analyte is present, more is available to be extracted by the fiber.

Another way to increase the mass of an analyte extracted is to change the partition coefficient between the fiber and the sample, K_{fs}. This can be accomplished by changing the extraction temperature. For analytes with a high affinity for the fiber, when the extraction temperature is increased, the partition coefficient of analyte between the headspace and the solvent is increased. Therefore, a higher mass of the analyte is extracted by the fiber. [4,5]. On the other hand, if an analyte has a lower affinity for the fiber, a small mass of the analyte will absorb onto the fiber. When the temperature is increased, the molecule is more likely to desorb from the fiber causing a lower mass of the analyte to be extracted by the fiber.

The partition coefficient between the headspace and the solvent (K_{hs}) can be affected by pH. At lower pH values, molecules are protonated and, as the pH increases, the molecules become deprotonated. The deprotonated molecules are more volatile (have

lower boiling points) and have a higher affinity for the headspace than the protonated form. Therefore, a larger mass of the deprotonated analyte is extracted [5].

Agitating the solution can also affect the mass of analyte that absorbs onto the fiber. As the analytes in the sample move from the solution into the headspace, stirring the sample helps to ensure that additional analytes in solution are able to transfer into the headspace. Therefore, the time required for equilibrium to be obtained between the solution and the headspace is decreased. This is especially useful for analytes with lower volatilities where only a small concentration of the analyte is in the headspace at equilibrium. Once the analytes are in the headspace they transfer to the fiber quickly because gasses have higher diffusion coefficients. [4].

The characteristics of the fiber can also be altered to affect the extraction of the analyte. The volume of the fiber, V_f, can be increased by lengthening the fiber or increasing the thickness of the fiber's coating. However, a larger fiber volume results in a longer equilibration time because more time is required for the analyte to adsorb into the fiber pores which are not as accessible in a thicker fiber [5]. When a thicker fiber coating is used, the molecules take longer to desorb from the fiber, lengthening the analysis time.

The type of fiber coating can affect the mass of the analyte extracted by changing the partition coefficient between the fiber and the sample, K_{fs} [4,5]. Different coatings have different chemical properties to extract different classes of analytes. Several types of fibers are commercially available. Polydimethylsiloxane (PDMS) is a common base used for the fibers. This coating is a non-polar coating that is used for extracting non-polar compounds and semi-polar compounds such as aromatics and esters. A

divinylbenzene (DVB) coating is often used in conjunction with PDMS coatings to broaden the range of analyte polarities that are extracted. The DVB coating is used to extract moderately polar compounds such as amines. Analytes adsorb, or are retained, in the pores of the DVB coating. This increases the sensitivity of the fiber to analytes present at trace levels. However, one drawback to the DVB coating is that it is fragile and can be stripped off the fiber easily. A Carboxen™ (CAR) coating is also used with a PDMS coating. Carboxen™ is made up of pores of various sizes and therefore allows for the adsorption and extraction of highly volatile compounds [4]. A combination fiber of the various coatings mentioned (PDMS, CAR, and DVB) is available and expands the range of analytes that can be extracted in a single extraction.

Because HS-SPME is a non-exhaustive extraction technique, the sample is not used in its entirety allowing for re-testing if necessary. In addition, because of the ability to pre-concentrate the analytes on the fiber, HS-SPME provides good sensitivity for the extraction of compounds present in the sample at trace levels, for example trace level impurities in MDMA tablets.

2.3. Gas Chromatography-Mass Spectrometry

Gas chromatography-mass spectrometry (GC-MS) is a common analytical technique used to separate a mixture into its components and to detect those components. Gas chromatography is a separation technique that is based on the interaction between the mixture's components and the mobile and stationary phases. After separation by the GC, the components enter the detector which, in the case of GC-MS, is a mass spectrometer. In the mass spectrometer, the analytes are ionized and fragmented, and the ions are separated according to the mass to charge (m/z) ratios.

2.3.1. Gas Chromatography

A schematic of a gas chromatograph (GC) is shown in Figure 2.2 with the major components labeled.

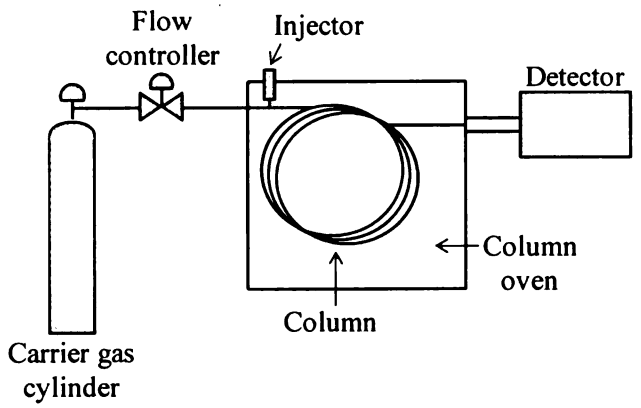

Figure 2.2: Schematic of a gas chromatograph

An inert carrier gas, or mobile phase, is required for GC analysis to move the sample through the system. Helium, hydrogen, and nitrogen are all common carrier gasses [6]. The flow rate and pressure of the carrier gas are regulated using gauges and controllers. For many GC-MS applications, flow rates are typically 1 mL/min.

The sample is introduced to the GC through the inlet. In order for a sample to be analyzed by GC, it must be volatile and thermally stable. The inlet is kept at high temperatures, generally at least 50 °C above the boiling point of the analytes to ensure that the sample volatilizes [6]. When an injection is performed, it is important that it be completed quickly to allow the sample to move onto the column in a tight band. If a sample volume is too large or the injection is made slowly, the sample spreads resulting in band broadening which causes peaks to become broader, affecting peak shape and resolution in the final chromatogram.

Sample injections can occur in the form of a liquid sample using a standard GC syringe (e.g. sample dissolved in solvent), a gas sample using a gas-tight syringe (e.g. from direct headspace sampling), or desorbed from a SPME fiber. Common inlets for liquid and gas injections contain a septum and a glass liner. The septum seals the inlet to prevent air from entering the instrument. The glass liner provides an inert surface in which to inject and volatilize the sample without retaining the sample. For SPME fiber analysis, a Merlin Microseal™ is used in place of the septum and a narrower glass inlet liner is used. The Merlin plays a similar role to the septum. The glass liner is narrower to focus analytes onto the column that desorb slowly from the fiber.

Once vaporized in the inlet, the sample is carried onto the column which is housed in an oven. In the column, the sample components interact with the stationary phase which slows the sample so that it does not travel through the column as quickly. Different components of the sample interact with the column stationary phase to different extents. Some components will have strong interactions with the column and will be slowed more than components that spend little time interacting with the stationary phase. This causes the separation of the sample into its individual components.

Several different stationary phases are available for columns. Polydimethyl siloxanes are a common group of stationary phases with the general form shown in Figure 2.3. In the polydimethyl siloxane coating, the R-groups are all methyl ($-CH_3$) groups making the stationary phase non-polar. For other stationary phases, the R-groups can be changed to a different group, such as a phenyl ($-C_6H_5$) group, to make the stationary phase more polar [6].

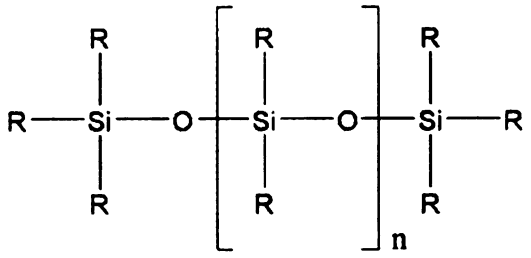

Figure 2.3: Polydimethyl siloxane phase in GC columns

The column is contained within an oven which heats the column at a specific rate as determined by the user. Temperature programming can increase the speed of analysis by increasing the temperature of the oven. When the analysis time is shorter, the sample spends less time on the column, and therefore band broadening is decreased. Often, the oven temperature will start low (e.g. 40-60 °C). After a given amount of time, the oven will start to heat the column at a given rate, for example 10 °C/minute, until reaching the desired final temperature (e.g. 280 °C). The different temperatures allow for the separation of the components based on their boiling points. Components with lower boiling points interact less with the column at low temperatures and elute from the column first. Components with higher boiling points interact more with the column and do not reach the detector until the higher oven temperatures are reached [6].

The separated sample components are then carried into the detector. The result of the GC analysis is a chromatogram that plots the abundance of molecules detected against the time at which they were detected, or the retention time. Each set of analytes (in sufficient concentration) that go through the detector appears in the output chromatogram as a peak. The retention time of the analyte will change when the temperature program or type of column are changed because the analyte will interact differently with the column.

2.3.2. Mass Spectrometry

A schematic of the sections of the mass spectrometer (MS) are shown in Figure 2.4. As shown in the figure, the system is under vacuum which typically operates at pressures of 30-40 mTorr. This greatly lengthens the mean free path of the sample molecules. In other words, the length of time between analyte collisions is much longer leading to fewer collisions between ions. When the ions collide, they are neutralized and therefore are not detected. Also, the vacuum reduces the possibility of contamination from the environment and protects surfaces from water vapor that would otherwise cause corrosion [6].

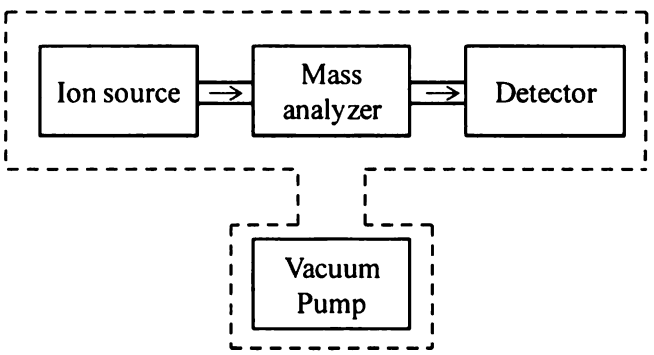

Figure 2.4: Schematic of a mass spectrometer

The GC column feeds into the MS through the transfer line. The transfer line is kept at high temperatures (e.g. 300 °C) to ensure that the separated components are not lost through condensation. The end of the column is located at the ion source to allow for the ionization of the sample.

One of the most common forms of ionization is electron ionization. This ionization source contains a heated filament that releases electrons at a particular energy, often 70 eV. The sample is introduced into the path of the electrons where ionization occurs. Typical bond energies in a molecule can range from 10 to 20 eV. Therefore, the

70 eV electrons supply ample energy to the molecule to ionize and fragment the molecule. Positive ions are formed during ionization due to the loss of an electron. Compared to the formation of positive ions, the formation of negative ions is inefficient and therefore few negative ions are produced. Ions of multiple charges can be formed during the ionization process; however, during electron ionization, singly charged ions are the most common. The fragments are useful in determining the structure of the sample molecule because the fragmentation pattern of a molecule is consistent under the same conditions [7].

A series of negatively charged focusing lenses attract the positive ions and focus them into a thin beam for transfer into the mass analyzer. Ion trap mass analyzers contain two end caps, which have openings to allow for the entry and exit of the ions and a ring electrode for RF voltage oscillation. Figure 2.5 shows a cross-section of an ion trap mass analyzer.

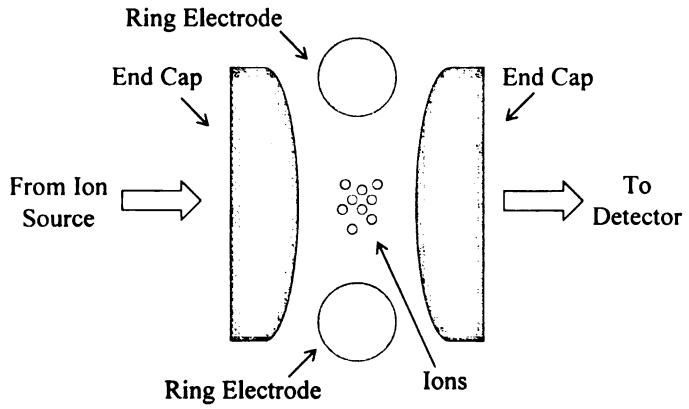

Figure 2.5: Schematic of an ion trap mass analyzer

The ions of different masses are held in the middle of the trap and move around in a figure-eight trajectory because of the voltage applied to the trap [7]. Inside the trap, helium is present to reduce the energy of the ions through collisions. This ensures that

the ions stay in a tight group in the center of the trap. At a particular RF voltage applied to the ring electrode, ions of a certain mass will become destabilized and leave the trap through an aperture in the exit end cap. As the voltage is cycled, all masses within a given range (for example 50-650 atomic mass units, amu) will be detected once in the cycle (if the mass is present) [7].

As the ions leave the mass analyzer they can be detected by a continuous dynode electron multiplier (EM) which converts the ions into a signal of electrons. The EM has a curved conical appearance and can have a voltage of -10 kV at the opening which changes to +10 kV at the end of the detector when operating in positive ion mode [6]. As the ions hit the surface of the EM, electrons are ejected. This starts a cascade of electrons. The ejected electrons are attracted to another region of the EM with a more positive voltage. The electrons strike the next section causing more electrons to be ejected. At the end of the multiplier, the electrons ejected constitute the current that is sent to the amplifier system and then to the data system.

The process of ionization, mass analysis, and detection can occur several times a second and is performed throughout the GC analysis. Therefore, every completely separated component of the sample will be detected by this process independently of the other components in the order they elute from the column.

The output of the mass spectrometer is a mass spectrum which contains the mass to charge ratios of the ions and the abundance at which they were detected. In a GC-MS analysis, every time point in the GC chromatogram has a corresponding mass spectrum. This allows for the definitive identification of compounds. The retention time of the

analyte from the GC and the fragmentation pattern from the MS is unique to that particular molecule.

2.4. Experimental Design

Experimental designs are used in research for many different applications. These statistical designs allow the experimenter to learn more about a system or procedure in fewer experiments than with a one-at-a-time experimental set-up, thus saving time and money. Experimental designs can be used to identify experimental parameters that affect the outcome, optimize important parameters in a process, or improve the robustness of a procedure [8,9]. Often, a screening design will be used to determine parameters that have a significant effect on the outcome followed by an optimization design to determine the optimum settings of the significant parameters.

In the process of setting up an experimental design, the parameters, or effects, to be studied are selected and the levels of the parameters are set. Levels are the number of values at which the parameter will be studied. For example, in a two-level design, high and low values of a parameter are studied. Also, the responses, or outcomes, are chosen based on what system is being studied.

Next the set of experiments are planned. Often the set of experiments to be performed are randomized to reduce experimental bias. If the set of experiments are to be completed on different days or are to utilize different batches of materials, the design can be divided into smaller sections called blocks. Dividing the experiments into blocks takes the differences between days or batches of material into account in the data analysis, often giving a more accurate view of the effects on the response. Some designs

employ a randomized block design in which each level of each parameter occurs once and only once in each block [10].

The confounding of the effects of parameters and interactions between parameters must been taken into account. If the parameters or interactions are confounded, it means that the data analysis cannot separate the effects of the confounded parameters or interactions, and they appear as one effect on the response [11]. The resolution of the design is related to the confounding. In a resolution III design, the effects of the main parameters are not confounded with other main parameters. However, one or more of the interactions may be confounded with a main parameter or with a two-factor interaction. In a resolution IV design, main parameters are not confounded with other main parameters or two-factor interactions. However, two-factor interactions may be confounded with one another. In a resolution V design, there is no confounding among the main parameters or the two factor-interactions.

2.4.1. Screening Design

Screening designs are employed by experimenters to examine parameters to determine which have a significant effect on the outcome. There are several types of screening designs including full factorial, fractional factorial, and Plackett-Burman designs [8]. Full factorial designs allow for the determination of the effects of the parameters and the interactions between the parameters on the experimental response.

2.4.1.1. Full Factorial Design

For full factorial designs, the number of experiments to be performed is based on Equation 2.6

$$E=K^N \tag{2.6}$$

where, E is the number of experiments, K is the number of levels, and N is the number of parameters. For a two-level design with four factors, 16 experiments must be performed. Fractional factorial designs, in which only a subset of the experiments in the full factorial design is performed, can be used when many parameters are being studied. However, not as much information about each parameter and interaction is learned from the fractional factorial design when compared to the information gained from a full factorial design.

In full factorial designs every combination of parameters at the various levels are studied. For example, for a two-level, three-parameter study, Table 2.1 lists an example set up of experiments. In the table, +1 indicates the high level and -1 indicates the low level. The levels are then translated into experimental values. For example, parameter A may be extraction temperature with a high value of 120 °C and a low value of 80 °C, parameter B may be extraction time with a high value of 20 minutes and a low value of 10 minutes, and parameter C is the concentration of the sample in solution with a high value of 2 M and a low value of 1 M. So, for experiment 1, an extraction temperature of 120 °C, an extraction time of 20 minutes, and a 2 M solution are used to complete the experiment.

Table 2.1: Example set up of full factorial design with three parameters

Experiment	Parameter A	Parameter B	Parameter C
1	+1	+1	+1
2	+1	+1	-1
3	+1	-1	+1
4	-1	+1	+1
5	+1	-1	-1
6	-1	+1	-1
7	-1	-1	+1
8	-1	-1	-1

2.4.1.2. Analysis of Full Factorial Design

After the design has been set up and the experiments have been completed, the experimental responses are used to build mathematical models using linear regression techniques. The model allows for the estimation of values for other settings of parameters not tested and is used to identify which parameters have a significant effect on the response [8].

Often, multivariate analysis of variance (MANOVA) is used to determine which parameters have a significant effect on the response when more than two variables are studied. The MANOVA calculations are a statistical technique that is used to separate variation due to random error (or uncontrolled factors) from variation due to changing a controlled factor. The calculations then determine if the change in the outcome due to the change in the control factor is significant.

The MANOVA calculations begin with the calculation of the sum of squares (SS) for each response for the parameters, the interactions between the parameters, the error (or residuals), and the total for the design based on the equations given in Table 2.2 [12]. Only two parameters are shown in the table; however, the calculations are the same if more parameters and interactions are involved in the design.

Table 2.2: Calculations for the sum of squares

Source of Variation	Sum of Squares
Parameter A	$SS_A = \left(\frac{\sum y_{A1}^2}{n} + \frac{\sum y_{A2}^2}{n}\right) - \frac{(\sum y)^2}{N}$
Parameter B	$SS_B = \left(\frac{\sum y_{B1}^2}{n} + \frac{\sum y_{B2}^2}{n}\right) - \frac{(\sum y)^2}{N}$
Interaction AB	$SS_{AB} = \left(\frac{\sum y_{A1B1}^2}{n_{A1B1}} + \frac{\sum y_{A2B1}^2}{n_{A2B1}} + \frac{\sum y_{A1B2}^2}{n_{A1B2}} + \frac{\sum y_{A2B2}^2}{n_{A2B2}}\right) - \frac{(\sum y)^2}{N} - SS_A - SS_B$
Error	$SS_{Error} = SS_{Total} - (SS_A + SS_B + SS_{AB})$
Total	$SS_{Total} = \left(\sum y^2\right) - \frac{(\sum y)^2}{N}$

In the table, variable y corresponds to the observed responses of the design. For the parameters, the subscripts A1 and A2, for example, correspond to the low level and high level of the parameter studied. Therefore y_{A1} corresponds to the responses from the design when parameter A was at its low level. The variable n corresponds to the number of experiments at the particular level and the variable N corresponds to the total number of experiments performed. Similar designations are used for parameter B. For the interactions, y is again the observed response. The subscript A1B1, for example, corresponds to the response when both A and B were at the low levels.

Next, the degrees of freedom, *df*, are calculated according to the equations given in Table 2.3. Degrees of freedom are the number of variables that are available to fit the

model. In the equations, the variable, T, is the number of levels of each parameter with the subscript corresponding to the parameter.

Table 2.3: Calculations for the degrees of freedom

Source of Variation	Degrees of freedom
Parameter A	$df_A = T_A - 1$
Parameter B	$df_B = T_B - 1$
Interaction AB	$df_{AB} = (T_A - 1)(T_B - 1)$
Error	$df_{Error} = df_{Total} - (df_A + df_B + df_{AB})$
Total	$df_{Total} = Number\ of\ Experiments - 1$

The mean squares (*MS*) and F-values are then calculated for each parameter, interaction, and error (or residuals) based on the equations given in Table 2.4.

Table 2.4: Calculations for the mean squares and F-values

Source of Variation	Mean Square	F-value
Parameter A	$MS_A = \frac{SS_A}{df_A}$	$F_A = \frac{MS_A}{MS_{Error}}$
Parameter B	$MS_B = \frac{SS_B}{df_B}$	$F_B = \frac{MS_B}{MS_{Error}}$
Interaction AB	$MS_{AB} = \frac{SS_{AB}}{df_{AB}}$	$F_{AB} = \frac{MS_{AB}}{MS_{Error}}$
Error	$MS_{Error} = \frac{SS_{Error}}{df_{Error}}$	

The significance of the parameter's or interaction's effect can be determined by comparing the calculated F-value to a critical F-value from a statistical table for the required confidence level. If the calculated F value is smaller than the critical F value,

then the effect is not significant at that confidence level. If the calculated F value is larger than the critical F value, the effect is significant at that confidence level [12].

2.4.2. Optimization Design

After determining the significant parameters in a procedure, the optimal setting of the parameters can be determined using an optimization design. A circumscribed central composite (CCC) design allows for the determination of second order interactions (squared terms) in addition to the interactions between parameters.

2.4.2.1. Circumscribed Central Composite Design

A CCC design contains a factorial design in conjunction with a star design and center points [9]. The factorial design is the same as discussed earlier. The star design involves setting experimental points at $\pm \alpha$ according to Equation 2.7

$$\alpha = [2^N]^{1/4} \tag{2.7}$$

where, N is the number of parameters. For two parameters, $\alpha = [2^2]^{1/4} = 1.41$. For three parameters, α equals 1.68. These experiments allow for the determination of the squared terms in the model. The center points involve experimental parameters in the middle of the design and the center point is often replicated to determine the error in the system [11].

Figure 2.6 shows a schematic of the correlation between the types of experimental points (factorial, star, and center) for a CCC design with two parameters being tested. In the figure, the small circles represent the factorial points, the stars represent the star points, and the diamond represents the center point. At each point, the first number in the ordered pair corresponds to the setting of one parameter while the second number in the ordered pair corresponds to the setting of the second parameter. The schematic is drawn

for a design with two parameters, but the same principal applies when three parameters are being studied.

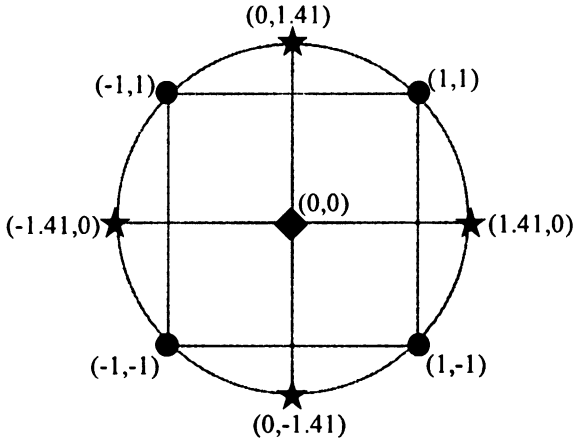

Figure 2.6: Schematic of set up of experiments for CCC design

These theoretical values (± 1, $\pm \alpha$, and 0) are then converted to experimental values to perform the set of experiments. For example, if extraction temperature with high and low levels of 120 °C and 80 °C, respectively, is considered, the factorial points can be converted to 80 °C (-1) and 120 °C (+1). The star points are converted to 72 °C (-1.41) and 128 °C (+1.41) and the center point is converted to 100 °C (0). Table 2.4 shows an example set of experiments for a CCC design. Only one center point is shown in this set up, however, the center point is usually replicated at least five times [9].

Table 2.5: Example set up of CCC design with two parameters

Experiment	Parameter A	Parameter B	Type of Point
1	+1	+1	Factorial
2	+1	-1	Factorial
3	-1	+1	Factorial
4	-1	-1	Factorial
5	+1.41	0	Star
6	0	+1.41	Star
7	-1.41	0	Star
8	0	-1.41	Star
9	0	0	Center

2.4.2.2. Analysis of Circumscribed Central Composite Design

After the experiments are completed, the responses are determined and a mathematical model is built for each response using linear regression analysis. Next, each response is optimized individually based on whether the response is to be maximized or minimized. The experimental data and model are used to determine the optimum settings for the parameters that result in the maximum (or minimum) for each response [13].

A desirability function combines the separate responses into a single function [14]. This function is then used to optimize the parameters based on all responses, not just each individually. Equation 2.8 is used to optimize the desirability of responses that are to be maximized [13,14].

$$d_{max} = \begin{cases} 0 & y < low \\ \left(\frac{y - low}{high - low}\right)^{s}, & low \leq y \leq high \\ 1 & y > high \end{cases} \tag{2.8}$$

As the response is maximized, the desirability, *d*, approaches one. The variable, *y*, is the predicted response from the model. The variable, *high*, is the value of *y* above which the desirability is at its maximum or one. The variable, *low*, is the lowest acceptable value of *y*, and any value lower would yield an unacceptable desirability of zero [13,14].

The variable, *s*, is the shape of the desirability function. When *s* is set at one, the desirability function is linear. If *s* is less than one, the desirability is almost equally acceptable over the range. If *s* is greater than one, only the values closest to the maximum (or minimum) are acceptable, thus limiting the range of acceptable values

[13,14]. Figure 2.7 shows the shape of the desirability function when different values of *s* are used.

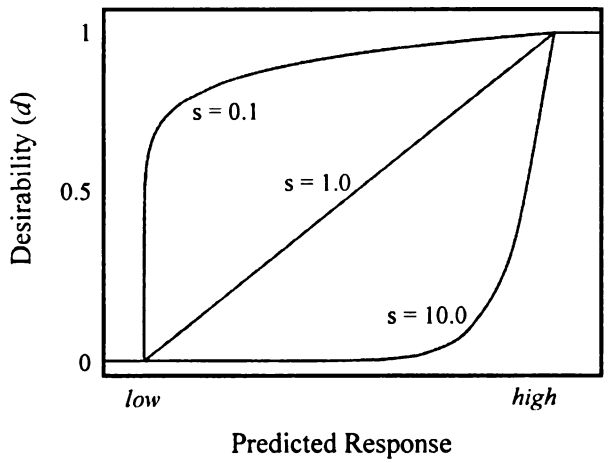

Figure 2.7: Graph of desirability function for maximization at different values of *s* (adapted from references 13 and 14)

Equation 2.9 is used to optimize the desirability of responses that are to be minimized [13,14].

$$d_{min} = \begin{cases} 1 & y < low \\ \left(\frac{y - high}{low - high}\right)^s, & low \leq y \leq high \\ 0 & y > high \end{cases} \tag{2.9}$$

Overall, as the response is minimized, the desirability *d* approaches one. This equation is the opposite of the equation for d_{max}. The variable *y* is the predicted response based on the model. The variable *low* is the value of *y* below which the desirability is at its maximum or one. The variable *high* is the highest acceptable value for *y*, and any value above it would result in an unacceptable desirability of zero.

To determine the overall desirability *D* of the system, the set of parameters that yields the highest value for *D* according to Equation 2.10 is determined [13,14]

$$D = (d_1^{l1} \times d_2^{l2} \times \ldots \times d_j^{lj})^{\frac{1}{(\Sigma l)}} \tag{2.10}$$

where, d_I, etc. is the desirability of the individual responses and I is the impact of each response. The impact of each response is set on a scale of one to five according the user's determination of the importance of the response. Five indicates high importance and one indicates low importance [13,14]. The resulting optimum set of parameters theoretically gives the optimum results based on the range of parameters studied in the design.

2.5. Retention Time Alignment

Chromatograms of replicates of the same sample can be retention time aligned to overcome instrumental drift between analyses. The Line Up software (Infometrix, Bothell, WA) utilizes a correlation optimized warping algorithm to align the chromatograms. For this algorithm, a target chromatogram is chosen, and the chromatograms to be aligned are compared to the target one at a time. The alignment starts at the end of the chromatogram and then moves towards the beginning. The algorithm divides the chromatogram into sections. The user defined "slack" parameter sets the number of data points to be included in each of the sections. The user defined "warp" parameter specifies how many data points the section can be stretched or compressed when matching the chromatogram to the target. The closeness of the match is determined by calculating the Pearson product moment correlation (PPMC) coefficient (discussed in section 2.6.) between the target and the aligned chromatogram for each section. When the highest PPMC coefficient is determined for the section, the algorithm moves to the next section of the chromatogram, again maximizing the PPMC coefficient. This process continues through the length of the chromatogram, resulting in the aligned chromatograms. The process is repeated for all other chromatograms in the sample set.

2.6. Pearson Product Moment Correlation Coefficients

Pearson product moment correlation (PPMC) coefficients are used to determine the similarity between two variables according to Equation 2.11.

$$r = \frac{\sum\{(x - \bar{x})(y - \bar{y})\}}{\sqrt{[\sum(x - \bar{x})^2][\sum(y - \bar{y})^2]}} \tag{2.11}$$

For chromatographic applications, the x variables correspond to one chromatogram and the y variable corresponds to the second chromatogram. The variable r can have a value between +1 and -1. Correlation values greater than zero indicate a positive correlation, with values from 0.8-1 indicating strong positive correlation. Values less than zero indicate a negative correlation, while a correlation value of zero indicates no correlation [15].

2.7. References

[1] Kingston HM ed, Haswell SJ ed. Microwave-Enhanced Chemistry: Fundamentals, Sample Preparation and Applications. American Chemical Society, Washington, D.C.; 1997.

[2] Kaufmann B, Christen P. Recent Extraction Techniques for Natural Products: Microwave-Assisted Extraction and Pressurised Solvent Extraction. Phytochemical Analysis 2002; 13: 105-113.

[3] Eskilsson CS, Bjorklund E. Analytical-Scale Microwave-Assisted Extraction. J Chromatog A 2000; 902: 227-250.

[4] Wercinski SA ed. Solid Phase Microextraction: A Practical Guide. Marcel Dekker, Inc., New York; 1999.

[5] Pawliszyn J. Solid Phase Microextraction: Theory and Practice. Wiley-VCH, New York; 1997.

[6] Skoog DA, Holler FJ, Nieman TA. Principles of Instrumental Analysis. Thomson Learning, Inc., United States; 1998.

[7] De Hoffmann E, Stroobant V. Mass Spectrometry: Principles and Applications. John Wiley and Sons, Inc., England; 2007.

[8] Araujo PW, Brereton RG. Experimental Design I. Screening. Trends Anal Chem 1996; 15: 26-31.

[9] Araujo PW, Brereton RG. Experimental Design II. Optimization. Trends Anal Chem 1996; 15: 63-70.

[10] Peterson RG. Design and Analysis of Experiments. Marcel Dekker, New York City; 1985.

[11] Antony J. Design of Experiments for Engineers and Scientists. Butterworth-Heinemann, Amerdam; 2003.

[12] Frigon NL, Mathews D. Practical Guide to Experimental Design. John Wiley and Sons, Inc., New York; 1997.

[13] Statgraphics. Design of Experiments – Multiple Response Optimization. StatPoint, Inc., Herndon, VA; 2005.

[14] Derringer G, Suich R. Simultaneous Optimization of Several Response Variables. J Qual Tech 1980; 12: 214-219.

[15] Devore JL. Probability and Statistics for Engineering and the Sciences, 4th Ed. Duxbury Press, Belmont, CA; 1995.

Chapter 3 Materials and Methods

3.1. Sample Preparation

3.1.1. Simulated Sample

A simulated 3,4-methylenedioxymethamphetamine (MDMA) sample of known components was prepared for use in the microwave optimization studies. Benzylamine hydrochloride (0.5-2% of sample), 2-phenethylamine hydrochloride (0.5-2% of sample) methamphetamine hydrochloride (0.5-2% of sample), MDMA (0.1% of sample), and ephedrine (0.5-2% of sample) were purchased from Sigma-Aldrich (St. Louis, MO) and used as received. Caffeine (92-98% of sample; Eastman, Rochester, NY) was included as an adulterant. All components were homogenized with a mortar and pestle. Due to cost, MDMA (0.1% of sample) was only used in the simulated tablet for the selection of the buffer for microwave-assisted extraction (MAE).

3.1.2. MDMA Exhibits

Three exhibits of MDMA tablets were received from the Michigan State Police Forensic Science Division. An exhibit is a set of tablets with similar physical properties that is obtained by the police at one time from one location. For each exhibit, the physical characteristics of the tablets were recorded, and several tablets from each exhibit were homogenized with a mortar and pestle for use. Photographs of representative tablets from each exhibit are shown in Figure 3.1.

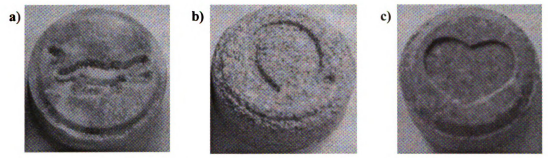

Figure 3.1: Representative tablets from each exhibit: a) exhibit MSU900-01 (pink, purple, and green); b) exhibit T-17 (blue); c) exhibit T-27 (pink)

3.2. Optimization of Microwave-Assisted Extraction Procedure

3.2.1. Optimization of Extraction Buffer

An Ethos EX Microwave Lab Station (Milestone Inc.; Shelton, CT) was used for all microwave-assisted extractions. When the MDMA sample is introduced to the buffer, the sample has the potential to alter the pH of the solution. Buffers were used as the extraction solvent instead of water alone due to the ability of the buffer to maintain the pH of the solution. Based on a review of the literature, three different buffers at three different pH values and concentrations were investigated [1-5].

Preliminary studies were performed with a 0.05 M carbonate buffer, pH 10, which was prepared using sodium bicarbonate (Sigma) and 2 M sodium hydroxide (Spectrum, New Brunswick, NJ). Phosphate buffers at concentrations of 1 M, 0.5 M, and 0.1 M were prepared using potassium phosphate-monobasic, KH_2PO_4 (Mallinckrodt, Paris, KY) and sodium phosphate-dibasic, $Na_2HPO_4 \cdot 7H_2O$ (Jade Scientific, Canton, MI). For each concentration, buffers at three different pH values (6, 7, and 8) were prepared using 2 M sodium hydroxide (Spectrum) to adjust the pH. Tris buffers at concentrations of 1 M, 0.5 M, and 0.1 M were prepared using tris(hydroxymethylaminomethane) (Mallinckrodt).

For each concentration, buffers at three different pH values (7, 8, and 9) were prepared using concentrated hydrochloric acid (EM; Gibbstown, NJ) to adjust the pH.

Extractions were performed using each buffer at each pH and concentration. A 75 mg mass of the simulated sample was transferred to a Teflon™ microwave vessel (Milestone Inc.) and 10 mL of the appropriate buffer was added. The vessel was then assembled according to the manufacturer's recommendations and a fiber optic temperature probe was inserted into the reference vessel to accurately monitor the temperature during the extraction. Figure 3.2 shows a schematic of the assembled reference vessel.

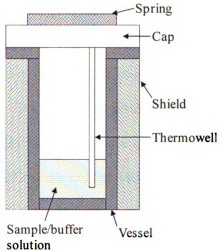

Figure 3.2: Schematic of assembled microwave vessel with sample

After the assembled microwave vessels were placed in the microwave unit, the instrument was programmed to heat for 15 minutes (ramp time) to 100 °C (extraction temperature) and hold at 100 °C for 15 minutes (extraction time). During the extraction, the vessels were rotated in the microwave to allow for even heating of all samples. At the end of the extraction, the vessels were allowed to cool to 50 °C before being opened.

Then, 5 mL of the extract were transferred to a 10 mL amber glass vial (Supelco, Bellefonte, PA) containing a stir bar.

The solution was further extracted using a headspace solid-phase microextraction (HS-SPME) procedure previously developed in our laboratory. The vial was pre-heated at 70 °C for five minutes, with stirring. A StableFlex divinylbenzene/Carboxen™/ polydimethylsiloxane (DVB/CAR/PDMS) fiber (Supelco, Bellefonte, PA) was exposed to the headspace for 20 minutes, with stirring. Finally, the fiber was retracted and analyzed by gas chromatography-mass spectrometry (GC-MS) using a Thermo Focus gas chromatograph with a Polaris Q mass spectrometer (Thermo Fisher Scientific Inc., Waltham, MA).

The Teflon™ microwave vessel was c leaned by rinsing with distilled water, acetone, and methanol. Next, 10 mL of fresh distilled water were added to the vessel which was then assembled. The vessel was then cleaned in the microwave with a 10 minute ramp to 160 °C and a 20 minute hold at 160 °C. After cooling, the water in the vessels was discarded, and the vessels were rinsed with fresh distilled water. The cleanliness of the vessels was assessed by performing blank extractions which were performed exactly as described for sample extraction, but with no simulated sample present.

Triplicate extractions of the simulated sample followed by the blank extractions were performed for each of the buffers. The optimum buffer was chosen based on the number of simulated sample components extracted, the precision of the extraction, and the level of simulated sample component carryover between extractions.

3.2.2. Determination of Significant Parameters

A full factorial experimental design was performed to screen for significant parameters in the MAE procedure. Ramp time, extraction time, and extraction temperature were studied, and the high and low values for each parameter were determined based on practical limitations (Table 3.1).

Table 3.1: High and low parameters for full factorial screening design

Parameter	High Value	Low Value
Ramp Time (min)	20	10
Extraction Time (min)	20	10
Extraction Temperature (°C)	120	80

The experimental design was generated using Statgraphics Centurion software (Version XV, Statpoint, Inc., Herndon, VA). For the screening design, a block randomized set of 16 experiments in four blocks was generated. Each block contained four extractions: two center point extractions and two other extractions. Center point extraction parameters included the middle point of the high and low values for each parameter, in this case a 15 minute ramp time, 15 minute extraction time, and 100 °C extraction temperature. The two other extractions tested the various combinations of the high and low values for the parameters.

Preliminary extractions indicated that methamphetamine carryover was present in the microwave vessel between extractions. This was potentially due to adsorption of the sample onto the Teflon™ microwave vessel. To overcome the carryover problem, quartz inserts were used which theoretically minimize carryover because the sample would not adsorb onto the quartz. For this study, 50 mg of the simulated sample were placed in 5.5 mL of 1 M phosphate buffer (pH 8) in the quartz insert. The insert was then placed in the

Teflon™ microwave vessel with 10 mL buffer in the vessel. The buffer in the vessel outside of the insert was required for accurate temperature monitoring by the fiber optic probe in the thermowell. The vessel was assembled according to the manufacturer's recommendation (Figure 3.3) and extracted using the ramp time, extraction time, and extraction temperature specified in the full factorial design given in Appendix C.

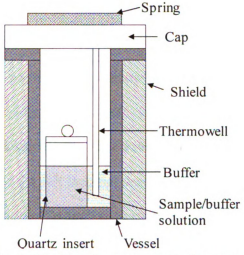

Figure 3.3: Schematic of assembled microwave vessel with quartz insert and sample

After MAE, 5 mL of the extract was transferred to an amber glass vial for subsequent extraction by HS-SPME using a similar procedure as previously described (section 3.2.1) except with a 40 minute extraction time rather than 20 minutes. All extracts were analyzed by GC-MS.

Integrated peak areas of each component of the simulated sample were used as the responses for the appropriate extraction. Using Statgraphics software, statistically significant extraction parameters for each tablet component were determined based on multivariate analysis of variance (MANOVA).

The quartz inserts were cleaned between each sample extraction by rinsing with distilled water, acetone, and methanol. Next 10 mL distilled water were added to the

insert which was then placed in the vessel with 15 mL distilled water. The vessels with the quartz inserts were then cleaned in the microwave with a 10 minute ramp to 130 °C and a 20 minute hold at 130 °C. After the vessels cooled, the water was discarded, and the inserts were rinsed with fresh distilled water.

3.2.3. Optimization of Significant Parameters

After determining that ramp time, extraction time, and extraction temperature were significant parameters for MAE, a circumscribed central composite (CCC) optimization design was performed to determine the optimum settings for these parameters. Statgraphics software was used to generate the CCC design with 23 randomized experiments (Appendix D). The values for the factorial points of the CCC design were the same as for the full factorial design discussed in section 3.2.2. For the star points, ramp time and extraction time were studied with at 23 minutes and 7 minutes while extraction temperature was studied at 134 °C and 67 °C. Extractions were performed exactly as described in section 3.2.2 except using the ramp rate, extraction time, and extraction temperature specified in the CCC design. The inserts were cleaned between each extraction using the procedure given in section 3.2.2.

As before, integrated peak areas of each simulated sample component were used as the responses for the appropriate extraction. Using Statgraphics software, mathematical models were developed for each sample component based on the peak area for each extraction. The responses were then optimized based on whether the goal was to maximize or minimize the peak area. A desirability function was used to combine the desired responses (peak areas) into a single function to optimize the extraction parameters.

3.3. Optimization of Headspace Solid-Phase Microextraction Procedure

After selecting the optimum buffer for use in MAE, it was necessary to determine the optimum HS-SPME extraction time and extraction temperature for future MAE/HS-SPME extractions. For the optimization, a homogenized sample from one MDMA exhibit (MSU900-01) was extracted using HS-SPME with no prior microwave extraction. All HS-SPME extractions used a 23-gauge StableFlex divinylbenzene/ Carboxen™/polydimethylsiloxane (DVB/CAR/PDMS) fiber (Supelco; Bellefonte, PA) that was conditioned daily before use as recommended by the manufacturer. After conditioning, the fiber was analyzed by GC-MS to ensure that the fiber was clean.

For the extraction, 50 mg the homogenized MDMA exhibit was placed in 5 mL of 1 M phosphate buffer at pH 8 in a 10 mL amber glass vial containing a stir bar. The vial was pre-heated by suspending it in a water bath at the specified extraction temperature for five minutes with stirring. Extraction time and extraction temperature were studied empirically; that is, one parameter was changed while the other was held constant. Extraction times of 10-60 minutes in 10 minute increments were studied while holding the extraction temperature at 70 °C. Then, extraction temperatures of 40-80 °C were studied using an extraction time of 40 minutes. At the end of the extraction time, the fiber was retracted and analyzed by GC-MS. The optimum HS-SPME extraction time and temperature were determined based on the combination that offered a compromise between the number and abundance of the impurities extracted and acceptable chromatography.

3.4. Liquid-Liquid Extraction Procedure

The procedures for liquid-liquid extraction (LLE) were adapted from the method developed by van Deursen *et al.* [1]. Phosphate buffer (0.33 M at pH 7) was prepared using potassium phosphate-monobasic (Mallinckrodt) and sodium phosphate-dibasic (Jade Scientific) with 2 M sodium hydroxide (Spectrum) used to adjust the pH.

For the extraction, 200 mg of either the simulated sample or the MDMA exhibits were placed in 4 mL of the phosphate buffer. The sample was vortexed for 10 seconds followed by sonication for 10 minutes and centrifugation for eight minutes. After adding 400 µL of toluene (Mallinckrodt) with eicosane (Aldrich) as an internal standard (0.020 mg/mL), the sample was gently agitated, then sonicated for 10 minutes, and centrifuged for five minutes. The toluene layer was transferred to a GC vial insert (Restek, West Chester, PA). Manual injections were made using 1 µL of sample with 0.5 µL air.

3.5. Gas Chromatography-Mass Spectrometry

A Thermo Focus gas chromatograph with a Polaris Q ion trap mass analyzer (Thermo Fisher Scientific Inc.) was used for all analyses. The GC was equipped with a Rxi™-5ms column (30 m, 0.25 mm id, 0.25 µm df; Restek). The mass spectrometer was operated in full scan mode from 50-650 m/z with the electron ionization source operating at 70 eV.

For HS-SPME extractions, a Merlin Microseal™ septum replacement (Merlin Instrument Company, Half Moon Bay, CA) was used instead of a traditional septum. A narrow splitless inlet liner with an internal diameter of 0.8 mm was used for HS-SPME extractions to better focus the components that desorb from the fiber onto the head of the column. The GC-MS parameters used for HS-SPME experiments are given in Table 3.2.

Blank MAE/HS-SPME extractions were analyzed using the same GC-MS parameters for samples with a minor change to the GC temperature program: the hold at the end of the program was reduced to one minute for time efficiency.

For LLE, a BTO 17 mm CenterGuide septum (Restek) and a traditional split/splitless liner were used. The GC-MS parameters used for LLE injections were based on those reported by van Duersen *et al.* [1] and are given in Table 3.2.

Table 3.2: GC-MS parameters for HS-SPME analysis and LLE analysis

	MAE/HS-SPME and HS-SPME	LLE
Injection Port	260°C; splitless 1 minute, then 100:1 split	250°C; 50:1 split
Carrier Gas	Helium, 1 mL/min	Helium, 0.5 mL/min
Oven Program		
Initial	60°C for 2 minutes	90°C for 1 minute
Ramp	8°C/minute	8°C/minute
Final	300°C for 15 minutes	300°C for 10 minutes
MS Transfer Line	275 °C	275 °C
Ion Source	225 °C	225 °C
MS Solvent Delay	2 minutes	4 minutes

Using instrument software (Xcaliber 1.4, Thermo Fisher Scientific Inc.), peak areas of the simulated sample components were integrated and used in subsequent data analysis.

3.6. Comparison of Extraction Procedures

Replicate extractions of the simulated sample were performed to compare the precision of the optimized MAE/HS-SPME procedure (four replicates) and the optimized HS-SPME procedure (five replicates) with the LLE procedure based on the literature [1] (three replicates). For each extraction procedure, the relative standard deviation (RSD) of the integrated peak area for each component in the simulated sample was calculated.

The three homogenized MDMA exhibits were then extracted in triplicate by each extraction procedure. The extraction procedures were evaluated based on the number of

impurities extracted, the overall chromatography, and the precision of the extraction for each exhibit. Rather than calculate RSD values for the individual impurities in each exhibit to assess precision, Pearson product moment correlation (PPMC) coefficients were calculated between each pair-wise combination of replicates to assess the correlation among replicate chromatograms. Prior to calculating PPMC coefficients, chromatograms were retention time aligned using a commercially available retention time alignment algorithm (Line Up, Infometrix, Bothell, WA).

Using the HS-SPME chromatograms, the three MDMA exhibits were compared based on the identity of the impurities extracted by the three extraction procedures. The origin of the impurities as well as the synthetic route used to synthesize the MDMA in the exhibit was investigated.

3.7. References

[1] van Deursen MM, Lock ERA, Poortman-van der Meer AJ. Organic Impurity Profiling of 3,4-Methylenedioxymethamphetamine (MDMA) Tablets Seized in the Netherlands. Sci Justice 2006; 46: 135-152.

[2] Andersson K, Jalava K, Lock E, Huizer H, Kaa E, Lopes A, Poortman-van der Meer A, Cole MD, Dahlen J, Sippola E. Development of a Harmonised Method for the Profiling of Amphetamines IV. Optimisation of Sample Preparation. Forensic Sci Int 2007; 169: 64-76.

[3] Kuwayma K, Tsujikawa K, Miyaguchi H, Kanamori T, Iwata Y, Inoue H, Saitoh S, Kishi T. Identification of Impurities and the Statistical Classification of Methamphetamine using Headspace Solid Phase Microextraction and Gas Chromatography-Mass Spectrometry. Forensic Sci Int 2006; 160: 44-52.

[4] Palhol F, Boyer S, Naulet N, Chabrillat M. Impurity Profiling of Seized MDMA Tablets by Capillary Gas Chromatography. Anal Bioanal Chem 2002; 374: 274-281.

[5] Swist M, Wilamowski J, Zuba D, Kochana J, Parczewski. Determination of Synthesis Route of 1-(3,4-methylenedioxyphenyl)-2-propanone (MDP2P) based on Impurity Profiles of MDMA. Forensic Sci Int 2005; 149: 181-192.

Chapter 4 Results and Discussion

4.1. Sample Preparation

4.1.1. Simulated MDMA Sample

The components in the simulated sample, which was used to optimize the microwave-assisted extraction (MAE) parameters, were chosen to provide a wide span of retention times and peak abundances in the resulting impurity profiles. Benzylamine and phenethylamine were chosen because of their structural similarity to methamphetamine, MDMA, and impurities commonly observed in MDMA tablets. Methamphetamine and caffeine were included because they are common adulterants added to the synthesized MDMA before it is pressed into tablet form [1]. Ephedrine was included because it is a common starting material for the synthesis of methamphetamine [2]. MDMA was included to make the simulated tablet as realistic as possible; however, it was not included in the data analysis due to the low quantity present in the sample.

4.1.2. MDMA Exhibits

The physical characteristics of the three MDMA exhibits used throughout this study are given in Table 4.1. The average diameter, height, and mass were calculated based on ten tablets selected from each of the exhibits.

Table 4.1: Physical characteristics of MDMA exhibits (averages based on ten tablets)

Exhibit Identity	Number of Tablets in Exhibit	Tablet Color	Tablet Logo	Tablet Shape	Average Diameter (mm)	Average Height (mm)	Average Mass (g)
MSU900-01	100	Pink/green/ purple	Alligator	Circular, beveled edge	8.0	5.0	0.2705
T-17	20	Blue	Horseshoe	Circular, beveled edge	8.0	4.0	0.2423
T-27	20	Pink	Heart	Circular, beveled edge	8.0	4.8	0.2693

4.2. Optimization of Microwave-Assisted Extraction Procedure

4.2.1. Selection of Extraction Buffer

The goal of the buffer study was to determine the optimum buffer for use with MAE. It was desired that the buffer extract all components of the simulated sample with acceptable precision and no carryover between extractions. The simulated sample was extracted in triplicate using the different buffers at different pH values and different concentrations. For each set of triplicates, the percent relative standard deviations (RSD) of the peak areas of the simulated sample components were calculated. Blank extractions were performed and analyzed following each sample extraction and cleaning procedure to determine if sample carryover was detected.

4.2.1.1. Investigation of Phosphate Buffers

Phosphate buffers at pH 6, 7, and 8 were studied to correspond to the buffering range of phosphate which has a pK_a of 7.2 [3]. Buffers of lower pH were not studied because basic impurities, which are commonly found in MDMA tablets, are extracted more efficiently at higher pH values [4]. Buffer concentrations of 1 M, 0.5 M, and 0.1 M were studied based on a review of the literature [2,4,5]. The average peak areas and RSD

values for the simulated sample in phosphate buffers analyzed in triplicate are summarized in Table 4.2.

Table 4.2: Average abundance and RSD values of simulated sample components in phosphate buffers (average peak areas based on three replicates)

Buffer pH	Impurity	pK_a	1 M		0.5 M		0.1 M	
			Average Peak Area	% RSD	Average Peak Area	% RSD	Average Peak Area	% RSD
6	Benzylamine	9.3	*	*	*	*	*	*
	Phenethylamine	9.8	*	*	*	*	*	*
	Methamphetamine	10.0	2.49E+07	8.47	1.22E+07	10.84	1.31E+07	27.88
	Ephedrine	10.0	*	*	*	*	*	*
	Caffeine	14.0	7.92E+07	27.34	4.33E+07	44.66	3.42E+07	57.64
7	Benzylamine	9.3	5.05E+07	28.21	4.33E+07	14.59	5.88E+07	15.12
	Phenethylamine	9.8	*	*	*	*	*	*
	Methamphetamine	10.0	3.44E+08	7.53	2.84E+08	4.47	2.58E+08	7.37
	Ephedrine	10.0	1.12E+07	27.28	8.68E+06	34.04	6.93E+06	23.12
	Caffeine	14.0	1.74E+08	20.82	1.52E+08	33.98	1.18E+08	4.30
8	Benzylamine	9.3	5.33E+08	1.86	3.23E+08	20.21	2.66E+08	15.58
	Phenethylamine	9.8	1.26E+08	5.58	6.96E+07	11.80	5.71E+07	27.05
	Methamphetamine	10.0	1.28E+09	1.09	1.29E+09	1.43	1.23E+09	5.46
	Ephedrine	10.0	9.73E+07	7.90	**	**	**	**
	Caffeine	14.0	2.10E+08	5.43	1.29E+08	23.68	1.17E+08	6.92

* denotes that the impurity was not detected

** denotes that the impurity co-eluted with a siloxane peak from the fiber

As the concentration of the buffer increased, the average peak area of the simulated sample components generally increased indicating a higher concentration of sample was extracted. As the concentration of the buffer increased, the stability of the solution increased which makes the solution more thermally stable. A more stable solution would experience less degradation when exposed to microwave energy than a less stable solution. Therefore, phosphate buffers of higher concentration are more desirable.

At lower pH values, not all components of the simulated sample were extracted. Also, as the pH of the buffer increased, the abundance of the peaks generally increased. This is due to the pK_a of the components. In a solution with the pH less than the pK_a of the component, the salt (or protonated) form of the component dominates the equilibrium between the salt and the free base form. The protonated form is less volatile than the free base form which indicates that the protonated form has a lower affinity for the headspace than the free base form during headspace-solid phase microextraction (HS-SPME) [6,7]. Because the components of the sample generally move from the sample solution to the headspace and then from the headspace to the fiber [7], more of the analyte in the headspace implies that more of the analyte is available for HS-SPME. To illustrate the effect of pH on the extraction of the simulated sample, Figure 4.1 shows chromatograms of the simulated sample extracted from 1 M phosphate buffers at pH 6 and pH 8.

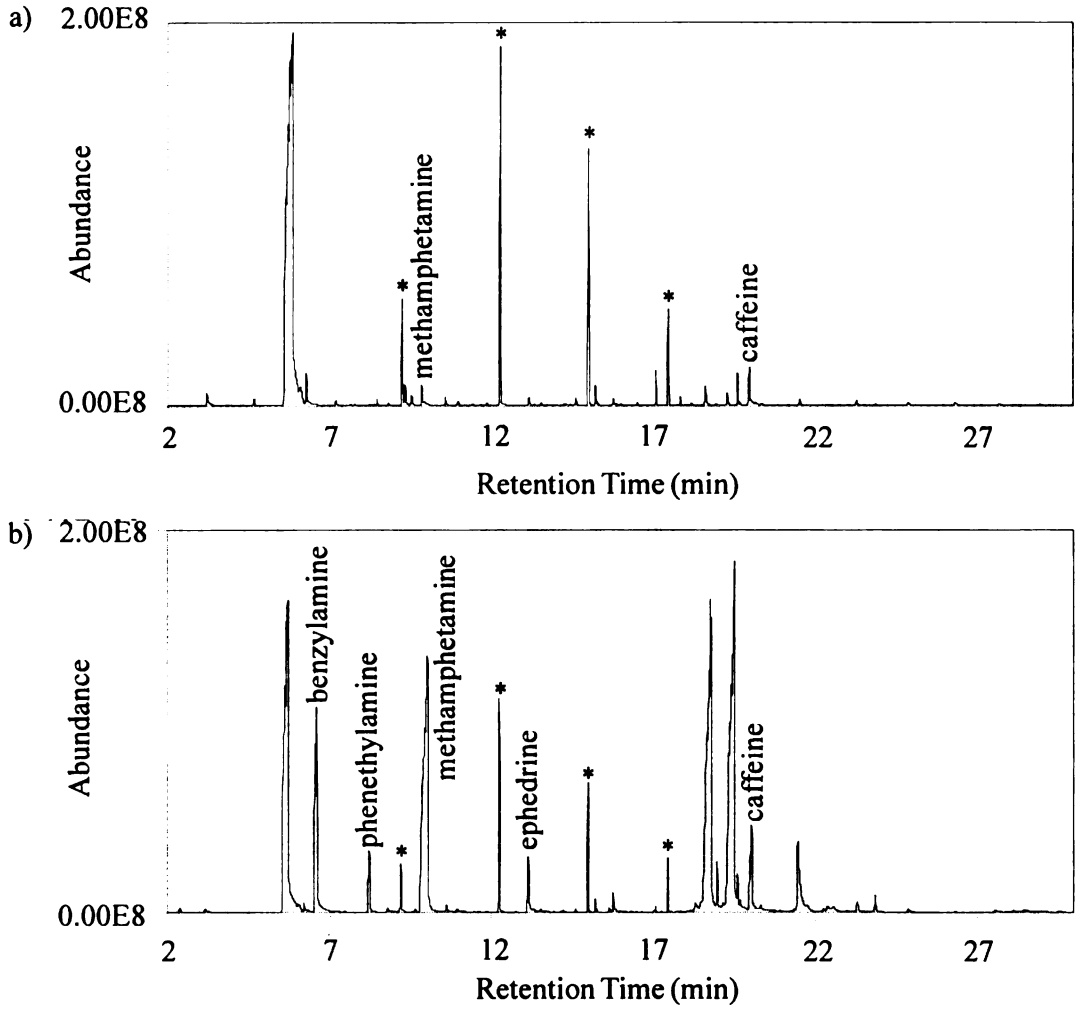

Figure 4.1: Chromatograms of the simulated sample in 1 M phosphate buffer at a) pH 6 and b) pH 8; an * indicates that a peak was present in the blank

At pH 6, benzylamine, phenethylamine, and ephedrine were not extracted. Methamphetamine and ephedrine both have a pK_a of 10.0, but ephedrine was not detected at pH 6 while methamphetamine was detected. This was due to the lower boiling point of methamphetamine making it more volatile than ephedrine. The higher methamphetamine volatility gives methamphetamine a higher affinity for the headspace than ephedrine, therefore allowing methamphetamine to be extracted at higher abundances.

For HS-SPME, acceptable RSD values usually fall between 1% and 10% [7]. The RSD value for caffeine was high (greater than 27%) for all concentrations at pH 6, and the RSD value for methamphetamine was high (greater than 10%) at 0.5 M and 0.1 M. This may be due to the sample not being completely homogenized when the aliquots were taken for extraction. Another contributing factor may be slight fluctuations in the temperature of the water bath (plus or minus 2-3 °C) during HS-SPME. These factors combined can decrease the precision observed because the extraction conditions are not the same between replicate extractions.

At all concentrations of phosphate buffers at pH 6, there was no sample carryover in the microwave vessel after the cleaning procedure. Despite the adequate cleaning of the microwave vessels, the phosphate buffers of pH 6 were not chosen as the optimum buffer because not all components of the simulated sample were extracted. Also, the components that were extracted (methamphetamine and caffeine) were not extracted precisely, as shown by the high RSD values.

For pH 7 phosphate buffers, phenethylamine was not extracted at any buffer concentration. Overall, high RSD values (greater than 10%) were observed for benzylamine, ephedrine, and caffeine (in 1 M and 0.5 M buffers at pH 7). Again, this could have been due the lack of homogeneity in the sample or changes in the extraction temperature (plus or minus 2-3 °C). At all concentrations, there was no sample carryover in the microwave vessel after cleaning. However, phosphate buffers of pH 7 were not chosen as the optimum buffer because not all components were extracted and components that were extracted did not show good precision.

All simulated sample components were extracted using pH 8 phosphate buffers. At pH 8, using the 0.5 M and 0.1 M concentration buffers, ephedrine co-eluted with a siloxane from the fiber making accurate identification and peak area integration difficult. Therefore the RSD value for ephedrine was not calculated for these concentrations. The co-elution and higher fiber bleed may have been due to a new fiber being used. After several extractions, there was no further co-elution between ephedrine and siloxane using this fiber. At 0.5 M and 0.1 M, RSD values were high for benzylamine (greater than 15%) and phenethylamine (greater than 11%) again due to slight changes in the sample and extraction temperature between replicate extractions. The RSD values were acceptable (less than 10%) for all impurities at the 1 M concentration pH 8. The concentration of the buffer can influence the partition coefficient between the sample and the headspace affecting the equilibration between the two phases. The 1 M buffer is more stable than the 0.5 M and 0.1 M buffers. Therefore, the simulated sample may be more stable in the 1 M buffer during MAE, allowing for a more precise extraction.

The 0.5 M and 0.1 M buffers (pH 8) showed methamphetamine and benzylamine carryover in the microwave vessel between extractions, and hence, these buffers were not chosen as the optimum buffer. There was no sample carryover in the microwave vessels between extractions with at 1 M concentration. Because the simulated sample is more soluble in the higher concentration buffer, more of the sample goes into solution and less is left in the microwave vessel following the extraction. The 1 M phosphate buffer at pH 8 was chosen as the optimum phosphate buffer for MAE because all components were extracted with acceptable RSD values and there was no carry-over of the sample in the microwave vessel between extractions.

4.2.1.2. Investigation of Tris Buffers

Tris buffers were studied at pH 7, 8, and 9 to correspond to the buffering range of tris(hydroxymethylaminomethane) which has a pK_a of 8.1 [3]. Buffers of higher pH were avoided because methamphetamine and MDMA are extracted more efficiently at higher pH values [4]. Based on a review of the literature, buffer concentrations of 1 M, 0.5 M, and 0.1 M were studied [5]. The average peak area and RSD values for the simulated sample analyzed in triplicate in the tris buffers are summarized in Table 4.3.

Table 4.3: Average abundance and RSD values of simulated sample components in tris buffers (average peak area based on three replicates)

Buffer pH	Impurity	pK_a	1 M		0.5 M		0.1 M	
			Average Peak Area	% RSD	Average Peak Area	% RSD	Average Peak Area	% RSD
7	Benzylamine	9.3	1.70E+07	***	1.62E+07	***	1.04E+07	3.29
	Phenethylamine	9.8	*	*	*	*	*	*
	Methamphetamine	10.0	3.12E+08	***	5.51E+06	***	1.34E+07	29.72
	Ephedrine	10.0	*	*	*	*	*	*
	Caffeine	14.0	3.02E+07	***	2.37E+07	***	4.32E+07	6.45
8	Benzylamine	9.3	1.57E+07	27.45	8.14E+07	8.64	4.72E+07	29.58
	Phenethylamine	9.8	*	*	*	*	*	*
	Methamphetamine	10.0	1.73E+08	5.06	2.52E+08	5.55	1.95E+08	10.27
	Ephedrine	10.0	**	**	**	**	**	**
	Caffeine	14.0	4.06E+07	33.64	1.06E+08	44.32	9.40E+07	44.95
9	Benzylamine	9.3	4.22E+08	4.16	4.25E+08	8.04	4.32E+08	4.08
	Phenethylamine	9.8	1.65E+08	14.13	1.47E+08	11.24	1.24E+08	5.94
	Methamphetamine	10.0	1.19E+09	1.35	1.17E+09	2.15	1.09E+09	2.51
	Ephedrine	10.0	**	**	**	**	**	**
	Caffeine	14.0	1.07E+08	22.18	9.25E+07	54.13	8.87E+07	3.36

* denotes that the impurity was not detected

** denotes that the impurity co-eluted with a siloxane peak from the fiber

***denotes that impurity was present but the buffer was only analyzed once; therefore, no RSD value was calculated for the particular concentration/pH combination

For tris buffers of pH 7, phenethylamine and ephedrine were not extracted at any buffer concentration, and replicates of 1 M and 0.5 M tris buffers at pH 7 were not completed. Therefore, RSD values for these two buffers were not calculated. The pH 7 tris buffers showed no carryover in the microwave vessel from the simulated sample between extractions. However, because not all impurities were extracted, tris buffers of pH 7 were not chosen as the optimum buffer for MAE.

At all concentrations of tris buffer at pH 8, phenethylamine was not extracted, and ephedrine was extracted but co-eluted with a siloxane peak from the fiber. At all concentrations there was no sample carryover in the microwave vessel between extractions. However, because not all impurities were extracted, tris buffers of pH 8 were not chosen as the optimum buffer for MAE.

For tris buffers of pH 9 all impurities were extracted; however, ephedrine co-eluted with a siloxane peak making peak area integration difficult. Therefore, no RSD value was calculated for ephedrine. However, methamphetamine carryover in the microwave vessel was observed at all concentrations and benzylamine carryover was observed in the 1 M buffer. Therefore, tris buffers of pH 9 were not chosen as the optimum buffer for MAE.

4.2.1.3. Investigation of Carbonate Buffer

A 0.05 M carbonate buffer at pH 10 was chosen based on a review of the literature [8,9] for preliminary work at the start of this project. The average peak areas (n=3) and RSD values were determined for the components of the simulated sample in the carbonate buffer and are summarized in Table 4.4.

Table 4.4: Average abundance and RSD values of simulated tablet components in carbonate buffer (average peak area based on three replicates)

Buffer pH	Impurity	pK_a	0.05 M	
			Average Peak Area	% RSD
10	Benzylamine	9.3	4.05E+08	5.89
	Phenethylamine	9.8	2.64E+08	8.72
	Methamphetamine	10.0	1.92E+09	1.71
	Ephedrine	10.0	1.60E+08	8.26
	Caffeine	14.0	1.55E+08	7.74

All impurities were extracted in the carbonate buffer with good precision. However, because methamphetamine carryover was observed in the microwave vessels between extractions, carbonate buffer was not chosen as the optimum buffer for MAE.

Thus, the optimum buffer selected for all subsequent extractions was a 1 M phosphate buffer at pH 8. The simulated sample components were extracted with good precision from this buffer, and no sample carryover was seen in the microwave vessel between extractions.

4.2.2. Determination of Significant Parameters

Using the simulated sample, a full factorial screening design was performed to determine if the microwave parameters of ramp time, extraction time, and extraction temperature were significant in the extraction of organic impurities. The full factorial design was chosen because the parameters and the interactions between the parameters could be studied and the significance of each determined.

The high values for ramp time and extraction time (20 minutes) were chosen for time efficiency as longer extractions would become impractical. The low value for ramp time (10 minutes) w as chosen to allow the microwave sufficient time to reach the extraction temperature. The low value for the extraction time (10 minutes) was selected to allow time for the sample to dissolve into solution. The high extraction temperature

(120 °C) was selected to avoid possible thermal decomposition of the sample while the low extraction temperature (80 °C) was chosen to ensure that the sample completely dissolved into solution.

After the set of experiments was completed (see Appendix C), the peak areas of the simulated sample components were integrated. Using Statgraphics software, multivariate analysis of variance (MANOVA) was performed to determine which of the microwave parameters had a significant effect on the extraction of the simulated sample components. Ephedrine was not included in the analysis because it co-eluted with a siloxane peak from another new fiber that made accurate peak area determination difficult.

Because of the blocked experimental design, the interactions between the parameters were confounded with the block effects, or the day to day differences. This means that the effects of the interactions and the effects of the blocks could not be differentiated from one another. Because this design was an initial screening used only to determine which of the parameters had an effect on the extraction, the confounding with the block effects was not problematic.

Using MANOVA, the sum of squares for each of the main effects, the interactions plus blocks, and blocks alone were calculated, and the degrees of freedom were determined. The mean square value of each parameter and interaction was calculated followed by the determination of the F-ratio for each parameter and interaction. The significance of this value was determined by comparing the calculated F-value to a critical F-value at the 95% confidence level. Complete MANOVA tables for each of the simulated sample components can be found in Appendix E.

For benzylamine, the interaction between extraction time and extraction temperature had a significant effect on the peak area. Because the interaction between extraction time and extraction temperature was significant, both parameters were important and investigated further in the subsequent optimization design. For methamphetamine, three parameters and interactions significantly affected the peak area: extraction temperature, the interaction between ramp time and extraction time, and the interaction between extraction time and extraction temperature. For caffeine and phenethylamine, no parameter or interaction of parameters had a significant effect on the peak areas. Because all three parameters (ramp time, extraction time, and extraction temperature) had a significant effect on the peak area of one or more of the components, all three parameters were included in the optimization design.

4.2.3. Optimization of Significant Parameters

To optimize the microwave ramp time, extraction time, and extraction temperature, the parameters were studied in a circumscribed central composite design using the simulated sample. The circumscribed central composite design was chosen because it allowed for the second order interactions to be determined and more complete mathematical models to be built [10]. After the set of experiments was completed (see Appendix D), the peak areas of the simulated sample components were integrated. Again, ephedrine was not included in the data analysis because of co-elution with a siloxane peak from the fiber.

Using Statgraphics software, the first step in determining the optimum parameters was to model the data collected during the experiments. Linear regression analysis was

used to fit a second-order mathematical model for each component's peak area. This resulted in four models, one for each sample component.

Next, the peak area of each impurity was optimized individually based on whether the goal was to maximize or minimize the area. The peak areas of methamphetamine and caffeine were minimized. In MDMA tablets, these compounds are adulterants, not impurities. Therefore, these peaks should be minimized to avoid over-extraction and broad peaks that can mask impurities present at low concentrations. Meanwhile, benzylamine and phenethylamine were maximized because they represent impurities in the MDMA tablets, and the goal is to maximize the extraction of impurities.

A desirability function was created for each simulated sample component individually. Then, the desirability of each individual component was combined to determine the optimum settings for the MAE. This allowed for the determination of the extraction parameters that allowed the methamphetamine and caffeine peaks to be minimized and the benzylamine and phenethylamine peaks to be maximized. The variable, *s*, or the shape of the desirability function, was set to one (linear) for all responses (or peak areas).

The impact, or importance, was set for each component on a scale of 1-5. The impact of methamphetamine was set to 5 because it was important to minimize the carryover of methamphetamine between samples. Also, it was important to minimize the possibility of a broad methamphetamine peak masking impurities present at lower concentrations. Minimizing caffeine was not of great importance because there was no carryover of caffeine between experiments, and the peak is not so broad as to mask other impurities present at similar retention times. Therefore, the impact was set to 2.

Benzylamine and phenethylamine maximization was important in maximizing the levels of impurities present in the sample, and the impact was set to 5. The optimum MAE parameters determined from the desirability function are shown in Table 4.5.

Table 4.5: Optimum microwave parameters from the CCC design

Parameter	Optimum
Ramp Time (min)	23
Extraction Time (min)	23
Extraction Temperature (°C)	100

To visualize the estimated peak area at various settings, including the optimum settings, of the parameters, estimated response surface graphs were drawn for the components. To determine the estimated response, the values of the parameters were entered into the mathematical model constructed for the particular component. The plot was then constructed from the responses of several different sets of conditions. A separate plot was created for each component.

For example, Figure 4.2 shows the estimated response surface for methamphetamine. For this plot, the extraction temperature was held at 100 °C in the equation for methamphetamine, and the values for the parameters of ramp time and extraction time were varied. Although the peak areas are shown as discrete lines, the peak area is a continuum. The peak area at the optimum setting is marked with a plus sign (+).

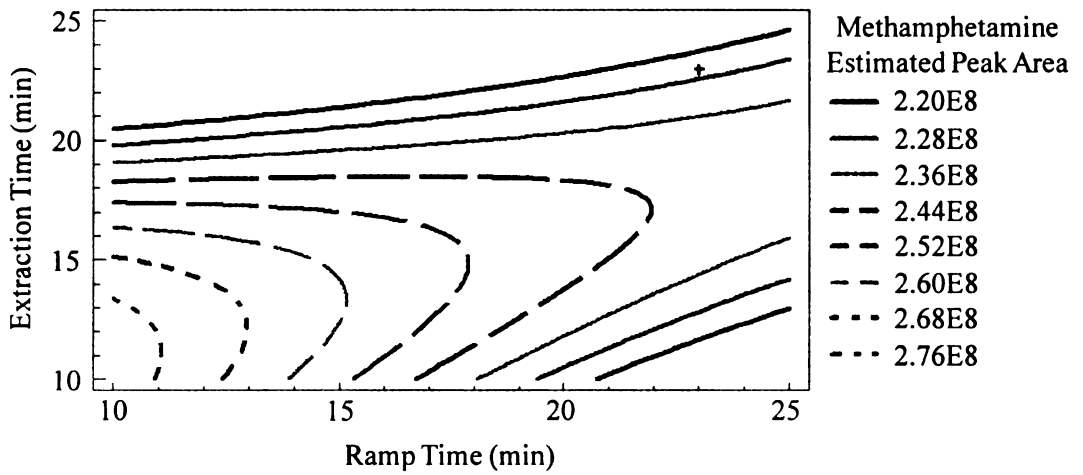

Figure 4.2: Estimated response surface for methamphetamine from CCC design with a plus sign (+) indicating the response at the optimum settings for the MAE parameters

At the optimum settings of the parameters (23 minute ramp time and 23 minute extraction time), the predicted peak area for methamphetamine is between 2.20E8 to 2.28E8 which are the lowest values calculated for the estimated peak area. This result is expected since the desired outcome of methamphetamine is minimization. From this plot, it can be seen that a 10 minute ramp time and 20 minute extraction time gives similar results to a 23 minute ramp time and 23 minute extraction time. However, these values for the parameters were not chosen because the peak areas of the other components are at their maximum or minimum at a ramp time and extraction time closer to 23 minutes. The optimum parameters represent a compromise of parameter settings based on all the responses.

4.3. Optimization of Headspace Solid-Phase Microextraction Procedure

Using 1 M phosphate buffer at pH 8 and the homogenized batch of exhibit MSU900-01, the optimum HS-SPME extraction time and extraction temperature were investigated. The samples for this study were not microwave extracted prior to HS-SPME to determine the effect of HS-SPME on the extraction of the MDMA exhibit. For

the HS-SPME optimization, extraction times of 10-60 minutes in 10 minute increments and extraction temperatures of 40-80 °C in increments of 10 °C were studied. The extraction time range was chosen for time efficiency while the extraction temperature range was chosen for practical limitations of the water bath. The number of impurities extracted and the peak shape were evaluated to determine the optimum HS-SPME extraction time and extraction temperature.

4.3.1. Optimization of Extraction Time

When the extraction temperature was held at 70 °C, the longer extraction times (40, 50, and 60 minutes) extracted five more impurities from the MDMA exhibit than the shorter extraction times (10, 20, and 30 minutes). In general, impurities were extracted at higher abundances at longer extraction times because of the pre-concentration of the impurities on the fiber. For impurities with a higher affinity for the fiber than the headspace, the longer extraction time allowed more time for the impurities to absorb or adsorb onto the fiber. However, if the impurities have a lower affinity for the fiber, it is possible that the longer extraction time would give more time for the impurities to desorb from the fiber. This did not appear to be the case for the impurities extracted from the exhibit because the longer extraction times had more abundant peaks across the retention time range of the chromatogram.

Even though more impurities and components were extracted in higher abundances at longer extraction times, the high abundance is not always desirable. Figure 4.3 shows a comparison of chromatograms for the 60, 40, and 10 minute extractions, all with an extraction temperature of 70 °C. At longer extraction times (60 and 40 minutes, Figure 4.5a and b, respectively), the higher abundances of MDMA and

caffeine led to poor peak shape and broadened peaks with 60 minutes showing the worst peak shape. The broad peaks are caused by the high concentration of the sample overloading the gas chromatograph (GC) column resulting in band broadening. Therefore, the longest extraction times, 50 and 60 minutes, were not investigated further as there is a greater chance that trace level impurities present in the retention time range of MDMA and caffeine would be masked by the broad peaks.

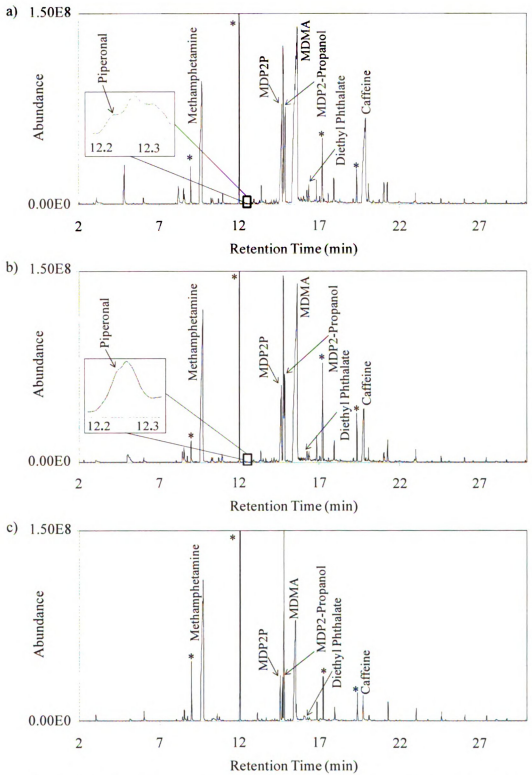

Figure 4.3: Chromatograms of HS-SPME extractions at a) 60 minutes, b) 40 minutes, and c) 10 minutes; an asterisk (*) indicates that a peak was present in the blank

At the shorter extraction times (10 minutes, Figure 4.3c), many impurities were extracted at lower abundances. Piperonal, which co-eluted with an unidentified compound, was not detected above the baseline noise at the 10 minute extraction time. The detection of piperonal is important for determining the synthetic route of 3,4-methylenedioxyphenyl-2-propanone (MDP2P) which is a common starting material in the synthesis of MDMA. Forty minutes (Figure 4.3b) was chosen as the optimum extraction time because it offered a compromise between higher impurity abundance and improved peak shape.

4.3.2. Optimization of Extraction Temperature

When the extraction time was held at 40 minutes, the higher extraction temperatures (70 and 80 °C) extracted impurities at higher abundances than the lower extraction temperatures (40, 50, and 60 °C). At higher extraction temperatures, more of a compound volatilizes than at lower extraction temperature because the compounds have a higher partition coefficient between the headspace and the sample. Thus, more of the sample is in the headspace to absorb onto the fiber [7,11]. By lowering the temperature, less of the compound volatilizes; and therefore, less of the sample is available in the headspace to absorb or adsorb onto the fiber resulting in less abundant peaks in the chromatogram.

However, at higher extraction temperatures, higher volatility compounds may actually desorb from the fiber during the extraction time due to the lower partition coefficient [7,11] For example, Figure 4.4 shows a comparison of extractions at 80 °C and at 40 °C. An unidentified peak with a retention time of 2.17 minutes (labeled "a")

was extracted at a higher abundance with an extraction temperature of 40 °C than with an extraction temperature of 80 °C.

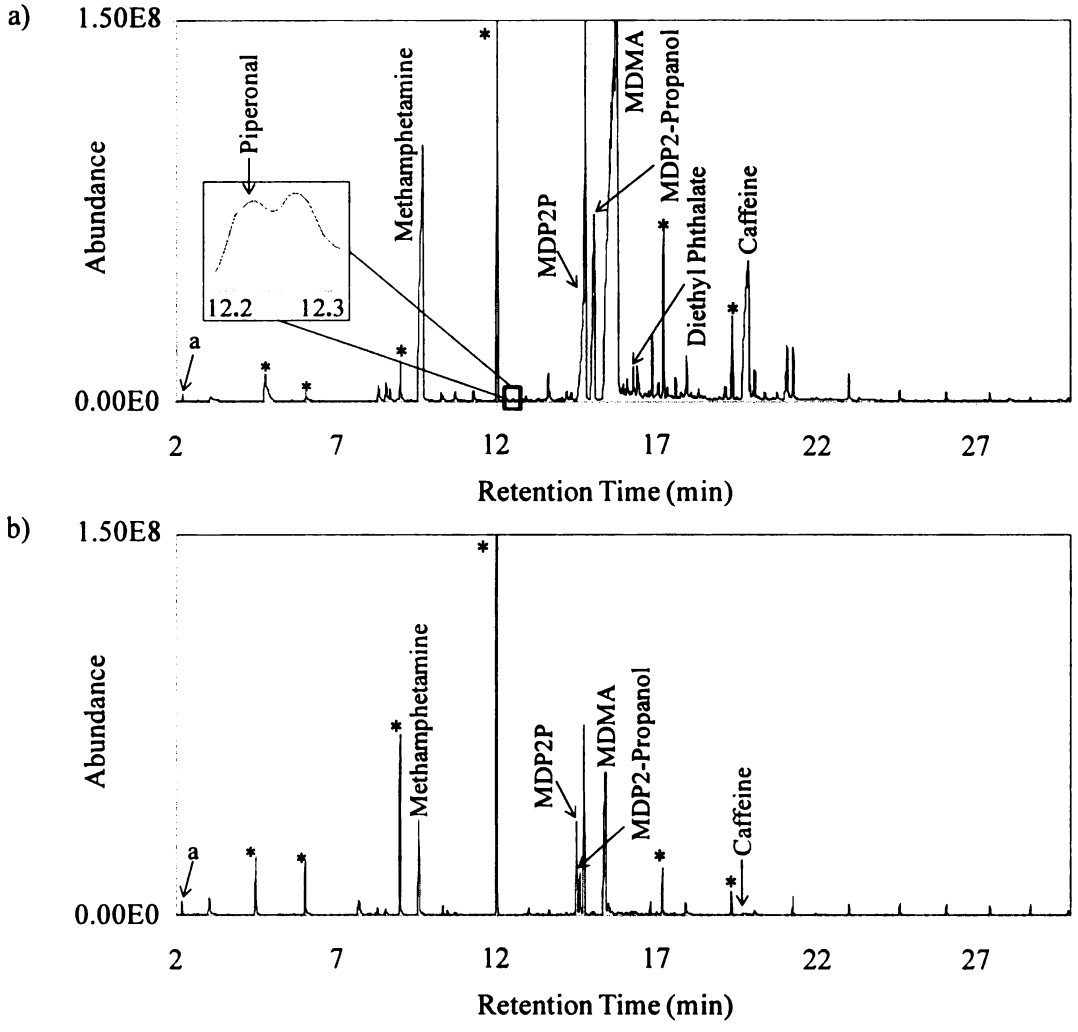

Figure 4.4: Chromatograms of HS-SPME extractions at a) 80 °C and b) 40 °C; an asterisk (*) indicates that the peak was present in the blank

Even though impurities were extracted at higher abundances at 80 °C, the broad MDMA peak may have masked additional impurities present at trace levels that elute at a similar retention time to MDMA. Therefore, 80 °C was not chosen as the optimum extraction temperature. At lower extraction temperatures, for example 40 °C, the broad peaks were not observed; however, some impurities such as piperonal and isosafrole were

not extracted above the baseline noise due to their lower volatility. The detection of these impurities is important because their presence indicates the possible synthetic route used to synthesize the MDP2P [12]. Ultimately, an extraction temperature of 70 °C was chosen as the optimum temperature for the extraction of organic impurities because impurities were extracted at higher abundance than the lower temperatures while maintaining better chromatography than the 80 °C extraction. Therefore, the optimum HS-SPME conditions were a 40 minute extraction at 70 °C.

Thus, based on the results of the optimization studies, the optimum MAE/HS-SPME procedure involves a microwave extraction with a 23 minute ramp time to 100 °C and a 23 minute extraction at 100 °C. The subsequent HS-SPME parameters include a five minute pre-heat at 70 °C and a 40 minute extraction at 70 °C.

4.4. Comparison of MAE/HS-SPME, HS-SPME, and LLE

4.4.1. Simulated Sample

To determine the precision of each of the three extraction procedures (MAE/HS-SPME, HS-SPME, and liquid-liquid extraction, LLE), replicate extractions of the simulated sample were performed by each of the procedures (four replicates for MAE/HS-SPME, five replicates for HS-SPME, and three replicates for LLE). For each set of replicates, the peak areas of each simulated sample component were integrated and RSD values were calculated (Table 4.6).

Table 4.6: Relative standard deviations for simulated sample components extracted by the three procedures

Component	%RSD		
	MAE/HS-SPME (n=4)	HS-SPME (n=5)	LLE (n=3)
benzylamine	4.61	5.74	**
phenethylamine	28.32	3.46	**
methamphetamine	9.81	5.50	9.37
ephedrine	*	4.88	**
caffeine	8.73	6.35	7.61

* Co-elution with siloxane from fiber; ** Component not detected

For SPME, acceptable RSD values range from 1-10%. The MAE/HS-SPME procedure showed good precision with RSD values less than 10% for benzylamine, methamphetamine, and caffeine. Ephedrine co-eluted with a siloxane peak, therefore making accurate peak area integration difficult. The co-elution may have been due to a new fiber being used. Phenethylamine showed poor precision resulting in a RSD value greater than 25%. Phenethylamine may not be thermally stable at the higher temperatures reached by the microwave (100 °C), and therefore is not extracted precisely.

The HS-SPME procedure showed a precise extraction of the simulated sample with all components being extracted with RSD values less than 10%. The LLE procedure only extracted two of the simulated sample components and did so with RSD values less than 10%. Despite similar precision in extraction for the three procedures, more of the simulated sample components were extracted using MAE/HS-SPME and HS-SPME than with LLE.

4.4.2. MDMA Exhibits

Homogenized batches of the three MDMA exhibits were extracted in triplicate by each of the three extraction procedures (MAE/HS-SPME, HS-SPME, and LLE). For each exhibit, the ability of the three extraction procedures to extract impurities was

assessed based on the number and identity of impurities. To compare the precision of the extraction procedures, the triplicate chromatograms were retention time aligned and Pearson product moment correlation (PPMC) coefficients were calculated between replicate extractions for each exhibit.

A full list of all compounds extracted from the three MDMA exhibits is given in Appendix F. The compounds extracted from the exhibits have been divided into two groups: impurities and other components. Impurities are chemical compounds which originate from the reactions involved in synthesizing the MDMA. Other components are additives, adulterants, and main active ingredients. Components include caffeine, fatty acids, methamphetamine, MDMA, lidocaine, and phthalates (not present in the blank).

The GC-MS parameters for the LLE analysis are based on the literature [4]. This set of parameters differs from the parameters optimized for MAE/HS-SPME and HS-SPME analysis in two ways that affect the retention time of impurities and components: the carrier gas flow rate and the initial starting temperature of the GC oven. The flow rate for LLE analysis is 0.5 mL/min while for MAE/HS-SPME and HS-SPME it is 1 mL/min. The initial GC oven temperature for LLE is 90 °C while for MAE/HS-SPME it is 60 °C. Therefore, a difference in retention times of approximately four minutes is expected when comparing LLE to MAE/HS-SPME or HS-SPME. Also, retention time differences of about 0.1 minutes are observed when comparing MAE/HS-SPME and HS-SPME chromatograms due to slight changes in the instrument as a result of routine maintenance, for example cutting the end of the column.

4.4.2.1. MDMA Exhibit MSU900-01

In total, 62 different compounds were extracted from exhibit MSU900-01 by the three extraction procedures and are summarized in Table 4.7.

Table 4.7: Number of impurities and components extracted from MDMA exhibit MSU900-01

Extraction	Number of Impurities	Number of Other Components
MAE/HS-SPME	42	6
HS-SPME	46	5
LLE	8	6

Figures 4.5, 4.6, and 4.7 show the chromatograms of exhibit MSU900-01 extracted by MAE/HS-SPME, HS-SPME, and LLE, respectively. The chromatograms have been truncated to show only the region from 2-30 minutes as this is the region of interest. Peaks in the chromatograms are labeled with the identity of the component or impurity. Peaks labeled with an asterisk (*) are present in the blank, some of which are siloxanes from the SPME fiber.

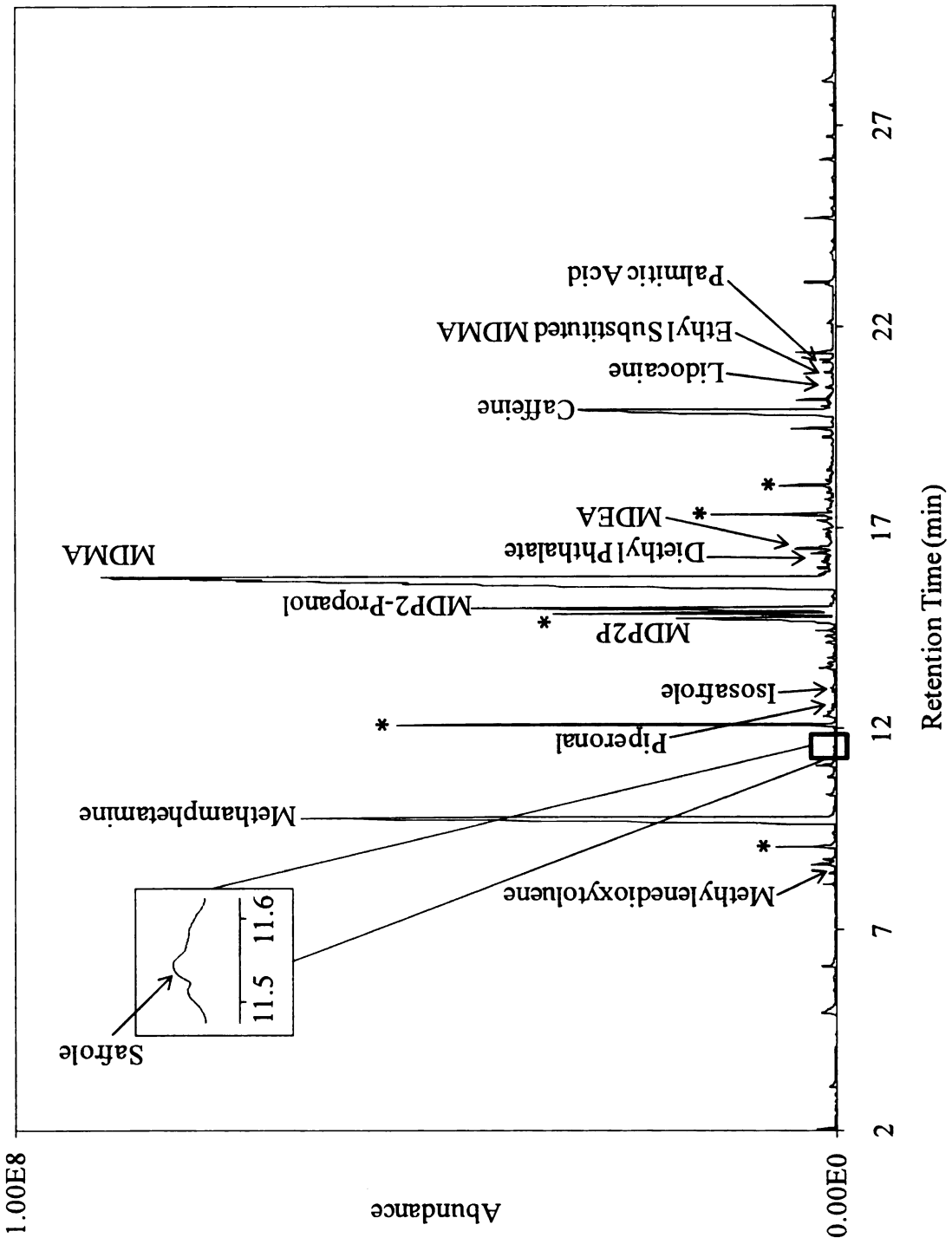

Figure 4.5: Chromatogram of MDMA exhibit MSU900-01 extracted by MAE/HS-SPME; an asterisk (*) indicates that the peak was present in the blank

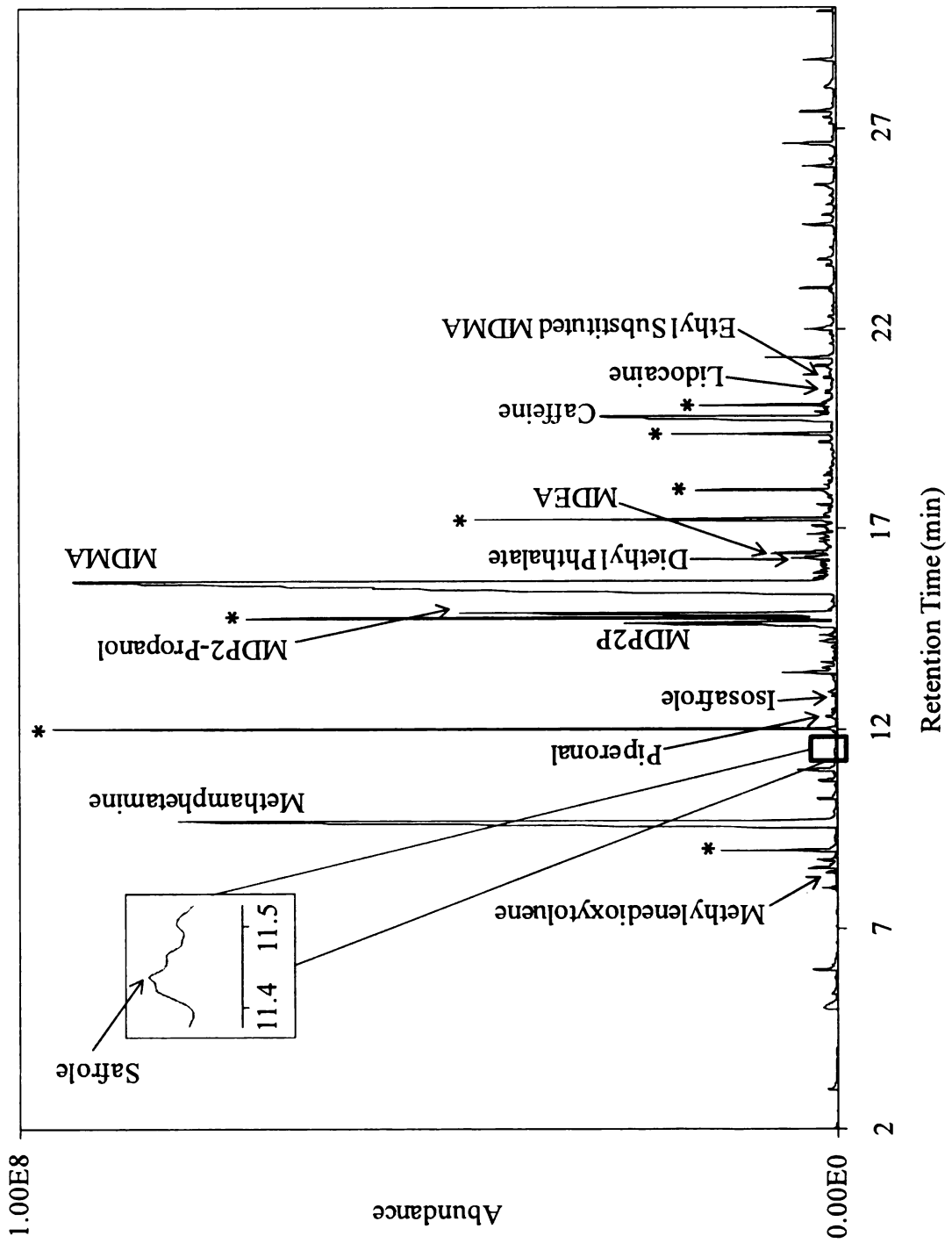

Figure 4.6: Chromatogram of MDMA exhibit MSU900-01 extracted by HS-SPME; an asterisk (*) indicates that the peak was present in the blank

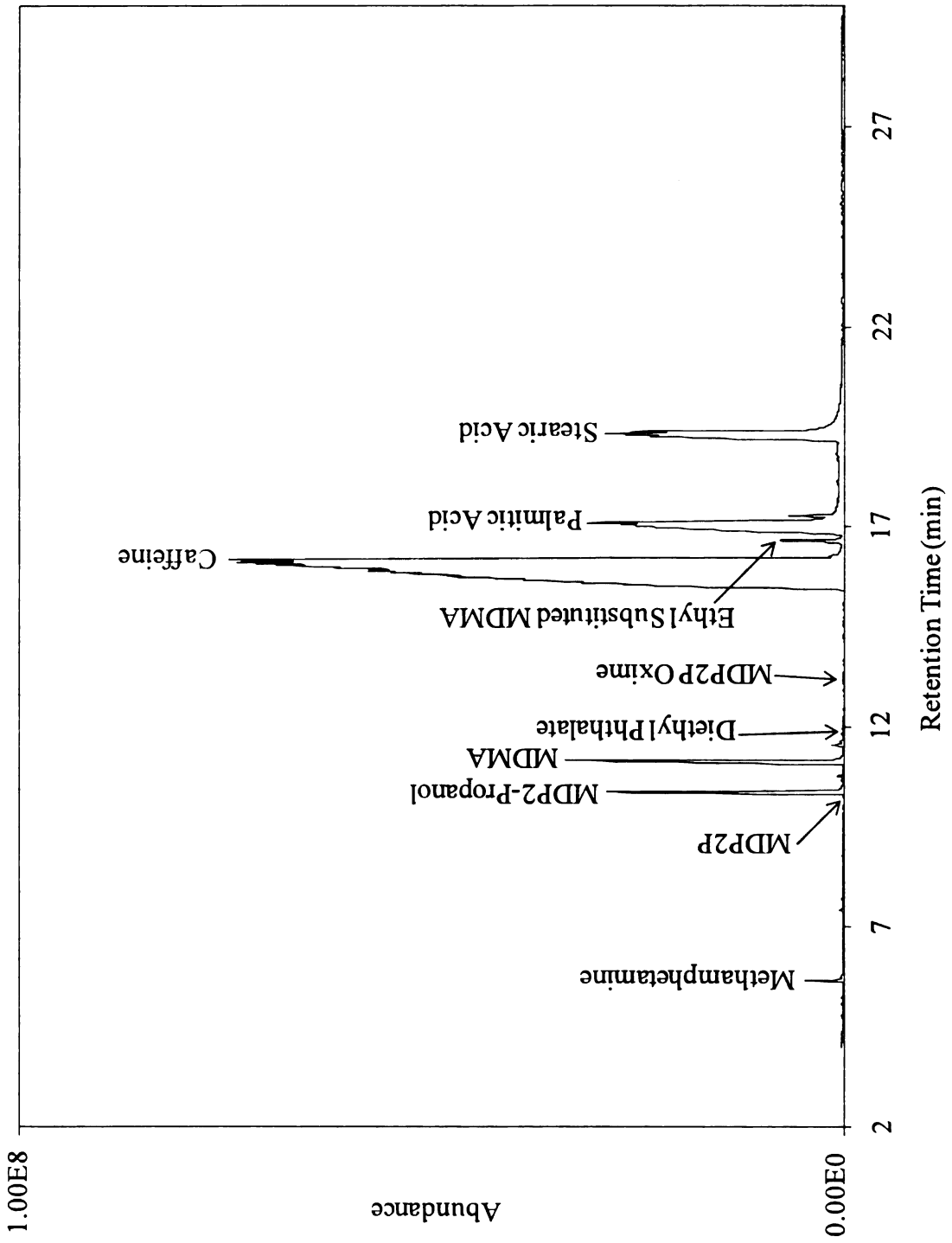

Figure 4.7: Chromatogram of MDMA exhibit MSU900-01 extracted by LLE

More impurities were extracted from exhibit MSU900-01 using MAE/HS-SPME and HS-SPME than LLE. Headspace solid-phase microextraction pre-concentrates the impurities on the SPME fiber allowing the impurities to be extracted and detected above the background noise. However, there is no pre-concentration in LLE [4] and compounds present in the sample at trace levels may not be detected above the background noise in the chromatogram.

The impurity 3,4-methylenedioxytoluene was extracted using MAE/HS-SPME and HS-SPME, but not using LLE. This impurity is a by-product formed during the synthesis of MDP2P from safrole. This lack of detection was a limitation of the GC temperature program used for LLE analysis. The initial temperature of the GC program for LLE analysis was 90 °C with a four minute solvent delay to prevent saturation of the detector. After four minutes, the mass spectrometer turned on at which time the oven temperature was approximately 114 °C. Therefore, compounds with boiling points lower than 114 °C were not observed in the chromatogram. In contrast, for MAE/HS-SPME and HS-SPME, the initial oven temperature was 60 °C and the mass spectrometer delay was only two minutes, which allowed the sample to desorb from the fiber. Therefore, more impurities were observed at the beginning of the MAE/HS-SPME and HS-SPME chromatograms.

The impurities safrole, piperonal, and isosafrole were also only detected by MAE/HS-SPME and HS-SPME; however, this is due to the pre-concentration of the impurities on the SPME fiber. The presence of these impurities is indicative of the synthetic route used to synthesize MDP2P. Safrole is a common starting material for

MDP2P and is often extracted from sassafras oil, a naturally occurring substance [12]. Piperonal and isosafrole are intermediates in the synthesis of MDP2P [13].

The impurities MDP2P and 3,4-methylenedioxyphenyl-2-propanol (MDP2-propanol) were extracted by all three procedures but at higher concentrations by MAE/HS-SPME and HS-SPME. The impurity MDP2-propanol is a product of a side reaction in the synthesis of MDMA from MDP2P using reductive amination [8]. During the reductive amination, MDP2P is converted to an imine intermediate by amination reaction with methylamine. The intermediate is then reduced to MDMA during which a side reaction occurs converting the MDP2P to the alcohol form (MDP2-propanol).

The impurity 3,4-methylenedioxyethylamphetamine (MDEA), which is chemically similar to MDMA, was extracted by MAE/HS-SPME and HS-SPME at similar levels but not extracted by LLE due to its low concentration in the exhibit. While the origin of this impurity has not been tested or confirmed, it is possible that it originates from the amination of MDP2P by ethylamine ($CH_3CH_2NH_2$) which is an impurity present in methylamine (CH_3NH_2) [12].

Some tablet impurities, such as 1-(3,4-methylenedioxyphenyl)-2-propanone oxime (MDP2P oxime), were extracted by LLE but were not extracted by MAE/HS-SPME and HS-SPME. This oxime impurity originates from the synthesis of MDP2P from safrole through the β-nitroisosafrole route (see synthesis route 2 in Appendix A) [12]. Liquid-liquid extraction has the advantage of extracting components of low volatility that are not extracted by MAE/HS-SPME or HS-SPME thus giving complementary information to the SPME profiles. Therefore, more information about the sample can be gained if both HS-SPME (or MAE/HS-SPME) and LLE are used.

The impurity N-methyl-(1,2-methylenedioxy)-4-(1-ethyl-2-aminopropyl) benzene (ethyl substituted MDMA) was extracted by all three procedures. While the exact origin of this impurity is not known, it is similar in structure to N-ethyl,N-methyl(1,2-methylenedioxy)-4-(2-aminopropyl)benzene which is a by-product of the reductive amination of MDP2P by ethylamine which is an impurity in methylamine [12]. Therefore, the impurity detected in the chromatogram may be an indicator of the reductive amination route of MDMA synthesis.

A similar number of tablet components were extracted from exhibit MSU900-01 by all three extraction procedures. Although these components are not organic impurities which are the focus of this work, their extraction and detection in the tablet is important to provide additional information on the tablet production and manufacturing process.

Methamphetamine, MDMA, diethyl phthalate, and caffeine were extracted by all three procedures. Methamphetamine and caffeine are adulterants which are added to the synthesized MDMA before it is pressed into tablets to enhance the effects of the MDMA [1]. Diethyl phthalate is a plasticizer which is used as a binder in the tableting process [9]. Methamphetamine and diethyl phthalate were extracted in higher abundances by MAE/HS-SPME and HS-SPME than by LLE because of the pre-concentration of the compounds on the SPME fiber.

Caffeine was extracted at higher concentrations by LLE than by MAE/HS-SPME and HS-SPME. In the LLE chromatogram, the broad caffeine peak had a baseline width of 0.8 minutes whereas in the MAE/HS-SPME chromatogram, the caffeine peak had a baseline width of 0.2 minutes. In LLE, other extracted compounds that have a similar retention time to caffeine would likely be masked by the broad caffeine peak. In contrast,

using MAE/HS-SPME and HS-SPME, these compounds are less likely to be masked because the caffeine peak is narrower. The higher concentration of caffeine in LLE is due to its volatility. With a sublimation point of 180 °C [14], caffeine has a low volatility that limits its extraction by MAE/HS-SPME and HS-SPME, but does not affect its extraction by LLE. Even though caffeine has a high sublimation point, caffeine is still extracted by HS-SPME due to the high concentration in the sample. According to Equation 4.1 (which was previously discussed in Chapter 2), as the concentration of the compound in the initial solution, C_o, increases, a higher mass of the compound, n_f, will be extracted by the fiber.

$$n_f = \frac{K_{fs} V_f V_s C_o}{K_{fs} V_f + K_{hs} V_h + V_s} \tag{4.1}$$

Lidocaine, a local anesthetic that can be added to the MDMA before it is pressed into tablets, was detected in the MAE/HS-SPME and HS-SPME chromatograms. The MAE/HS-SPME and HS-SPME allow for components and impurities present at trace levels to be pre-concentrated on the fiber, thus allowing the compounds to be extracted and detected above the baseline. However, in LLE, trace level impurities may be difficult to detect above the background noise since there is no pre-concentration.

Fatty acids such as palmitic acid and stearic acid are used as lubricants in the tableting process [9]. Palmitic acid was extracted by both MAE/HS-SPME and LLE, with LLE extracting the component at higher concentrations because of the low volatility of the component. However, the fatty acid was not extracted using SPME alone. Theoretically, a highly efficient extraction is achieved by MAE allowing for all components to be extracted into solution. In contrast, during HS-SPME alone, the entire sample did not completely dissolve into solution. Analytes transfer more readily from

solution into the headspace than from a solid into the headspace. Therefore, following MAE, the entire sample was in solution and more of the sample transferred into the headspace for extraction.

Meanwhile, stearic acid was only extracted by LLE. Because of the higher boiling point of the stearic acid compared to palmitic acid, the HS-SPME equilibrium would favor the solution and little of the component would be present in the headspace to be extracted by the fiber. The mass extracted by the fiber, if any, was too small to be detected above the background. Therefore stearic acid was not observed in the MAE/HS-SPME or HS-SPME chromatograms. However, because LLE is not dependent on the volatility of the compound, stearic acid was extracted by LLE.

To determine the precision of the extraction procedures, the chromatograms were retention time aligned, and, using the entire chromatogram, the average PPMC coefficients of each set of triplicates and their standard deviations were calculated and are shown in Table 4.8.

Table 4.8: Average PPMC coefficients and standard deviations of MDMA exhibit MSU900-01 associated with each extraction procedure

Extraction	Average PPMC (n=3)	Standard Deviation
MAE/HS-SPME	0.9501	0.0264
HS-SPME	0.9271	0.0399
LLE	0.9330	0.0190

A PPMC coefficient between 0.8-1.0 indicates a strong positive correlation [15]. Ideally, PPMC coefficients of replicates should be at least 0.99, indicating close to perfect correlation between the replicates. However, variability in the sample, sample preparation, and extraction procedure among replicate extractions can cause lower PPMC coefficients. For example, the sample may not have been completely homogenized prior

to analysis. Also, slight fluctuations in the temperature of the water bath used for HS-SPME (plus or minus 2-3 °C) could have caused the variation between replicate extractions. Retention time misalignments also could have contributed to the lower PPMC coefficients. For example, in the chromatogram of this exhibit, several small peaks were present at the beginning of the chromatogram (first 10 minutes) that were only slightly higher than the baseline noise. These peaks were not well aligned by the alignment algorithm which may have contributed to the lower PPMC coefficients. Despite these factors, the PPMC coefficients of the replicates were greater than 0.92 indicating a strong correlation among replicates and a precise extraction.

The PPMC coefficient of the MAE/HS-SPME replicates is higher than HS-SPME. Because the sample was entirely in solution following MAE, the MAE/HS-SPME extraction was more precise than with HS-SPME alone. The standard deviation shows the range of differences in the PPMC coefficients among the replicates. The standard deviation of the HS-SPME procedure was higher than the standard deviation for the MAE/HS-SPME replicates showing that the replicates of the MAE/HS-SPME procedure were more similar than the replicates of the HS-SPME procedure. The LLE procedure showed a similar PPMC coefficient to HS-SPME; however, for LLE, the standard deviation was approximately half that for HS-SPME. Again, this is due to misalignments in the HS-SPME chromatograms, mainly in the early eluting peaks.

4.4.2.2. MDMA Exhibit T-17

In total, 66 different impurities and components were extracted from exhibit T-17 by the different procedures and are summarized in Table 4.9.

Table 4.9: Number of impurities and components extracted from MDMA exhibit T-17

Extraction	Number of Impurities	Number of Other Components
MAE/HS-SPME	40	5
HS-SPME	35	5
LLE	23	7

Figures 4.8, 4.9, and 4.10 show the chromatograms of exhibit T-17 extracted by MAE/HS-SPME, HS-SPME, and LLE, respectively. The chromatograms have been truncated to show only the region from 2-30 minutes as this is the region of interest. Peaks in the chromatograms are labeled with the identity of the component or impurity. Peaks labeled with an asterisk (*) are present in the blank, some of which are siloxanes from the SPME fiber.

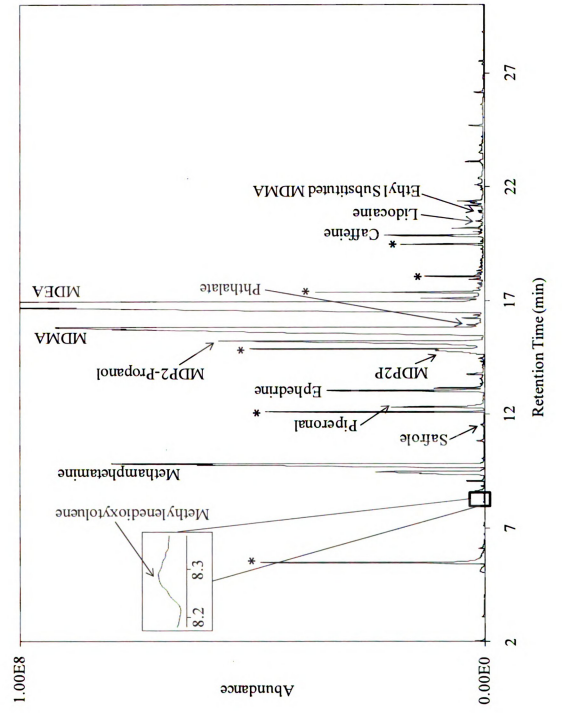

Figure 4.8: Chromatogram of MDMA exhibit T-17 extracted by MAE/HS-SPME; an asterisk (*) indicates that the peak was present in the blank

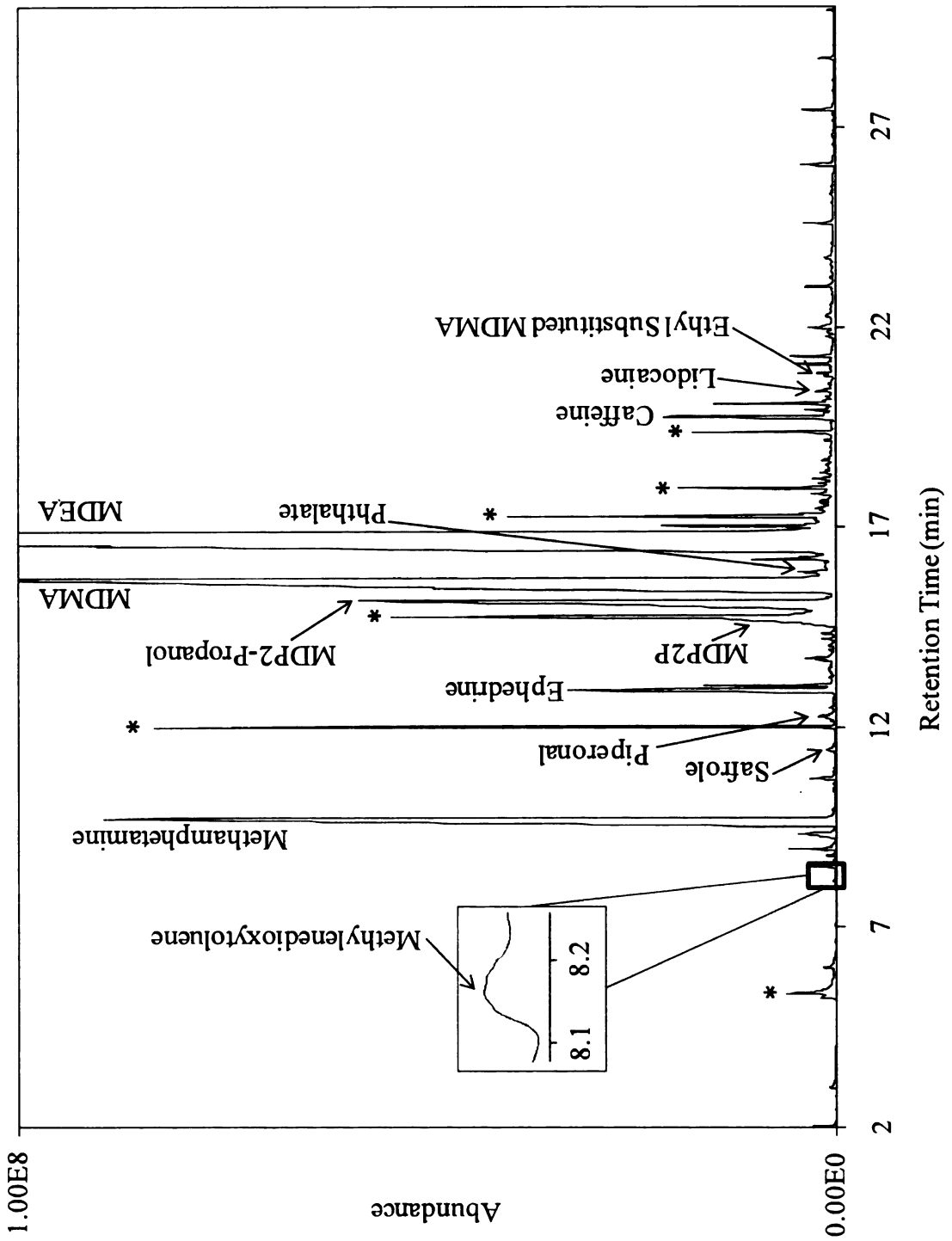

Figure 4.9: Chromatogram of MDMA exhibit T-17 extracted by HS-SPME; an asterisk (*) indicates that the peak was present in the blank

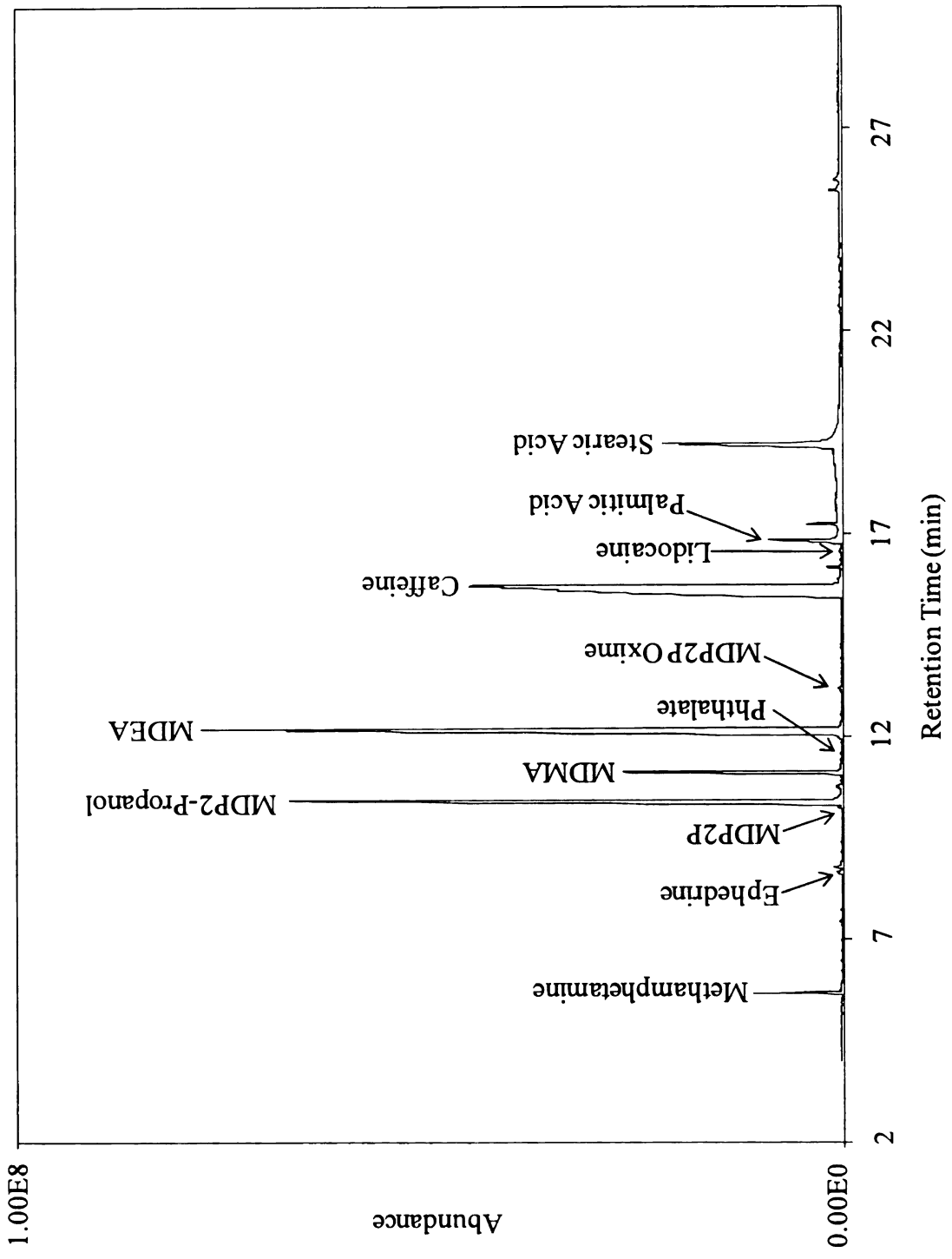

Figure 4.10: Chromatogram of MDMA exhibit T-17 extracted by LLE

More impurities were extracted using the MAE/HS-SPME and HS-SPME procedures than using the LLE procedure due to pre-concentration of the impurities on the SPME fiber. There were five more impurities extracted by MAE/HS-SPME than by HS-SPME alone due to the theoretically higher extraction efficiency of the microwave which extracts the entire sample into solution. In HS-SPME alone, some of the sample remains in the solid state. Compounds in solution move more easily into the headspace than compounds that are in the solid form. Therefore, with the entire sample in solution more impurities were extracted by MAE/HS-SPME.

The impurities 3,4-methylenedioxytoluene, safrole, and piperonal were extracted by both MAE/HS-SPME and HS-SPME. Ephedrine, which is a starting material in the synthesis of methamphetamine [2], was extracted by all three procedures. Ephedrine can also be an adulterant added to the MDMA after the MDMA was synthesized. However due to the low abundance of ephedrine in the LLE chromatogram, it is more likely that the ephedrine was present in the tablets at low levels suggesting it was an impurity from the synthesis of methamphetamine.

The impurities MDP2P and MDP2-propanol were extracted by all three procedures. The MDP2P was extracted at trace levels in the LLE chromatogram due to its low concentration in the sample and the lack of pre-concentration in LLE. In the chromatograms of all three procedures, MDEA was the most abundant peak. The impurity N-methyl-(1,2-methylenedioxy)-4-(1-ethyl-2-aminopropyl) benzene (ethyl substituted MDMA) was extracted by MAE/HS-SPME and HS-SPME but was not extracted by LLE. Once again, MDP2P oxime was only extracted by LLE due to its volatility.

More tablet components were extracted by LLE than by the other two procedures because LLE is not dependent on the volatility of the compound. For example, the fatty acids palmitic acid and stearic acid were only extracted by LLE. However, palmitic acid was extracted by MAE/HS-SPME from exhibit MSU900-01. Palmitic acid and stearic acid were present in lower concentrations in exhibit T-17 compared to exhibit MSU900-01 as is evident from the less abundant peaks. When a lower concentration of a compound is present in the starting solution, there is less available for extraction by the fiber based on Equation 4.1. Therefore, the fatty acids were not detected above the baseline in MAE/HS-SPME or HS-SPME for exhibit T-17 while palmitic acid was detected from exhibit MSU900-01 by MAE/HS-SPME.

Methamphetamine, MDMA, caffeine, and lidocaine were extracted by all three procedures. A phthalate peak was detected by all three procedures but at higher concentrations in the MAE/HS-SPME and HS-SPME chromatograms due to its pre-concentration on the SPME fiber.

The average PPMC coefficients and the standard deviations of the triplicate chromatograms for each extraction procedure are shown in Table 4.10.

Table 4.10: Average PPMC coefficients and standard deviations of MDMA exhibit T-17 associated with each extraction procedure

Extraction	Average PPMC (n=3)	Standard Deviation
MAE/HS-SPME	0.9943	0.0016
HS-SPME	0.9975	0.0008
LLE	0.9812	0.0050

The three extraction procedures have similar PPMC coefficients of 0.98 or higher indicating a very strong correlation between the replicates. There were fewer misalignments for exhibit T-17 than for exhibit MSU900-01 resulting in the higher

PPMC coefficients for exhibit T-17. The low standard deviations show that the replicate extractions were very similar indicating good precision.

4.4.2.3. MDMA Exhibit T-27

In total, 75 different impurities and components were extracted from exhibit T-27 and are summarized in Table 4.11.

Table 4.11: Number of impurities and components extracted from MDMA exhibit T-27

Extraction	Number of Impurities	Number of Other Components
MAE/HS-SPME	50	6
HS-SPME	46	5
LLE	14	6

Figures 4.11, 4.12, and 4.13 show the chromatograms of exhibit T-27 extracted by MAE/HS-SPME, HS-SPME, and LLE, respectively. The chromatograms have been truncated to show only the region from 2-30 minutes as this is the region of interest. Peaks in the chromatograms are labeled with the identity of the component or impurity. Peaks labeled with an asterisk (*) are present in the blank, some of which are siloxanes from the SPME fiber.

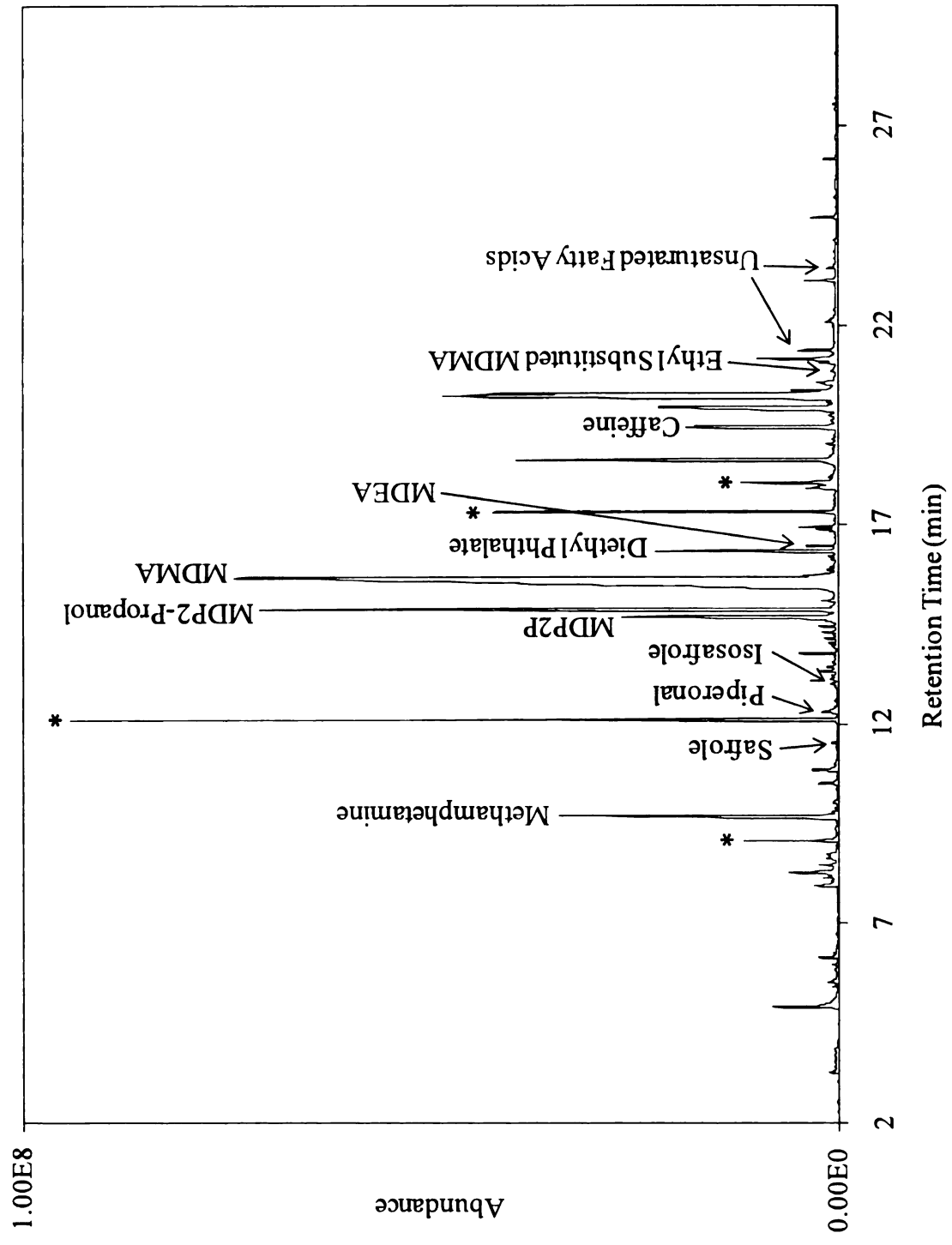

Figure 4.11: Chromatogram of MDMA exhibit T-27 extracted by MAE/HS-SPME; an asterisk (*) indicates that the peak was present in the blank

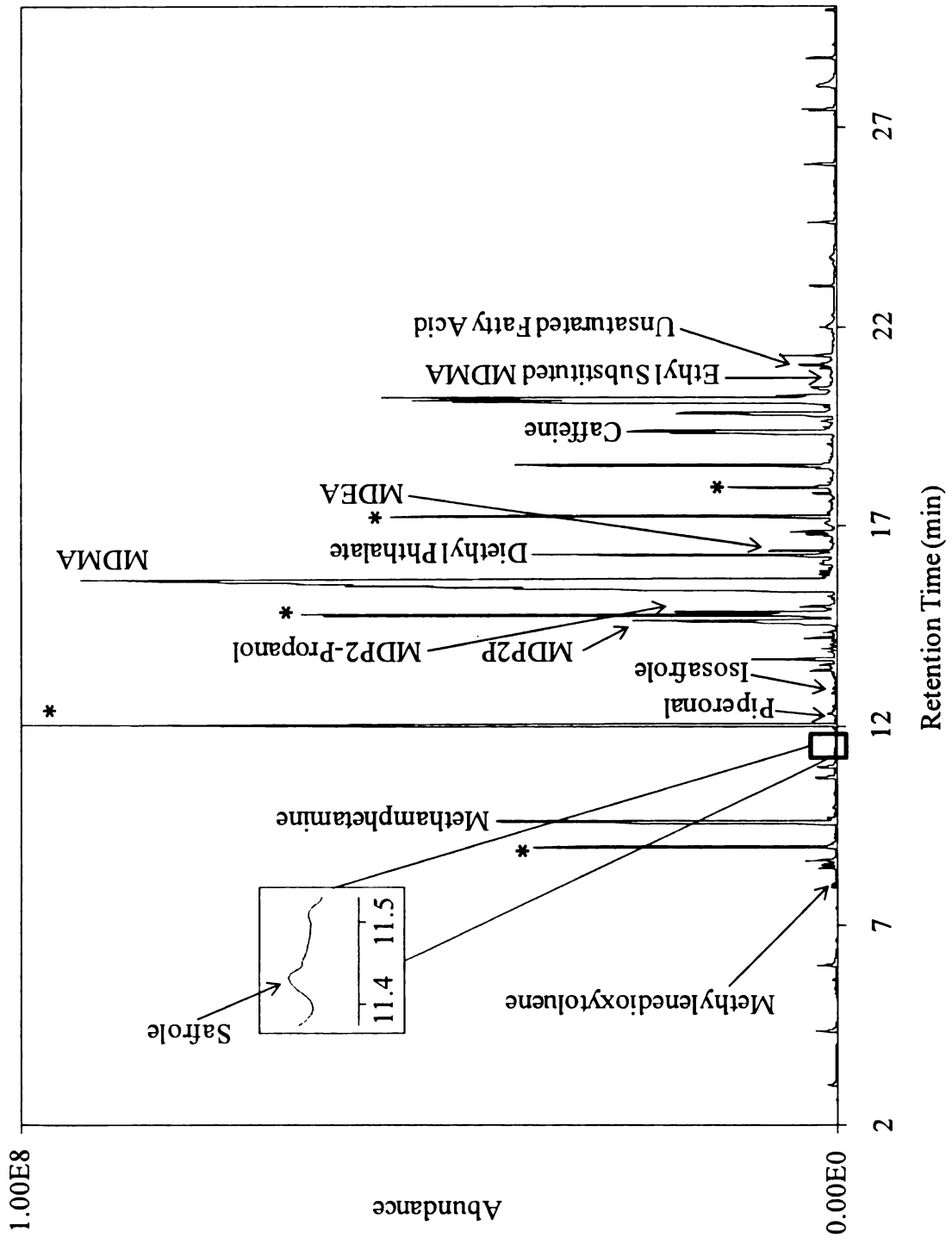

Figure 4.12: Chromatogram of MDMA exhibit T-27 extracted by HS-SPME; an asterisk (*) indicates that the peak was present in the blank

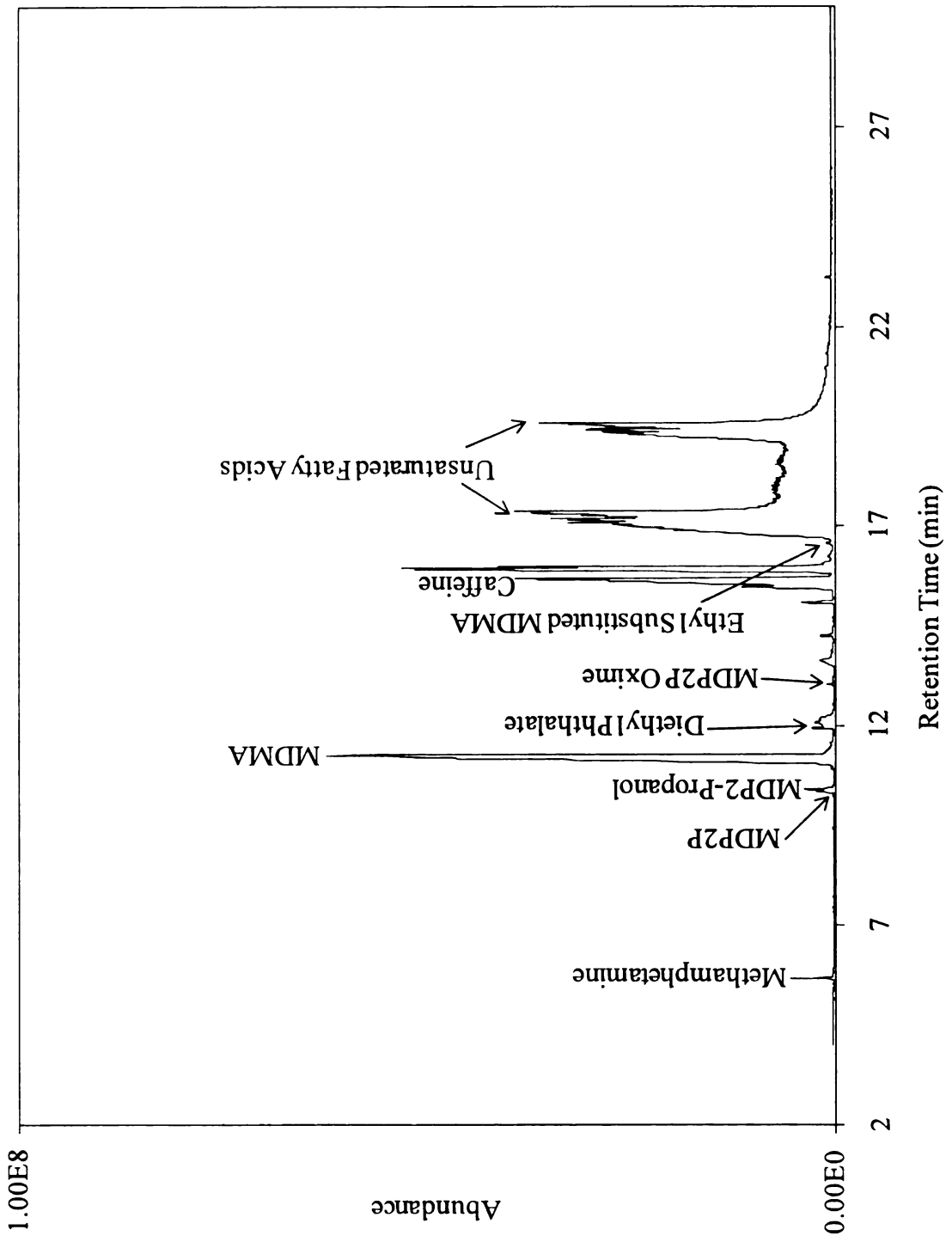

Figure 4.13: Chromatogram of MDMA exhibit T-27 extracted by LLE

More impurities were extracted by the MAE/HS-SPME and HS-SPME procedures than by the LLE procedure. The MAE/HS-SPME procedure extracted six impurities that eluted during the first ten minutes of the GC-MS analysis that were not present in the HS-SPME extract analysis. Higher molecular weight compounds may be degrading during the MAE resulting in the formation of lower molecular weight compounds with lower boiling points. Because these compounds have not yet been identified, this hypothesis cannot be confirmed.

The impurity 3,4-methylenedioxytoluene was only detected in the HS-SPME chromatogram. The impurity may have been present in the MAE/HS-SPME extract, but other unidentified peaks were present in the retention time range may have masked the impurity since it is only present at trace levels. The impurities safrole, piperonal, isosafrole, and MDEA were extracted by both MAE/HS-SPME and HS-SPME but not detected in the LLE chromatograms because of their low concentration. The impurities MDP2P and MDP2-propanol were extracted by all three procedures, but at lower abundances by LLE than the other two extractions due to the lack of pre-concentration. The impurity N-methyl-(1,2-methylenedioxy)-4-(1-ethyl-2-aminopropyl) benzene (ethyl substituted MDMA) was extracted by all three procedures at similar abundances. The impurity MDP2P-oxime was extracted by LLE but not by MAE/HS-SPME or HS-SPME due to its low volatility

The components methamphetamine, MDMA, diethyl phthalate, caffeine, and fatty acids were extracted by all three procedures. Unsaturated fatty acids were extracted in higher concentrations by LLE resulting in broad peaks. Unsaturated fatty acids are best separated by polar GC columns while saturated fatty acids can be separated by non-polar

columns [16]. The column used for this research, an Rxi™-5ms, is a non-polar column composed of a 5% diphenyl and 95% dimethylpolysiloxane stationary phase. Therefore, it is possible that the fatty acids present in exhibit T-27 are unsaturated fatty acids resulting in the poor chromatography. The fatty acids were extracted by MAE/HS-SPME and HS-SPME but in low concentrations due to the low volatility of the components.

The average PPMC coefficients and the standard deviation associated with the triplicates of each extraction procedure are shown in Table 4.12. As mentioned earlier, ideally, PPMC coefficients of replicates should be at least 0.99. The values for these replicates show strong correlation, but not as strong as expected for replicates. This is again possibly due to slight changes in the extraction procedure such as the small fluctuations in the temperature of the water bath. The HS-SPME procedure shows the lowest PPMC coefficient, but still indicates a strong correlation. The higher PPMC coefficients for MAE/HS-SPME and LLE indicate these two procedures are more precise than the HS-SPME procedure. The standard deviations of the MAE/HS-SPME and LLE procedures are lower than the standard deviation for the HS-SPME procedure. This indicates that the replicates for MAE/HS-SPME and LLE are more similar than replicates of the HS-SPME procedure.

Table 4.12: Average PPMC coefficients and standard deviations of exhibit T-27 associated with each extraction procedure

Extraction	Average PPMC (n=3)	Standard Deviation
MAE/HS-SPME	0.9798	0.0044
HS-SPME	0.9388	0.0221
LLE	0.9776	0.0093

4.4.3. Summary

Table 4.13 summarizes the number of impurities and other components extracted from each exhibit by each extraction procedure. As evident in the table, the number of impurities extracted from each exhibit by MAE/HS-SPME and HS-SPME is greater than the number of impurities extracted by LLE. The number of other components extracted from each of the exhibits by each of the procedures is similar. The average PPMC coefficients and standard deviations are also shown in the table. The PPMC coefficients of the replicates indicate a strong positive correlation among replicates of each MDMA exhibit extracted by each procedure. However, as mentioned previously, these PPMC coefficients are not as strong as expected for replicates (expect 0.99 or greater) because of small changes in the extraction procedure between replicates.

Table 4.13: Summary of number of impurities and components extracted from each MDMA exhibit by each extraction procedure; also shown are average PPMC coefficients and standard deviations for each exhibit extracted by each procedure

Exhibit	Extraction	Number of Impurities	Number of Other Components	Average PPMC (n=3)	Standard Deviation
A	MAE/HS-SPME	42	6	0.9501	0.0264
	HS-SPME	46	5	0.9271	0.0399
	LLE	8	6	0.9330	0.0190
B	MAE/HS-SPME	40	5	0.9943	0.0016
	HS-SPME	35	5	0.9975	0.0008
	LLE	23	7	0.9812	0.0050
C	MAE/HS-SPME	50	6	0.9798	0.0044
	HS-SPME	46	5	0.9388	0.0221
	LLE	14	6	0.9776	0.0093

Despite extracting more impurities than LLE and HS-SPME with good precision, MAE/HS-SPME has several downsides that make its use for the organic impurity profiling of MDMA tablets unrealistic at this point. The MAE/HS-SPME procedure requires the use of an additional instrument which increases the cost of analysis. In addition, extra time is required to complete the analysis, and because vessels and inserts are reused, there is the possibility of sample carryover between extractions.

The HS-SPME procedure extracts more impurities than the LLE procedure with similar precision. During this procedure, the sample is left unattended for 40 minutes allowing the scientist to continue with other work. Because the vials used for HS-SPME can be discarded, the possibility of carryover is overcome using HS-SPME alone, assuming the fiber is properly cleaned after each experiment. However, special equipment must be purchased to use HS-SPME which increases the cost of analysis. For example, the fibers and fiber holder as well as different GC inlet parts (e.g. liner, Merlin Microseal™, etc.) must be purchased.

The LLE procedure extracts the fewest impurities from the MDMA exhibits of the three procedures studied. Because the LLE procedure uses equipment commonly found in the laboratory (e.g. sonicator, centrifuge, and vortex), the cost of analysis is relatively low. However, the procedure requires more hands-on time during the extraction because no single step in the extraction procedure is longer than 10 minutes. Therefore, sufficient time for other work is not available.

If the costs of the fibers and other equipment can be absorbed, HS-SPME is the best choice for extracting organic impurities from seized MDMA exhibits among the three procedures discussed in this work. The HS-SPME procedure offers a compromise

between the other two procedures: it extracts more impurities than LLE, but does so at a lower cost and shorter analysis time than MAE/HS-SPME. As mentioned earlier, LLE extracts components that were not extracted by HS-SPME. Therefore, if sufficient time, sample, and equipment are available, more information about the MDMA sample can be obtained by performing both HS-SPME and LLE with different aliquots of the same exhibit.

4.5. Comparison of MDMA Exhibits

Because HS-SPME is the best choice for extracting impurities from MDMA tablets, the HS-SPME chromatograms of each of the MDMA exhibits were used to compare the exhibits to one another and to determine the possible synthetic route used to manufacture the MDMA in each exhibit.

4.5.1. Comparison of MDMA Exhibits MSU900-01, T-17, and T-27

The impurities 3,4-methylenedioxytoluene, safrole, and piperonal were extracted from all three exhibits. These impurities are present from the synthesis of MDP2P which was also extracted from all three exhibits. Isosafrole, an intermediate in the synthesis of MDP2P from safrole, was extracted from exhibits MSU900-01 and T-27 but not from exhibit T-17. The presence of safrole and piperonal in all three exhibits suggests that the MDP2P in all exhibits was synthesized from safrole. However, the oxidation of isosafrole may have been more efficient for exhibit T-17 (see reaction schemes in Appendix A).

The utility of LLE in addition to HS-SPME is illustrated by the presence of the impurity MDP2P oxime in the LLE chromatograms of all three exhibits. This impurity indicates that the MDP2P was synthesized from the reduction of β-nitroisosafrole. Based

on the presence of safrole, piperonal, and MDP2P oxime, it is likely that the MDP2P oxime in all three exhibits was synthesized through Route 2 shown in Appendix A [12].

The presence of N-methyl-(1,2-methylenedioxy)-4-(1-ethyl-2-aminopropyl) benzene in all three exhibits suggests that the reductive amination route may have been used to convert MDP2P to MDMA. This impurity is structurally similar to N-ethyl,N-methyl(1,2-methylenedioxy)-4-(2-aminopropyl)benzene which is a by-product of the reductive amination of MDP2P by ethylamine, an impurity in methylamine [12]. Also, MDP2-propanol is formed during the reduction of MDP2P to MDMA. However, because the impurities N-methyl-(1,2-methylenedioxy)-4-(1-ethyl-2-aminopropyl) benzene and MDP2-propanol are not limited to the reductive amination route, the hypothesis that the reductive amination route was used to manufacture the MDMA in the three exhibits cannot be proven.

There are many similar active ingredients and other tablet components including adulterants and additives. Methamphetamine, MDMA, and caffeine were present in all three exhibits. Exhibits MSU900-01 and T-17 both contained lidocaine which was not present in exhibit T-27. Diethyl phthalate was extracted from exhibits MSU900-01 and T-27; however, a different, unidentified, phthalate was extracted from exhibit T-17. Fatty acids were only extracted by HS-SPME from exhibit T-27.

The exhibits can be discriminated from one another based on the presence and the levels of the impurities present in the tablets. In addition to the lack of isosafrole, the presence of ephedrine and the high abundance of MDEA in exhibit T-17 discriminate exhibit T-17 from the other two exhibits, MSU900-01 and T-27. Exhibit T-27 contained three major unidentified impurities (numbers 75, 81, and 87 in Appendix F) which were

not present in either of the other two exhibits thus discriminating exhibit T-27 from exhibits MSU900-01 and T-17. Even though the MDP2P and MDMA present in the three exhibits could have been synthesized by the same synthetic route, the three exhibits were likely produced by different laboratories because many tablet impurities and components were present in different concentrations [9].

4.5.2. Comparison of MDMA Exhibits T-17 and CJ-FS05

A fourth MDMA exhibit was available for comparison: CJ-FS05. Exhibit CJ-FS05 was obtained from the Michigan State Police Forensic Science Division Laboratory in Northville, MI, in March of 2007. This exhibit had similar physical characteristics to exhibit T-17, which was obtained from the Michigan State Police Forensic Sciences Division Laboratory in Bridgeport, MI, in January of 2009. Only one tablet was available for analysis from exhibit CJ-FS05. This tablet was ground with a mortar and pestle, and three 50 mg aliquots were extracted by the same HS-SPME procedure as used for the other MDMA exhibits. The resulting impurity profiles of exhibit CJ-FS05 were compared to profiles obtained from exhibit T-17. Figure 4.14 shows a comparison of the chromatograms of the two exhibits extracted by HS-SPME, and Appendix G lists all impurities and components extracted from these two exhibits.

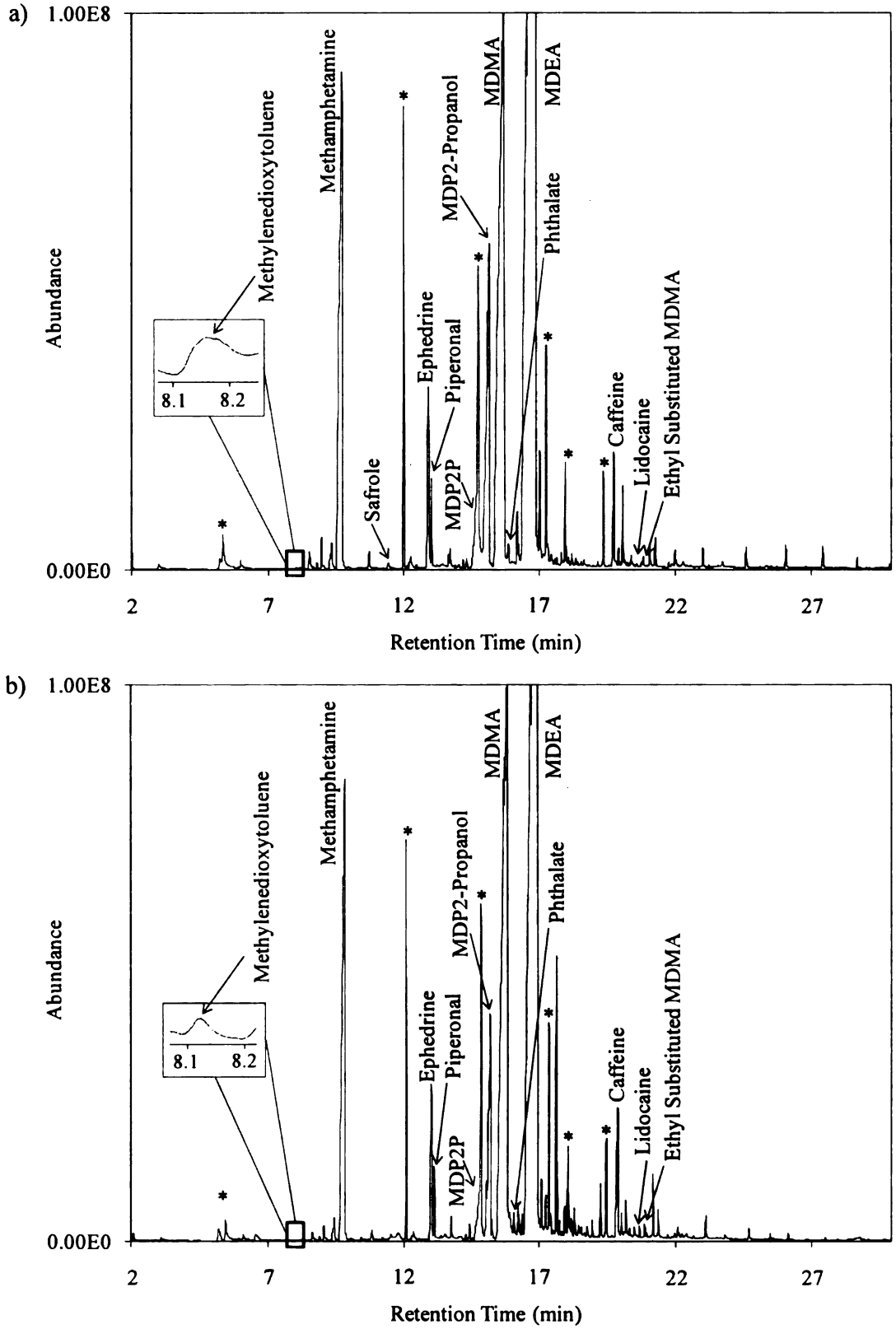

Figure 4.14: Chromatograms of MDMA exhibits a) T-17 and b) CJ-FS05 extracted by HS-SPME; an asterisk (*) indicates that the peak was present in the blank

As evident from the chromatograms, these two exhibits appear chemically similar. Most major peaks and identified peaks are present in both samples. However, the two exhibits differ by a few minor peaks. For example, safrole was extracted from exhibit T-17 but was not detected in exhibit CJ-FS05. Safrole was present in exhibit T-17 at trace levels; therefore, if safrole was present in exhibit CJ-FS05 at lower levels than in exhibit T-17, it would not have been detected above the baseline noise. Because these two samples have similar overall profiles that only differ slightly in impurities extracted and relative abundances, it is possible that these samples were produced by the same laboratory using the same synthetic route but potentially with the MDMA produced in different batches, which is consistent with the physical characteristics [9]. However, since only one tablet was available from exhibit CJ-FS05, a definitive conclusion cannot be made.

4.6. Summary

A MAE/HS-SPME procedure was optimized for the extraction of organic impurities from seized MDMA tablets. Using a 1 M phosphate buffer at pH 8, the MAE part of the procedure included a 23 minute ramp time to 100 °C and a 23 minute extraction time at 100 °C. The HS-SPME part of the procedure included a 5 minute pre-heat at 70 °C and a 40 minute extraction at 70 °C. This combination of procedures was compared to a LLE procedure available in the literature [4] and to the HS-SPME procedure alone using a simulated MDMA sample and seized MDMA tablets.

While MAE/HS-SPME extracted more impurities overall than HS-SPME alone or LLE, HS-SPME alone was determined to be the most practical procedure for the extraction of organic impurities of the extraction procedures studied. The limitations of

MAE/HS-SPME, which included a longer extraction time, higher costs, and contamination problems, made the MAE part of the extraction impractical. The shortcomings of LLE, which included fewer impurities extracted, made LLE a less desirable extraction procedure than HS-SPME.

Three MDMA exhibits were differentiated based on their chemical composition using HS-SPME alone. However, it was ultimately determined that HS-SPME and LLE gave complimentary information to one another, and therefore, if time and money allow, both procedures should be performed. Using both HS-SPME and LLE, the possible synthetic routes used to manufacture the MDP2P and the MDMA were determined for the three MDMA exhibits.

4.7. References

[1] Byrska B, Zuba D. Profiling of 3,4-Methylendioxymethamphetamine by Means of High-Performance Liquid Chromatography. Anal Bioanal Chem 2008; 390: 715-722.

[2] Kuwayma K, Tsujikawa K, Miyaguchi H, Kanamori T, Iwata Y, Inoue H, Saitoh S, Kishi T. Identification of Impurities and the Statistical Classification of Methamphetamine using Headspace Solid Phase Microextraction and Gas Chromatography-Mass Spectrometry. Forensic Sci Int 2006; 160: 44-52.

[3] C. Thompson. 2004 http://www.umt.edu/medchem/teaching/Lecture5-Pharmaceutics%20(buffer-partition).pdf <Accessed 8 June 2009>.

[4] van Deursen MM, Lock ERA, Poortman-van der Meer AJ. Organic impurity profiling of 3,4-methylenedioxymethamphetamine (MDMA) tablets seized in the Netherlands. Sci Justice 2006; 46: 135-152.

[5] Andersson K, Jalava K, Lock E, Huizer H, Kaa E, Lopes A, Poortman-van der Meer A, Cole MD, Dahlen J, Sippola E. Development of a Harmonised Method for the Profiling of Amphetamines IV. Optimisation of Sample Preparation. Forensic Sci Int 2007; 169: 64-76.

[6] Coumbaros JC, Kirkbride KP, Klass G. Application of Solid-Phase Microextraction to the Profiling of an Illict Drug: Manufacturing Impurities in Illicit 4-Methoxyamphetamine. J Forensic Sci 1999; 44: 1237-1242.

[7] Pawliszyn J. Solid Phase Microextraction: Theory and Practice. Wiley-VCH, New York; 1997.

[8] Swist M, Wilamowski J, Zuba D, Kochana J, Parczewski. Determination of Synthesis Route of 1-(3,4-methylenedioxyphenyl)-2-propanone (MDP2P) based on Impurity Profiles of MDMA. Forensic Sci Int 2005; 149: 181-192.

[9] Palhol F, Boyer S, Naulet N, Chabrillat M. Impurity profiling of seized MDMA tablets by capillary gas chromatography. Anal Bioanal Chem 2002; 374: 274-281.

[10] Araujo PW, Brereton RG. Experimental Design II. Optimization. Trends Anal Chem 1996; 15: 63-70.

[11] Wercinski SA ed. Solid Phase Microextraction: A Practical Guide. Marcel Dekker, Inc., New York; 1999.

[12] Gimeno P, Besacier F, Bottex M, Dujourdy L, Chaudron-Thozet H. A Study of Impurities in Intermediates and 3,4-Methylenedioxymethamphetamine (MDMA) Samples Produced via Reductive Amination Routes. Forensic Sci Int 2005; 155: 141-157.

[13] Gimeno P, Besacier F, Chaudron-Thozet H, Girard J, Lamotte A. A Contribution to the Chemical Profiling of 3,4-Methylenedioxymethamphetamine (MDMA) Tablets. Forensic Sci Int 2002; 127: 1-44.

[14] Moffat AC, Jackson JV, Moss MS, Widdop B. Clarke's Isolation and Identification of Drugs. Pharmaceutical Society of Great Britain, London; 1986.

[15] Devore JL. Probability and Statistics for Engineering and the Sciences, 4th Ed. Duxbury Press, Belmont, CA; 1995.

[16] Baer I, Margot P. Analysis of Fatty Acids in Ecstasy Tablets. Forensic Sci Int 2009; doi 10.1016/ i.forsciint.2009.03.015.

Chapter 5 Conclusions and Future Work

5.1. Conclusions

A microwave-assisted extraction (MAE) procedure was developed and optimized for the extraction of organic impurities from seized MDMA tablets. Three different types of buffers at three different pH values and concentrations were studied to determine the optimum buffer for use with the microwave extraction. Using a simulated sample containing benzylamine, phenethylamine, methamphetamine, ephedrine, and caffeine, the optimum buffer for use with the microwave was determined to be 1 M phosphate buffer at pH 8. This buffer allowed for the precise extraction of all components with no sample carryover in the vessels between extractions. Buffers of lower pH did not extract all components of the simulated sample or extracted components with poor precision. Buffers of higher pH extracted all components; however, carryover of the sample in the microwave vessel between sample extractions limited the use of high pH buffers.

A full factorial experimental design in four blocks was used to determine the microwave parameters that had an effect on the extraction of impurities from MDMA samples. Using the simulated sample, the parameters of ramp time, extraction time, and extraction temperature were studied. Ramp time and extraction time were studied at times of 10 and 20 minutes with a center point of 15 minutes, while the extraction temperature was studied at 80 °C and 120 °C with a center point of 100 °C. From this experimental design, all three parameters were found to have a significant effect on the extraction of the simulated sample components.

The three parameters of ramp time, extraction time, and extraction temperature were then optimized using the simulated sample in a circumscribed central composite

(CCC) experimental design. In the CCC design the range of values for the ramp time and extraction time was 7-23 minutes and the range of values for the extraction temperature was 66-134 °C. Using a desirability function, the optimum parameters determined were determined to be a 23 minute ramp time to 100 °C and a 23 minute extraction time at 100 °C. These parameters allowed for the minimization of the methamphetamine and caffeine peaks while allowing for the maximization of benzylamine and phenethylamine peaks.

Because of the efficient extraction of the microwave, a second, more selective extraction technique, headspace solid-phase microextraction (HS-SPME), was utilized to selectively extract the organic impurities from the sample. The HS-SPME parameters of extraction time and extraction temperature were optimized empirically. The extraction time was studied over a range of 10-60 minutes holding the extraction temperature at 70 °C. The extraction temperature was studied over a range of 40-80 °C holding the extraction time at 40 minutes. The shorter extraction times (10-30 minutes) and lower extraction temperatures (40-60 °C) did not extract as many impurities as the longer extraction times (40-60 minutes) and higher extraction temperatures (70-80 °C). However, the longest extraction times (50-60 °C) and highest extraction temperature (80 °C) resulted in the extraction of components, such as MDMA, in high concentrations resulting in broad peaks that could potentially mask impurities present at lower concentrations. An extraction time of 40 minutes and an extraction temperature of 70 °C were chosen as the optimum HS-SPME parameters because these parameters offered high impurity abundance without sacrificing chromatography.

Finally, the developed MAE/HS-SPME and HS-SPME procedures were compared to a liquid-liquid extraction (LLE) procedure from the literature [1] using three seized MDMA exhibits. The combination of MAE/HS-SPME allowed for the extraction of more impurities and components than HS-SPME and LLE. However, MAE/HS-SPME had limitations that restricted its use for organic impurity profiling such as increased extraction time and increased cost. Also, a problem of sample carryover in the microwave vessels and inserts between extractions limited the use of MAE for the extraction of impurities from MDMA exhibits. The LLE procedure required the least amount of new equipment therefore offering the lowest cost. However, more analyst involvement was required to complete the steps of the extraction and fewer components were extracted and detected. Because of these limitations, HS-SPME was determined to be the most practical extraction procedure of the three procedures studied for the extraction of organic impurities from MDMA exhibits. The HS-SPME procedure offered the extraction of more impurities than LLE and did not have the limitation of sample carryover between extractions like MAE. Also, the cost of HS-SPME analysis was less than the MAE/HS-SPME analysis because the microwave was not needed.

All three extraction procedures allowed for the extraction of impurities and components from the MDMA exhibits that helped to determine the synthetic route used to manufacture the MDMA in the exhibits. Using the chromatograms of the MDMA exhibits extracted by HS-SPME and LLE, the possible synthetic route for the synthesis of 3,4-methylenedioxyphenyl-2-propanone (MDP2P) and MDMA were determined. The MDP2P present in the exhibits could have been synthesized from safrole through the β-nitroisosafrole route (Route II shown in Appendix A). The MDMA may have been

synthesized using the reductive amination route (shown in Appendix B); however, few impurities were identified to establish this link and therefore the determination of the use of this route is a preliminary hypothesis. Based on the chromatograms of the MDMA exhibits obtained by HS-SPME, the three MDMA exhibits were successfully differentiated from one another based on chemical composition.

This work shows that the developed HS-SPME procedure can be utilized for organic impurity profiling of MDMA exhibits. Because of the pre-concentration of the impurities on the fiber, many impurities are extracted from MDMA samples, even those present at trace levels. Therefore, the synthetic route used to manufacture the MDMA could be determined with more certainty and more points of comparison among exhibits are available, thus aiding law enforcement in the connection of tablets from different MDMA exhibits.

Organic impurity profiling is more often performed in research laboratories than in local state and city crime laboratories. Often, local law enforcement laboratories are only interested in the active ingredients present in the MDMA tablets, such as MDMA and methamphetamine. Therefore, the MAE/HS-SPME and HS-SPME procedures optimized during this work (which were optimized for impurity extraction) are more likely to be utilized by research laboratories. However, HS-SPME may still be applicable to local crime laboratories. Because of the simple sample preparation (the sample is ground and placed in 5 mL of buffer) and the possibility of automation, the HS-SPME procedure could be optimized for the extraction of active ingredients and thus be relevant to local crime laboratories.

5.2. Future Work

Even though the MAE/HS-SPME procedure developed in this work has downfalls that hinder its use in a crime laboratory at this time, further work could be performed to successfully allow its use. Because one of the main downfalls of the use of the microwave was the sample carryover in the vessels between extractions, studies could be performed to determine a more efficient procedure to clean the microwave vessels and the quartz inserts. This would reduce the overall time required for MAE as well as overcome the contamination problem.

The application of Pearson product moment correlation (PPMC) coefficients can be expanded from comparing replicates of the same exhibit to comparing chromatograms from different exhibits. Other statistical procedures, such as hierarchical cluster analysis and principal components analysis, could also be applied to the data to determine the level of similarity or association among exhibits. By applying statistical procedures, the determination of the similarity of MDMA exhibits would be objective instead of subjective as was the case in this work, thus minimizing the possibility of experimenter bias.

As evident from this work, many unidentified impurities were extracted from the MDMA exhibits. Further work could be completed to determine the identity of these compounds. Tandem mass spectrometry is a technique that allows for the selection of target ions and further fragmentation of these ions in order to determine their structure. Ion trap mass spectrometers, like the one used in this work, have the ability to perform tandem mass spectrometry. By identifying more of the impurities extracted from MDMA

exhibits, more clues to the synthetic route used and more points of comparison among exhibits would be available.

Much of the work in identifying impurities in MDMA tablets has focused on the organic impurities. The study of the inorganic impurities present in the exhibits could also be useful for comparing tablets. Inductively-coupled plasma mass spectrometry (ICP-MS) can be used to identify trace metals present in the tablets. Once again, more points of comparison among exhibits increases the ability to link tablets from different MDMA exhibits to a common source or, alternatively, increase the certainty with which tablets are determined to be unrelated.

The extraction of organic impurities can assist law enforcement in determining the synthetic route used to manufacture the MDMA as well as link tablets from different exhibits to a common production source. Headspace solid-phase microextraction has proved useful in the extraction of the impurities. While some work still needs to be completed before the technique is fully applicable to crime laboratories, the extraction procedure shows promise in its eventual use.

5.3. References

[1] van Deursen MM, Lock ERA, Poortman-van der Meer AJ. Organic Impurity Profiling of 3,4-Methylenedioxymethamphetamine (MDMA) Tablets Seized in the Netherlands. Sci Justice 2006; 46: 135-152.

Appendix A: Synthesis Schemes of 3,4-Methylenedioxyphenyl-2-Propanone (MDP2P)

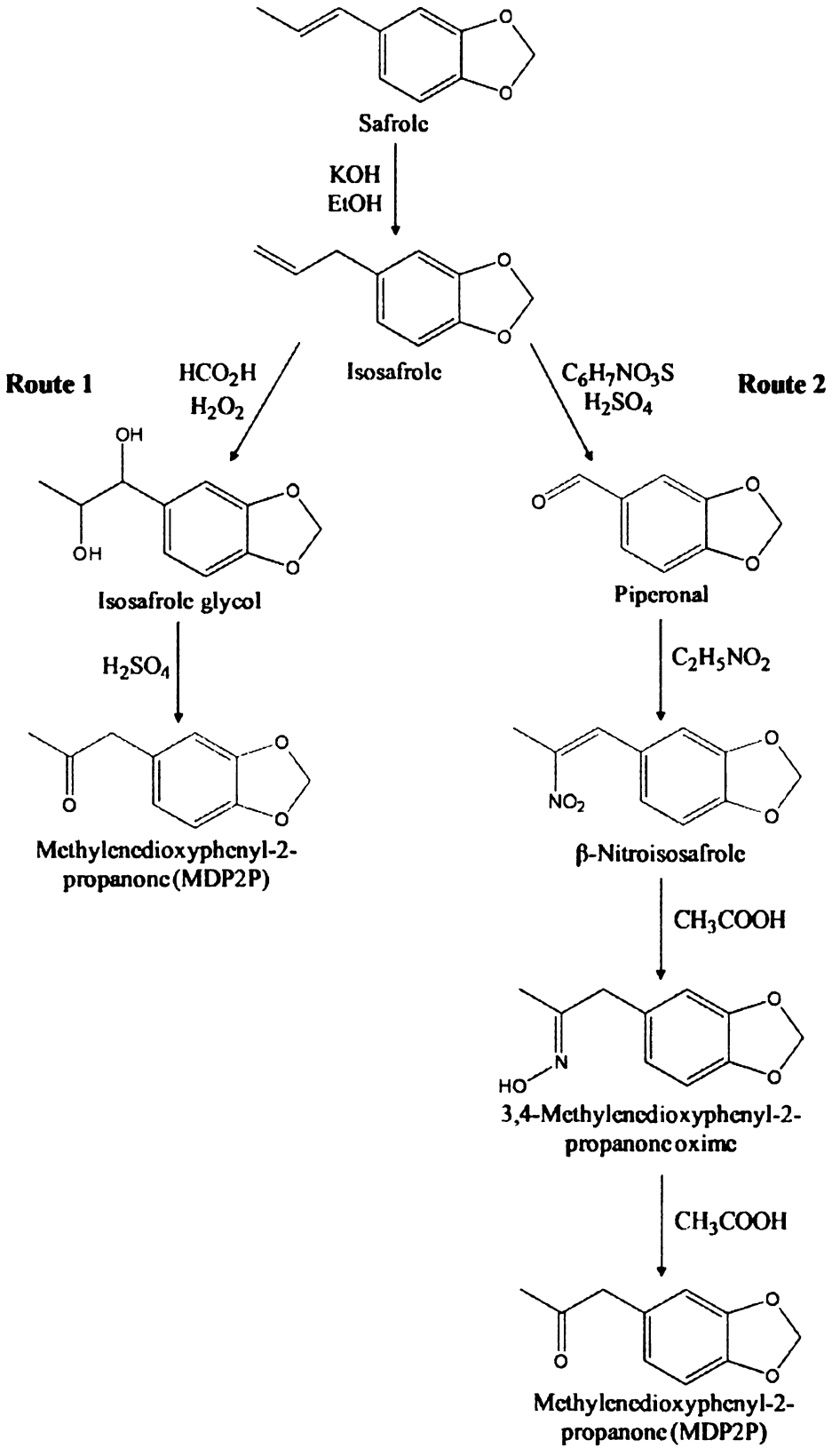

Appendix B: Synthesis Schemes of 3,4-Methylenedioxymethamphetamine (MDMA) from MDP2P

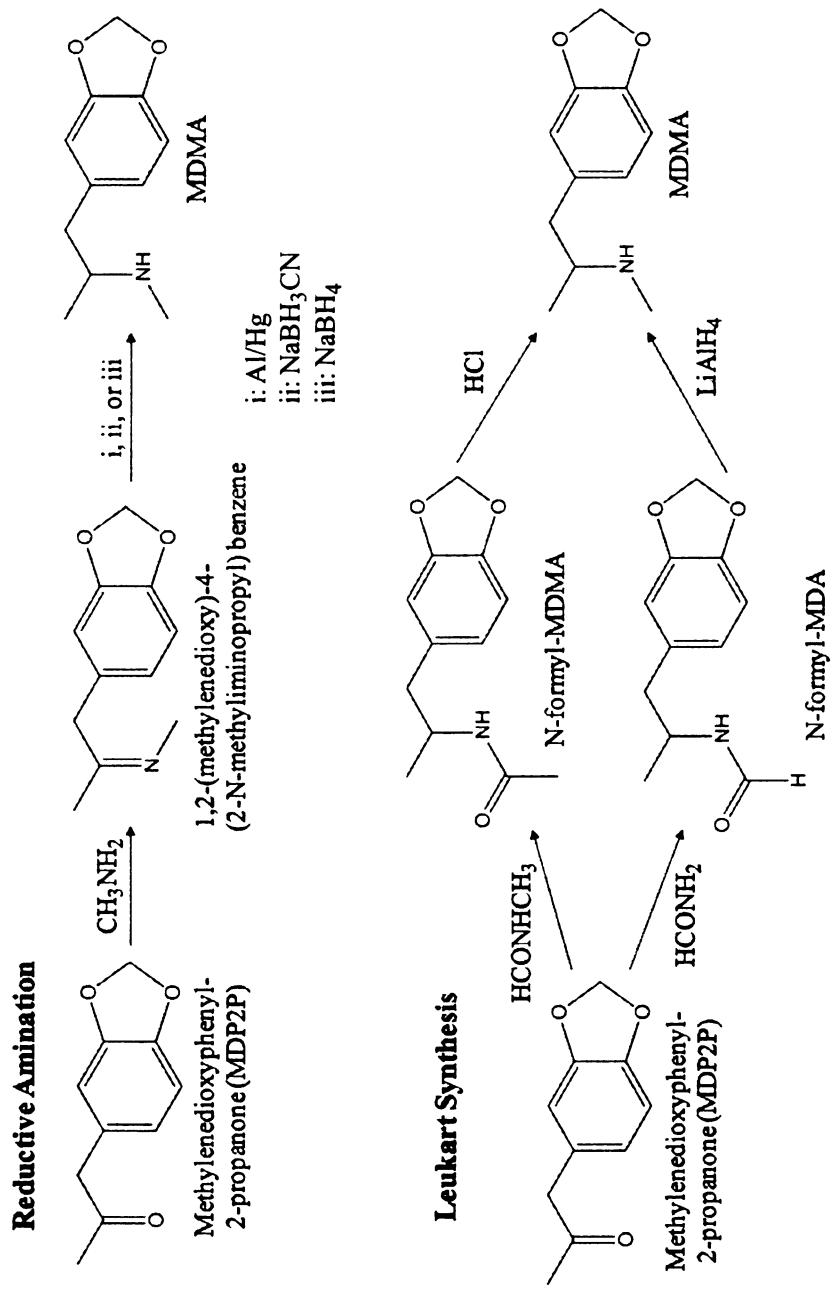

Appendix C: Experimental Runs for Full Factorial Screening Design

Block	Ramp Time (min)	Extraction Time (min)	Extraction Temperature (°C)
1	15	15	100
1	10	20	120
1	20	10	80
1	15	15	100
2	10	10	120
2	20	20	80
2	15	15	100
2	15	15	100
3	20	10	120
3	10	20	80
3	15	15	100
3	15	15	100
4	20	20	120
4	10	10	80
4	15	15	100
4	15	15	100

Appendix D: Experimental Runs for CCC Optimization Design

Run	Ramp Time (min)	Extraction Time (min)	Extraction Temperature (°C)	Type of Point
1	15	15	100	center point
2	10	10	80	factorial
3	20	20	80	factorial
4	15	15	66	star
5	15	15	134	star
6	15	15	100	center point
7	20	10	80	factorial
8	15	15	100	center point
9	10	20	80	factorial
10	15	15	100	center point
11	15	15	100	center point
12	15	15	100	center point
13	23	15	100	star
14	7	15	100	star
15	20	20	120	factorial
16	10	10	120	factorial
17	15	15	100	center point
18	15	15	100	center point
19	20	10	120	factorial
20	15	15	100	center point
21	10	20	120	factorial
22	15	23	100	star
23	15	7	100	star

Appendix E: MANOVA Table for Simulated Sample Components from Full Factorial Design

Benzylamine				
Source	Sum of Squares	Df	Mean Square	F-Ratio
A:Ramp Rate	9.63E+14	1	9.63E+14	4.65
B:Extraction Time	1.21E+14	1	1.21E+14	0.59
C:Extraction Temperature	9.50E+14	1	9.50E+14	4.58
AB+block	1.25E+14	1	1.25E+14	0.61
AC+block	1.52E+14	1	1.52E+14	0.73
BC+block	1.63E+15	1	1.63E+15	7.89
blocks	1.89E+15	3	6.31E+14	3.04
Total error	1.24E+15	6	2.07E+14	
Total (corr.)	5.55E+15	15		

Caffeine				
Source	Sum of Squares	Df	Mean Square	F-Ratio
A:Ramp Rate	2.03E+14	1	2.03E+14	0.06
B:Extraction Time	7.21E+14	1	7.21E+14	0.21
C:Extraction Temperature	3.67E+14	1	3.67E+14	0.11
AB+block	2.33E+15	1	2.33E+15	0.69
AC+block	1.51E+15	1	1.51E+15	0.45
BC+block	1.44E+15	1	1.44E+15	0.43
blocks	1.87E+16	3	6.24E+15	1.84
Total error	2.03E+16	6	3.39E+15	
Total (corr.)	4.45E+16	15		

Methamphetamine				
Source	Sum of Squares	Df	Mean Square	F-Ratio
A:Ramp Rate	4.84E+15	1	4.84E+15	2.85
B:Extraction Time	3.55E+15	1	3.55E+15	2.09
C:Extraction Temperature	8.27E+16	1	8.27E+16	48.6
AB+block	1.21E+16	1	1.21E+16	7.11
AC+block	7.64E+15	1	7.64E+15	4.49
BC+block	1.64E+16	1	1.64E+16	9.64
blocks	2.11E+16	3	7.02E+15	4.13
Total error	1.02E+16	6	1.70E+15	
Total (corr.)	1.60E+17	15		

Phenethylamine				
Source	Sum of Squares	Df	Mean Square	F-Ratio
A:Ramp Rate	6.90E+13	1	6.90E+13	0.07
B:Extraction Time	4.08E+11	1	4.08E+11	0
C:Extraction Temperature	2.29E+14	1	2.29E+14	0.22
AB+block	1.41E+15	1	1.41E+15	1.35
AC+block	1.01E+14	1	1.01E+14	0.1
BC+block	1.84E+14	1	1.84E+14	0.18
blocks	1.96E+15	3	6.53E+14	0.62
Total error	6.27E+15	6	1.04E+15	
Total (corr.)	9.56E+15	15		

Appendix F: Full List of Compounds Extracted from MDMA Exhibits MSU900-01, T-17, and T-27 using MAE/HS-SPME, HS-SPME, and LLE

Provisional Identity	m/z	Exhibit	MAE/HS-SPME RT (min)	HS-SPME RT (min)	LLE RT (min)
		MSU900-01	x	x	x
Unidentified 1	77, 81, 80, 78, 79, 53/59	T-17	2.26	x	x
		T-27	x	x	x
		MSU900-01	2.51	x	x
Unidentified 2	77, 137, 153, 155, 91, 133	T-17	2.51	x	x
		T-27	x	x	x
		MSU900-01	x	2.78	x
Unidentified 3	67, 57, 77, 55, 83	T-17	x	x	x
		T-27	x	x	x
		MSU900-01	x	x	x
Unidentified 4	83, 55, 77, 53, 67	T-17	x	2.79	x
		T-27	x	x	x
		MSU900-01	4.38	4.29	x
Unidentified 5	55, 81, 79, 67, 57	T-17	x	x	x
		T-27	4.48	x	x
		MSU900-01	x	x	x
Unidentified 6	133, 77, 78, 104, 151	T-17	x	4.36	x
		T-27	x	x	x
		MSU900-01	x	x	x
Unidentified 7	211, 213, 133	T-17	x	x	x
		T-27	5.42	x	x
		MSU900-01	5.72	5.79	x
Unidentified 8	193, 209, 105	T-17	x	x	x
		T-27	x	x	x
		MSU900-01	5.79	x	x
Unidentified 9	93, 66, 105, 65	T-17	x	x	x
		T-27	5.84	x	x

Provisional Identity	m/z	Exhibit	MAE/HS-SPME RT (min)	HS-SPME RT (min)	LLE RT (min)
Unidentified 10	93, 91, 77, 133	MSU900-01	x	x	x
		T-17	x	x	x
		T-27	6.05	x	x
Unidentified 11	117, 115, 55, 91, 77	MSU900-01	6.73	6.65	x
		T-17	6.70	6.65	x
		T-27	6.74	6.66	x
Unidentified 12	118, 91, 77	MSU900-01	x	7.08	x
		T-17	7.11	7.04	x
		T-27	x	x	x
Unidentified 13	91, 77, 58	MSU900-01	x	x	x
		T-17	x	x	x
		T-27	7.12	x	x
3,4-Methylenedioxytoluene	135, 136, 77, 78	MSU900-01	8.27	8.20	x
		T-17	8.27	8.17	x
		T-27	x	8.18	x
Unidentified 14	79, 77, 81, 91, 135, 136	MSU900-01	x	x	x
		T-17	x	x	x
		T-27	x	8.27	x
Unidentified 15	149, 105, 77, 79, 117	MSU900-01	x	x	x
		T-17	8.50	8.39	x
		T-27	x	x	x
Unidentified 16	91, 92, 65	MSU900-01	8.61	8.53	x
		T-17	8.64	8.54	x
		T-27	8.73	8.64	x
Unidentified 17	77, 105, 51	MSU900-01	9.41	9.33	x
		T-17	9.42	9.32	x
		T-27	x	x	x

Provisional Identity	m/z	Exhibit	MAE/HS-SPME RT (min)	HS-SPME RT (min)	LLE RT (min)
Methamphetamine	58, 91, 150	MSU900-01	9.78	9.71	5.67
		T-17	9.75	9.64	5.58
		T-27	9.67	9.61	5.67
Unidentified 18	139, 111, 57, 58	MSU900-01	x	x	x
		T-17	x	x	x
		T-27	9.89	x	x
Unidentified 19	152, 154, 118	MSU900-01	x	x	x
		T-17	x	x	x
		T-27	10.04	9.96	x
Unidentified 20	149, 58, 91, 105	MSU900-01	x	x	x
		T-17	10.05	9.96	x
		T-27	x	x	x
Unidentified 21	103, 131, 77, 149	MSU900-01	10.36	10.26	x
		T-17	x	x	x
		T-27	10.35	10.28	x
Unidentified 22	147, 148, 91, 89, 77	MSU900-01	x	x	x
		T-17	10.68	10.58	x
		T-27	x	x	x
Safrole	162, 131, 104/105, 77, 78	MSU900-01	11.54	11.45	x
		T-17	11.54	11.43	x
		T-27	11.52	11.46	x
Unidentified 23	135, 166, 77, 136	MSU900-01	x	x	x
		T-17	12.25	12.15	x
		T-27	x	x	x
Piperonal	149, 150, 121, 65	MSU900-01	12.31	12.25	x
		T-17	12.32	12.22	x
		T-27	12.31	12.28	x

Provisional Identity	m/z	Exhibit	MAE/HS-SPME RT (min)	HS-SPME RT (min)	LLE RT (min)
Unidentified 24	91, 116, 149, 131	MSU900-01	x	12.31	x
		T-17	x	x	x
		T-27	x	x	x
Unidentified 25	116, 91, 131, 130, 89	MSU900-01	12.51	12.41	x
		T-17	x	x	x
		T-27	x	12.40	x
Isosafrole	162, 131, 103, 104, 77, 78	MSU900-01	13.01	12.92	x
		T-17	x	x	x
		T-27	13.01	12.96	x
Ephedrine	58, 56, 77, 73, 91	MSU900-01	x	x	x
		T-17	13.04	12.91	8.63
		T-27	x	x	x
Unidentified 26	56, 91, 71, 58	MSU900-01	x	x	x
		T-17	x	x	8.67
		T-27	x	x	x
Unidentified 27	135, 136, 77, 178, 179	MSU900-01	x	x	x
		T-17	13.15	13.03	8.78
		T-27	x	x	x
Unidentified 28	57, 71, 85, 55	MSU900-01	x	x	x
		T-17	x	x	x
		T-27	x	13.21	x
Unidentified 29	117, 58, 115, 132	MSU900-01	x	x	x
		T-17			
		T-27	13.68	x	x
Unidentified 30	91, 105, 77, 79, 133	MSU900-01	13.77	13.68	x
		T-17	x	13.67	x
		T-27	13.77	13.68	x

Provisional Identity	m/z	Exhibit	MAE/HS-SPME RT (min)	HS-SPME RT (min)	LLE RT (min)
Unidentified 31	91, 119, 77, 105	MSU900-01	x	x	x
		T-17	x	x	x
		T-27	13.95	13.89	x
Unidentified 32	105, 91, 147, 77, 79	MSU900-01	x	x	x
		T-17	x	x	x
		T-27	14.03	13.94	x
Unidentified 33	91, 105, 77, 133, 120	MSU900-01	x	x	x
		T-17	x	x	x
		T-27	x	14.14	x
Unidentified 34	176, 175, 91	MSU900-01	14.30	14.20	x
		T-17	x	x	x
		T-27	x	x	x
Unidentified 35	91, 93, 77, 105, 79	MSU900-01	x	x	x
		T-17	14.32	14.20	x
		T-27	14.32	14.21	x
Unidentified 36	100, 117, 70/91/115, 132	MSU900-01	x	x	x
		T-17	x	x	x
		T-27	x	14.30	x
Unidentified 37	58, 100, 135, 136, 77	MSU900-01	x	x	x
		T-17	x	x	x
		T-27	14.38	x	x
Unidentified 38	177, 135, 163, 149, 121	MSU900-01	14.45	14.34	x
		T-17	x	x	x
		T-27	x	x	x
3,4-Methylenedioxyphenyl-2-propanone (MDP2P)	135, 77, 178, 79, 136	MSU900-01	14.71	14.63	10.26
		T-17	14.81	14.72	10.26
		T-27	14.67	14.60	10.27

Provisional Identity	m/z	Exhibit	MAE/HS-SPME RT (min)	HS-SPME RT (min)	LLE RT (min)
3,4-Methylenedioxyphenyl-2-propanol (MDP2-Propanol)	135, 136, 77, 180, 78, 79	MSU900-01	15.00	14.92	10.38
		T-17	15.10	15.08	10.36
		T-27	14.83	14.87	10.35
Unidentified 39	91, 92, 135, 65, 163	MSU900-01	x	x	x
		T-17	x	x	x
		T-27	x	x	10.58
Unidentified 40	91, 93, 105, 77, 79	MSU900-01	x	x	x
		T-17	x	x	x
		T-27	15.10	15.00	x
Unidentified 41	91, 161, 105, 119, 204	MSU900-01	x	x	x
		T-17	x	x	x
		T-27	x	15.24	x
Unidentified 42	99, 135	MSU900-01	x	15.31	x
		T-17	x	x	x
		T-27	x	x	x
3,4-Methylenedioxymethamphetamine (MDMA)	58, 135, 136, 194	MSU900-01	15.64	15.57	11.16
		T-17	15.68	15.58	11.12
		T-27	15.64	15.54	11.26
Unidentified 43	91, 135, 162, 92, 77, 65	MSU900-01	x	x	x
		T-17	x	x	11.41
		T-27	x	x	x
Unidentified 44	219, 194, 234, 191, 58	MSU900-01	x	x	x
		T-17	x	x	x
		T-27	15.94	15.87	x
Unidentified 45	58, 86/91/118/194	MSU900-01	15.99	15.90	11.55
		T-17	x	x	x
		T-27	x	x	x

Provisional Identity	m/z	Exhibit	MAE/HS-SPME RT (min)	HS-SPME RT (min)	LLE RT (min)
Phthalate	149, 65, 121, 194, 58	MSU900-01	x	x	x
		T-17	15.93	15.87	11.58
		T-27	x	x	x
Unidentified 46	91, 58, 70, 65, 86	MSU900-01	x	x	x
		T-17	x	x	11.98
		T-27	x	x	x
Unidentified 47	147, 89, 190, 194, 117	MSU900-01	16.15	16.05	x
		T-17	x	x	x
		T-27	16.13	x	x
Unidentified 48	154, 189, 401	MSU900-01	x	x	x
		T-17	x	x	x
		T-27	16.20	x	x
Unidentified 49	56, 135, 77, 191, 194	MSU900-01	x	x	x
		T-17	x	x	x
		T-27	x	16.06	x
Diethyl Phthalate	149, 177, 176	MSU900-01	16.35	16.26	11.95
		T-17	x	x	x
		T-27	16.32	16.28	11.95
3,4-Methylenedioxyethylamphetamine (MDEA)	72, 70, 77	MSU900-01	16.47	16.39	x
		T-17	16.52	16.47	12.18
		T-27	16.46	16.38	x
Unidentified 50	58, 72, 77, 135, 136	MSU900-01	x	x	x
		T-17	x	x	x
		T-27	x	x	12.08
Unidentified 51	58, 77, 135/136	MSU900-01	x	x	x
		T-17	x	x	x
		T-27	x	x	12.16

Provisional Identity	m/z	Exhibit	MAE/HS-SPME RT (min)	HS-SPME RT (min)	LLE RT (min)
Unidentified 52	169, 168, 167, 194	MSU900-01	16.77	16.67	x
		T-17	x	x	x
		T-27	x	x	x
Unidentified 53	161, 105, 91, 133, 189	MSU900-01	16.84	16.75	x
		T-17	x	x	x
		T-27	16.82	16.75	x
Unidentified 54	77, 105, 182, 181	MSU900-01	x	x	x
		T-17	x	x	x
		T-27	16.88	16.80	x
Unidentified 55	208, 72, 105, 77, 182	MSU900-01	x	x	x
		T-17	17.10	17.02	12.55
		T-27	x	x	x
Unidentified 56	105, 202, 119	MSU900-01	17.16	x	x
		T-17	x	x	x
		T-27	x	x	x
Unidentified 57	91, 86, 58, 92	MSU900-01	x	x	x
		T-17	x	x	12.98
		T-27	x	x	x
Unidentified 58	146, 117, 115, 77, 174	MSU900-01	x	x	x
		T-17	x	x	x
		T-27	17.39	17.30	13.04
Unidentified 59	100, 195, 70, 91	MSU900-01	x	x	x
		T-17	x	x	x
		T-27	17.43	17.34	x
1-(3,4-Methylenedioxyphenyl)-2-propanone oxime (MDP2P-oxime)	91, 146, 193, 135, 77	MSU900-01	x	x	13.12
		T-17	x	x	13.11
		T-27	x	x	13.13

Provisional Identity	m/z	Exhibit	MAE/HS-SPME RT (min)	HS-SPME RT (min)	LLE RT (min)
Unidentified 60	231, 175, 91, 246	MSU900-01	x	x	x
		T-17	x	x	13.19
		T-27	x	x	x
Unidentified 61	91, 231, 175, 92, 135	MSU900-01	x	x	13.19
		T-17	x	x	x
		T-27	x	x	13.20
Unidentified 62	195, 180, 165, 210	MSU900-01	17.59	17.49	x
		T-17	x	x	x
		T-27	x	x	x
Unidentified 63	129, 173, 115, 145, 103	MSU900-01	x	x	x
		T-17	x	x	x
		T-27	x	17.81	x
Unidentified 64	190, 208, 148, 91, 72	MSU900-01	x	x	x
		T-17	17.76	x	x
		T-27	x	x	x
Unidentified 65	190, 147, 148	MSU900-01	17.86	x	x
		T-17	17.92	17.82	x
		T-27	x	x	x
Unidentified 66	109, 173, 129, 80	MSU900-01	x	x	x
		T-17	x	x	x
		T-27	17.90	x	x
Unidentified 67	109, 80, 151, 81	MSU900-01	x	x	x
		T-17	x	x	x
		T-27	17.95	x	13.64
Unidentified 68	91, 176, 135	MSU900-01	x	x	x
		T-17	x	x	13.67
		T-27	x	x	x

Provisional Identity	m/z	Exhibit	MAE/HS-SPME RT (min)	HS-SPME RT (min)	LLE RT (min)
Unidentified 69	160, 109, 201	MSU900-01	x	x	x
		T-17	x	x	x
		T-27	18.23	x	x
Unidentified 70	58, 100, 208, 135, 77	MSU900-01	x	x	x
		T-17	18.30	18.20	13.92
		T-27	x	x	x
Unidentified 71	176, 177, 91, 92	MSU900-01	x	x	x
		T-17	x	x	14.02
		T-27	x	x	x
Unidentified 72	216, 115, 173, 143	MSU900-01	18.43	18.33	x
		T-17	x	x	x
		T-27	x	x	x
Unidentified 73	100, 58, 72, 135, 208	MSU900-01	x	x	x
		T-17	18.45	18.36	x
		T-27	x	x	x
Unidentified 74	115, 130, 193, 208, 178	MSU900-01	x	x	x
		T-17	x	x	x
		T-27	18.53	18.45	x
Unidentified 75	152, 154, 180, 138	MSU900-01	x	x	x
		T-17	x	x	x
		T-27	18.62	18.51	14.26
Unidentified 76	105, 132, 77, 91	MSU900-01	x	x	x
		T-17	18.81	x	x
		T-27	x	x	x
Unidentified 77	189, 188	MSU900-01	19.08	18.98	x
		T-17	x	x	x
		T-27	x	x	x

Provisional Identity	m/z	Exhibit	MAE/HS-SPME RT (min)	HS-SPME RT (min)	LLE RT (min)
Unidentified 78	91, 175, 92, 65, 120	MSU900-01	x	x	14.93
		T-17	x	x	x
		T-27	x	x	x
Unidentified 79	181, 167, 91, 166	MSU900-01	x	x	x
		T-17	x	x	x
		T-27	19.13	19.05	x
Unidentified 80	120, 91, 77, 175, 214	MSU900-01	19.25	19.15	x
		T-17	x	x	x
		T-27	x	x	x
Unidentified 81	91, 92, 103, 77, 65	MSU900-01	x	x	x
		T-17	x	x	x
		T-27	19.43	19.35	15.09
Unidentified 82	94, 78, 229	MSU900-01	x	x	x
		T-17	19.58	x	x
		T-27	x	x	x
Unidentified 83	134, 119, 91	MSU900-01	x	x	x
		T-17	x	x	x
		T-27	19.58	19.46	x
Unidentified 84	165, 91, 92, 150, 65	MSU900-01	x	x	x
		T-17	x	x	15.32
		T-27	x	x	x
Unidentified 85	166, 168, 131	MSU900-01	x	x	x
		T-17	x	x	x
		T-27	19.73	19.63	x
Caffeine	194, 193	MSU900-01	19.85	19.74	15.72
		T-17	19.83	19.74	15.69
		T-27	19.91	19.80	15.69

Provisional Identity	m/z	Exhibit	MAE/HS-SPME RT (min)	HS-SPME RT (min)	LLE RT (min)
Unidentified 86	194, 180, 91, 55, 193	MSU900-01	x	x	x
		T-17	x	x	15.90
		T-27	x	x	x
Unidentified 87	180, 182	MSU900-01	x	x	x
		T-17	x	x	x
		T-27	20.20	20.10	15.96
Unidentified 88	58, 165, 152, 167	MSU900-01	x	x	x
		T-17	20.35	20.26	x
		T-27	20.34	20.26	x
Lidocaine	86, 58, 72, 91	MSU900-01	20.48	20.38	x
		T-17	20.49	20.38	16.18
		T-27	x	x	x
Unidentified 89	91, 162, 119	MSU900-01	x	x	x
		T-17	x	x	x
		T-27	20.56	20.46	x
Unidentified 90	97, 70, 91, 162, 194	MSU900-01	x	x	x
		T-17	x	x	16.56
		T-27	x	x	x
N-methyl-(1,2-methylenedioxy)-4-(1-ethyl-2-aminopropyl) benzene	162, 58, 77, 135	MSU900-01	20.85	20.76	16.65
		T-17	20.86	20.77	x
		T-27	20.86	20.77	16.58
Unidentified 91	147, 277, 189, 292	MSU900-01	x	x	x
		T-17	20.95	20.84	x
		T-27	x	x	x
Unidentified 92	105, 77, 79, 146	MSU900-01	x	20.89	x
		T-17	x	x	x
		T-27	x	x	x

Provisional Identity	m/z	Exhibit	MAE/HS-SPME RT (min)	HS-SPME RT (min)	LLE RT (min)
Unidentified 93	180, 220, 115	MSU900-01	x	x	x
		T-17	x	x	x
		T-27	21.04	20.95	x
Palmatic acid	87, 55, 73, 129, 256	MSU900-01	21.10	x	17.10
		T-17	x	x	17.16
		T-27	x	x	x
Unsaturated fatty acid	55, 87, 73, 60, 129	MSU900-01	x	x	x
		T-17	x	x	x
		T-27	21.14	21.03	17.37
Unidentified 94	146, 147, 105, 77	MSU900-01	x	x	x
		T-17	21.29	21.17	x
		T-27	x	x	x
Unidentified 95	180, 166, 105, 79	MSU900-01	x	21.62	x
		T-17	x	x	x
		T-27	x	x	x
Unidentified 96	182, 227, 91, 205	MSU900-01	x	x	x
		T-17	21.87	x	x
		T-27	x	x	x
Unidentified 97	91, 176	MSU900-01	x	x	x
		T-17	x	x	x
		T-27	22.07	21.97	x
Unidentified 98	148, 168, 176, 73, 91	MSU900-01	x	x	x
		T-17	22.37	22.27	x
		T-27	x	x	x
Unidentified 99	196, 91, 98, 197	MSU900-01	23.04	22.92	x
		T-17	23.06	x	x
		T-27	x	x	x

Provisional Identity	m/z	Exhibit	MAE/HS-SPME RT (min)	HS-SPME RT (min)	LLE RT (min)
Unidentified 100	99, 117, 55, 100	MSU900-01	x	x	x
		T-17	x	32.22	x
		T-27	x	x	x
Stearic acid	87, 55, 73, 157, 284	MSU900-01	x	x	19.26
		T-17	x	x	19.23
		T-27	x	x	x
Unsaturated fatty acid	55, 87, 73, 60, 185	MSU900-01	x	x	x
		T-17	x	x	x
		T-27	23.41	x	19.58
Unidentified 101	160, 251, 129, 91	MSU900-01	x	23.56	x
		T-17	x	x	x
		T-27	x	x	x
Unidentified 102	168, 162, 281	MSU900-01	x	x	x
		T-17	x	x	x
		T-27	x	23.73	x
Unidentified 103	180, 97, 55, 135, 83	MSU900-01	24.11	24.02	x
		T-17	x	x	x
		T-27	24.11	x	x
Unidentified 104	91, 148	MSU900-01	x	x	x
		T-17	24.20	24.10	x
		T-27	x	x	x
Unidentified 105	182, 58, 162, 112	MSU900-01	24.93	24.83	x
		T-17	x	x	x
		T-27	x	x	x
Unidentified 106	194, 97, 69, 55	MSU900-01	25.19	25.09	x
		T-17	x	x	x
		T-27	25.19	x	x

Provisional Identity	m/z	Exhibit	MAE/HS-SPME RT (min)	HS-SPME RT (min)	LLE RT (min)
Unidentified 107	184, 72, 105	MSU900-01	x	25.18	x
		T-17	x	x	x
		T-27	x	x	x
Unidentified 108	182, 183, 98	MSU900-01	25.69	25.58	x
		T-17	x	x	x
		T-27	25.70	25.60	x
Unidentified 109	149, 91, 119, 284	MSU900-01	x	x	x
		T-17	25.81	25.71	x
		T-27	x	x	x
Unidentified 110	198, 72, 58	MSU900-01	26.33	26.23	x
		T-17	x	x	
		T-27	x	x	x
Unidentified 111	196, 197	MSU900-01	26.72	26.62	x
		T-17	26.73	x	x
		T-27	26.69	26.64	x
Unidentified 112	105, 149, 77	MSU900-01	x	x	22.60
		T-17	x	x	x
		T-27	x	x	x
Unidentified 113	135, 77, 270, 105	MSU900-01	x	x	x
		T-17	x	x	22.61
		T-27	x	x	x
Unidentified 114	149, 167, 91, 55	MSU900-01	x	x	23.22
		T-17	x	x	x
		T-27	x	x	x
Unidentified 115	135, 77, 270	MSU900-01	x	x	x
		T-17	26.80	x	x
		T-27	x	x	x

Provisional Identity	m/z	Exhibit	MAE/HS-SPME RT (min)	HS-SPME RT (min)	LLE RT (min)
Unidentified 116	293, 294, 190, 222	MSU900-01	x	27.13	x
		T-17	x	x	x
		T-27	x	x	x
Unidentified 117	160, 149, 167	MSU900-01	x	27.27	x
		T-17	x	x	x
		T-27	x	27.30	x
Unidentified 118	149, 167, 160, 176	MSU900-01	x	x	x
		T-17	x	27.32	23.21
		T-27	x	x	x
Unidentified 119	176, 149, 160	MSU900-01	27.39	x	x
		T-17	27.38	x	x
		T-27	27.39	x	x
Unidentified 120	149, 167	MSU900-01	x	x	x
		T-17	x	x	x
		T-27	x	x	23.23
Unidentified 121	135, 192, 77	MSU900-01	x	x	x
		T-17	27.99	x	23.83
		T-27	x	x	x
Unidentified 122	163, 204, 135, 105, 133	MSU900-01	28.11	28.03	x
		T-17	x	x	x
		T-27	x	28.05	x
Unidentified 123	260, 395	MSU900-01	29.15	29.05	x
		T-17	x	x	x
		T-27	x	x	x
Unidentified 124	163, 220, 135, 105	MSU900-01	x	x	x
		T-17	x	x	25.48
		T-27	x	x	x

Provisional Identity	m/z	Exhibit	MAE/HS-SPME RT (min)	HS-SPME RT (min)	LLE RT (min)
Unidentified 125	260, 204, 149	MSU900-01	29.72	29.64	x
		T-17	x	x	x
		T-27	x	x	x
Unidentified 126	218, 187, 157, 129	MSU900-01	x	x	x
		T-17	x	x	25.73
		T-27	x	x	x

Appendix G: Full List of Compounds Extracted from MDMA Exhibits T-17 and CJ-FS05 using HS-SPME (unidentified impurity numbers do not correspond to Appendix F)

Provisional Identity	m/z	T-17 RT (min)	CJ-FS05 RT (min)
Unidentified 1	137, 153, 82, 77, 91, 155	x	2.51
Unidentified 2	83, 55, 77, 67	2.79	2.87
Unidentified 3	133, 77, 78, 104, 151	4.36	x
Unidentified 4	117, 115, 77/91/118	6.65	x
Unidentified 5	94, 66, 65	x	6.65
Unidentified 6	118, 77, 91, 133	7.04	7.15
3,4-Methylenedioxytoluene	135, 136, 77, 78	8.17	8.26
Unidentified 7	146, 105, 79, 77, 91	8.39	8.49
Unidentified 8	91, 92, 65	8.54	8.62
Unidentified 9	105, 77, 51, 78, 106	9.32	9.41
Methamphetamine	58, 91, 150	9.64	9.73
Unidentified 10	146, 58, 105, 91	9.95	10.02
Unidentified 11	135, 108, 91, 82, 69, 58	x	10.42
Unidentified 12	147, 148, 91, 89, 77	10.58	10.66
Unidentified 13	107, 135, 77, 97	x	11.18
Safrole	162, 131, 103, 77, 104, 78	11.43	x
Unidentified 14	135, 166, 77, 136	12.15	12.24
Piperonal	149, 150, 121, 65	12.22	12.30
Ephedrine	58, 56, 77, 71, 91	12.91	13.00
Unidentified 15	135, 136, 77, 178, 179	13.03	13.12

Provisional Identity	m/z	T-17 RT (min)	CJ-FS05 RT (min)
Unidentified 16	91, 105, 77, 133, 79	13.67	x
Unidentified 17	91, 93, 77, 105, 79	14.20	14.30
3,4-Methylenedioxyphenyl-2-propanone (MDP2P)	135, 77, 178, 79, 136	14.72	14.76
3,4-Methylenedioxyphenyl-2-propanol (MDP2-propanol)	135, 136, 77, 180, 78, 79	15.12	15.20
3,4-Methylenedioxymethamphetamine (MDMA)	58, 135, 136, 194	15.58	15.64
Unidentified 18	149, 65, 121, 194, 58	15.87	x
3,4-Methylenedioyxethylamphetamine (MDEA)	72, 70, 77 (208)	16.47	16.50
Unidentified 19	208, 72, 105, 77	17.02	17.09
Unidentified 20	208, 207, 222, 72, 91	x	17.23
Unidentified 21	231, 208, 175, 133/246	x	17.62
Unidentified 22	195, 208, 167, 165	x	17.73
Unidentified 23	190, 147, 148, 208, 188	17.82	x
Unidentified 24	121, 208, 107, 163	x	17.82
Unidentified 25	135, 190, 107/208, 147, 148	x	17.92
Unidentified 26	107, 121, 149, 208	x	18.10
Unidentified 27	58, 100, 208, 135, 77	18.20	x
Unidentified 28	100, 58, 72, 135, 208	18.36	x
Unidentified 29	107, 149, 121, 208, 100	x	18.43
Unidentified 30	191, 192, 57	x	18.93
Unidentified 31	120, 91, 214, 77, 93/121	x	19.23
Caffeine	194, 193	19.74	19.86

Provisional Identity	m/z	T-17 RT (min)	CJ-FS05 RT (min)
Unidentified 32	58, 165, 152, 167	20.26	x
Lidocaine	86, 58, 72, 91	20.38	20.47
N-methyl-(1,2-methylenedioxy)-4-(1-ethyl-2-aminopropyl) benzene	162, 58, 77, 135	20.77	20.85
Unidentified 33	147, 277, 189, 292	20.84	x
Unidentified 34	146, 147, 105, 77	21.17	x
Unidentified 35	227, 143, 242, 228	x	22.23
Unidentified 36	148, 168, 176, 73, 91	22.27	x
Unidentified 37	217, 232, 215, 202, 231	x	22.65
Unidentified 38	99, 117, 55, 100	23.22	x
Unidentified 39	148, 190, 149	23.39	x
Unidentified 40	91, 148, 281	24.10	x
Unidentified 41	149, 91, 119, 284	25.71	25.80
Unidentified 42	191, 150, 164, 192	x	26.27
Unidentified 43	149, 167, 160, 176, 281	27.32	x
Unidentified 44	135, 192, 77	x	27.97